SOLID STATE FERMENTATION OF SOYBEAN HULLS FOR CELLULOLYTIC ENZYMES PRODUCTION: PHYSICOCHEMICAL CHARACTERISTICS, AND BIOREACTOR DESIGN AND MODELING

by

KHUSHAL BRIJWANI

B.S., University of Delhi, India, 2000
M.S., Central Food Technological Research Institute, University of Mysore, India, 2002
M.S., Satake Centre for Grain Process Engineering, University of Manchester, UK, 2003

AN ABSTRACT OF A DISSERTATION

submitted in partial fulfillment of the requirements for the degree

DOCTOR OF PHILOSOPHY

Department of Grain Science & Industry
College of Agriculture

KANSAS STATE UNIVERSITY
Manhattan, Kansas

2011

Abstract

The purpose of this study was to investigate micro- and macro-scale aspects of solid state fermentation (SSF) for production of cellulolytic enzymes using fungal cultures. Included in the objectives were investigation of effect of physicochemical characteristics of substrate on enzymes production at micro-scale, and design, fabrication and analysis of solid-state bioreactor at macro-scale. In the initial studies response surface optimization of SSF of soybeans hulls using mixed culture of *Trichoderma reesei* and *Aspergillus oryzae* was carried out to standardize the process. Optimum temperature, moisture and pH of 30ºC, 70% and 5 were determined following optimization. Using optimized parameters laboratory scale-up in static tray fermenter was performed that resulted in production of complete and balanced cellulolytic enzyme system. The balanced enzyme system had required 1:1 ratio of filter paper and beta-glucosidase units. This complete and balanced enzyme system was shown to be effective in the hydrolysis of wheat straw to sugars. Mild pretreatments– steam, acid and alkali were performed to vary physicochemical characteristics of soybean hulls – bed porosity, crystallinity and volumetric specific surface. Mild nature of pretreatments minimized the compositional changes of substrate. It was explicitly shown that more porous and crystalline steam pretreated soybean hulls significantly improved cellulolytic enzymes production in *T. reesei* culture, with no effect on xylanase. In *A. oryzae* and mixed culture this improvement, though, was not seen. Further studies using standard crystalline substrates and substrates with varying bed porosity confirmed that effect of physicochemical characteristics was selective with respect to fungal species and cellulolytic activity. A novel deep bed bioreactor was designed and fabricated to address scale-up issues. Bioreactor's unique design of outer wire mesh frame with internal air distribution and a near saturation environment within cabinet resulted in enhanced heat transfer with minimum moisture loss. Enzyme production was faster and leveled within 48 h of operation compared to 96 h required in static tray. A two phase heat and mass transfer model was written that accurately predicted the experimental temperature profile. Simulations also showed that bioreactor operation was more sensitive to changes in cabinet temperature and mass flow rate of distributor air than air temperature.

SOLID STATE FERMENTATION OF SOYBEAN HULLS FOR CELLULOLYTIC ENZYMES PRODUCTION: PHYSICOCHEMICAL CHARACTERISTICS, AND BIOREACTOR DESIGN AND MODELING

by

KHUSHAL BRIJWANI

B.S., University of Delhi, India, 2000
M.S., Central Food Technological Research Institute, University of Mysore, India, 2002
M.S., Satake Centre for Grain Process Engineering, University of Manchester, UK, 2003

A DISSERTATION

submitted in partial fulfillment of the requirements for the degree

DOCTOR OF PHILOSOPHY

Department of Grain Science & Industry
College of Agriculture

KANSAS STATE UNIVERSITY
Manhattan, Kansas

2011

Approved by:

Major Professor
Dr. Praveen V. Vadlani

Copyright

Abstract

The purpose of this study was to investigate micro- and macro-scale aspects of solid state fermentation (SSF) for production of cellulolytic enzymes using fungal cultures. Included in the objectives were investigation of effect of physicochemical characteristics of substrate on enzymes production at micro-scale, and design, fabrication and analysis of solid-state bioreactor at macro-scale. In the initial studies response surface optimization of SSF of soybeans hulls using mixed culture of *Trichoderma reesei* and *Aspergillus oryzae* was carried out to standardize the process. Optimum temperature, moisture and pH of 30ºC, 70% and 5 were determined following optimization. Using optimized parameters laboratory scale-up in static tray fermenter was performed that resulted in production of complete and balanced cellulolytic enzyme system. The balanced enzyme system had required 1:1 ratio of filter paper and beta-glucosidase units. This complete and balanced enzyme system was shown to be effective in the hydrolysis of wheat straw to sugars. Mild pretreatments– steam, acid and alkali were performed to vary physicochemical characteristics of soybean hulls – bed porosity, crystallinity and volumetric specific surface. Mild nature of pretreatments minimized the compositional changes of substrate. It was explicitly shown that more porous and crystalline steam pretreated soybean hulls significantly improved cellulolytic enzymes production in *T. reesei* culture, with no effect on xylanase. In *A. oryzae* and mixed culture this improvement, though, was not seen. Further studies using standard crystalline substrates and substrates with varying bed porosity confirmed that effect of physicochemical characteristics was selective with respect to fungal species and cellulolytic activity. A novel deep bed bioreactor was designed and fabricated to address scale-up issues. Bioreactor's unique design of outer wire mesh frame with internal air distribution and a near saturation environment within cabinet resulted in enhanced heat transfer with minimum moisture loss. Enzyme production was faster and leveled within 48 h of operation compared to 96 h required in static tray. A two phase heat and mass transfer model was written that accurately predicted the experimental temperature profile. Simulations also showed that bioreactor operation was more sensitive to changes in cabinet temperature and mass flow rate of distributor air than air temperature.

Table of Contents

List of Figures

List of Tables

Acknowledgements

It is my pleasure to express my deep sense of gratitude to my advisor Dr. Praveen Vadlani for his interest in my work, valuable suggestions, constant encouragement, help in matters related to my graduate studies and friendly support that were essential for the fulfillment of this endeavor. I place on record my deep sense of appreciation to Dr. Dirk Maier for serving on my committee, providing valuable suggestions throughout this project, support and encouragement. I would like to express my heartfelt thanks to Dr. Keith Hohn for his support and suggestions in this project, and serving on my committee. I am greatly thankful to Dr. Paul Seib for his technical insights and serving on my committee. Lastly, but not the least, support from Dr. Jon Faubion is greatly appreciated for serving on my defense, and providing helpful suggestions.

I am thankful to the Center for Sustainable Energy, and the Department of Grain Science & Industry for the fellowship and providing the funding to carry out the research work.

Thanks to my colleagues at bioprocessing lab– Liyan, Yixing, Erin, Anne, Kyle, Sunil, Anand and Harinder for wonderful time I had with them.

I wish to place on record the indebtedness to my beloved parents Shri T.D. Brijwani and Mrs. Aarti Brijwani for their affection and love. I am deeply thankful to my wife Monika for her continued support, affection, inspiration and patience in this journey.

Finally, to Almighty Lord who has given me the confidence, strength and wisdom to progress.

Chapter 1 - General Introduction

To attain DOE milestone to produce 60 billion gallons of ethanol by 2030, the emerging cellulosic technologies need to mature and several key steps need to be cost effectively developed. The most crucial stage in production of bioethanol from lignocellulosic biomass is the enzymatic saccharification of biomass into sugars, which are eventually fermented to ethanol by appropriate microorganism. A critical aspect of enzymatic conversion of biomass into sugars is associated enzyme dosage and cost. Due to the compositional complexity of lignocellulosic biomass multiple enzymes are required to complete the hydrolysis. This requires extensive dosage optimization of multiple enzymes that add cost. Cellulolytic enzyme system, collectively referred as group of multiple enzymes needed for biomass hydrolysis, is a complex system of enzymes composed of endoglucanase (1, 4-D-glucan-4-glucanohydrolase, EC 3.2.1.4), exoglucanase (1,-D-glucan-cellobiohydrolase, EC 3.2.1.91) and β-glucosidase (D-glucosidoglucohydrolase, cellobiase, EC 3.2.1.21) that act synergistically to degrade cellulosic substrate [1,2]. Xylanase (EC 3.2.1.8) complements this system; it is needed to elicit complete and efficient hydrolysis of the lignocellulosic biomass, which has appreciable amount of hemicellulose or xylan. For efficient hydrolysis it is important that all the desired activities should be present in balanced proportion with high titers. It is difficult to produce complete system in submerged fermentations, and consequently the commercial enzymes are rich in one activity and require supplementation of others.

Solid state fermentation (SSF) is one way where all the desired activities can be produced in a single process, thus avoiding complex and costly fermentations to produce three to four enzymes independently and then blending it to form a concoction. Another important feature of SSF is that it utilizes heterogeneous products of agriculture (mainly agricultural residues) and

by-products of agro-based industries [3]. In solid-state fermentation of cellulase production, cellulosic substrate acts as both the carbon source and as an inducer for cellulase production [4]. Both bacteria and fungi can use cellulose as a primary carbon source. Most bacteria, however, are incapable of degrading crystalline cellulose since their cellulase systems are incomplete. On the other hand, cellulolytic enzymes produced by some fungi generally involve all three types of enzymes, so are very useful in the saccharification of renewable pretreated lignocellulosic materials. *Trichoderma reesei* is the most widely employed fungus for production of cellulolytic enzymes and has been extensively studied [5]. Strains of *Trichoderma* can accumulate high activities of endo and exo-glucanase, but are poor in β-glucosidase [6], whereas the strains of *Aspergillus* are high in β- glucosidase activity [7].

Solid-state fermentation can be viewed as a discrete solid phase in which microorganisms grow on the surface of moist, discrete particles as well as inside and between them (Figure 1.1). The space between particles is occupied by a continuous gas phase [8]. Availability of oxygen in the open spaces between particles is a major challenge in SSF [9]. In their studies with model substrates of wheat flour disc and packed mass of wheat grains, Rahardjo et al. [10] stressed the importance of open spaces and surface area of particles in α-amylase production of *Aspergillus oryzae* in solid substrate fermentation. Because of the discrete nature of SSF the particulate nature is manifested. Only a few studies published to date have dealt with the influence of physicochemical characteristics of cellulosic substrate on cellulolytic enzyme production. And in these studies, there has been only an indirect mention of the influence of physicochemical attributes such as crystallinity on production of cellulases. For instance, Acebal et al. [11] demonstrated that chemically treated wheat straw, which had higher crystallinity than untreated straw by virtue of the treatment, resulted in higher titers of filter paper activity in *Trichoderma*

reesei QM 9414 than untreated wheat straw. Similarly, Evans et al. [12] showed that crystalline-cotton-induced cellulases exhibited better potential in hydrolyzing crystalline cellulose than Solka-Floc-induced cellulases. Moreover, all of these studies were performed in liquid cultures; no work has yet been attempted in a solid-state environment.

The successful commercialization of SSF depends upon its scalability. However, due to solid and discrete nature of the SSF with no mixing the scale-up is suffered from heat and mass transfer limitations. To understand limitations in scale-up we need to look at both temporally and spatially the phenomena taking place within the bioreactor space. Fig. 1.2 is a snap shot of processes occurring in any type of solid state bioreactor for any type of biotechnological product. There are two processes that occur simultaneously in a bioreactor containing moist substrate impregnated with fungal biofilm: transport phenomena and biological phenomena. The inter-particle space is occupied by gas phase.

Transport processes

1. Diffusion of O_2, CO_2, water vapor from the air flow into the inter-particle space surrounding the fungal biofilm. O_2 will be taken up and CO_2 and water vapor will be released into inter-particle space occupied by gas phase.
2. Diffusion of enzymes from the biofilm phase into substrate and reaction of enzymes with substrate.
3. Release of metabolic heat during growth and its exchange with gas phase surrounding the biofilm.

Biological phenomena

1. Transfer of nutrients (products of enzyme reaction) within hyphae
2. Growth including extension of hyphae both penetrative and aerial

3. Stress response by fungal cells to depleting oxygen and increasing temperature within bed
4. Cell death

Let expand aforementioned process into full blown macro-scale solid state bioreactor as shown in Fig. 3. It is noticeable that both heat and mass transport across the packed bed would be a major challenge to keep the fungal bed viable and alive. We must agree that fungal culture growing in a solid media would respond exactly in a same way when it is growing in few grams (Figure 1.2) and few thousand kilograms (Figure 1.3). However, as the scale grows, the transport limitation of heat and mass would play a significant role and may deviate the whole process from its optimal. In fact, a key prediction of the modeling work of Rajagopalan and Modak [13] was that few centimeters increase in bed height made heat and mass transport so worst that growth of *Aspergillus niger* on wheat bran medium came to a complete halt. Raghava Rao et al. [14] proposed an equation to estimate the maximum depth at which a bioreactor could be maintained without falling into hypoxia. The problem arising from the temperature gradients are more severe than problems arising from O_2 gradient within the inter-particle space especially in forced aerated bioreactor [15]. In their study Rajagopalan and Modak [13] showed that due to large rise in temperature especially at the center of the bed growth of fungal cells was virtually arrested even though oxygen concentration in the void space was above critical concentration. The work of Smits et al. [16] confirms that O_2 levels in the inter-particle spaces will generally not be a limiting factor as long as effective diffusivity of O_2 is of order of 4×10^{-6} m^2s^{-1}.

The foregoing indicates that temperature gradients are the major bottleneck in successful scale-up of static bioreactors that they limit the bed depth. Bed depth is important parameter to keep reasonable throughput of the bioreactor. Though the work so far has dealt the issues of heat

and mass transport limitations but mostly through by modeling or simulation studies. The experimental evidence in the literature is quite scanty.

Outline of this thesis

The current study aims at understanding both micro and macro scale aspects of SSF from flask to bioreactor level. This should lead to efficient process development and bioreactor design. At micro-scale we have investigated the role of physicochemical characteristics in controlling the cellulolytic enzyme production in both mono and mixed cultures of *Trichoderma reesei* and *Aspergillus oryzae* during SSF of soybean hulls. At macro-scale, a novel bioreactor has been designed that addresses heat and moisture transfer limitation common in deep bed bioreactor designs. The unique design features are instrumental in containing steep temperature gradients such that bed is maintained viable for the production of enzymes throughout its operational period. Finally, to extend the experimental observations of bioreactor operation into theoretical understanding a mathematical model of heat and mass transfer coupled to fungal growth has been developed that not only predict the experimental data but provides a valuable discourse on various phenomena happening within the bioreactor, as well as predicts the bioreactor performance in various scenarios. By viewing the SSF in both micro-scale (particulate nature) and macro-scale (bioreactor level) the current investigation addresses the entire spectrum of issues in SSF thus giving completeness to this work. This should promote advancement of knowledge that would eventually lead to successful commercialization of solid state fermentation.

Soybean hulls are the value added by-product of agricultural processing especially in mid-west region of United States. Its availability and rich cellulosic composition makes it valuable substrate for the production of cellulolytic enzymes in SSF. *Trichoderma reesei* is a

common fungal mold that has been used for cellulase production; however, its incapability of producing appropriate amount of beta-glucosidase is a major bottleneck. Chapter 2 discusses the potential of soybean hulls as probable candidate for large scale production of cellulolytic enzymes. By using mixed fungal culture of *T. reesei* and *A. oryzae* using soybean hulls supplemented with wheat bran a cellulolytic enzyme system is produced that has been shown to be effective in carrying out the complete hydrolysis of lignocellulosic biomass, wheat straw, into sugars that can be channelized for fuels and chemical production. Response surface methodology has been employed in optimizing the process conditions for mixed culture SSF of soybean hulls.

Due to discrete and particulate nature of SSF the physicochemical characteristics are directly manifested in influencing the enzyme production in fungal cultures. They offer a rich means of controlling enzyme production. Meaning by varying the characteristics it is possible to elicit a response in fungal cultures that has its impact on production of cellulolytic enzymes. Chapter 3 hypothesizes that pretreatments can be used as means to change physicochemical characteristics, such as crystallinity, bed porosity, and volumetric specific surface, of lignocellulosic biomass. The changes in physicochemical characteristics could influence the expression levels of cellulolytic enzymes in both monocultures and mixed cultures of *T. reesei* and *A. oryzae*. Further it explores if such effects are culture dependent or universal, and whether they affect all the enzyme activities or selective in action. Chapter 4 extends the results of chapter 3 further and explicitly demonstrates effect of bed porosity and crystallinity on cellulolytic enzymes production in both mono and mixed culture SSF of soybean hulls.

Deep bed bioreactors are preferred over most designs because of better control and process management. However, significant heat and mass transfer limitations in deep beds could jeopardize their commercial potential. After addressing the issues and fundamentals at micro-

scale where particle nature of substrate is in focus, the study touches the macro-scale aspects of SSF. It culminates in design and fabrication of novel bioreactor. Chapter 5 outlines the studies that benchmark performance of bioreactor in containing steep temperature gradients. It further highlights the cabinet usage restricts excessive moisture loss and prevents bed desiccation. Finally, it is shown that novel design leveraging on its enhanced convective heat transfer permits full capacity operation for production of cellulolytic enzymes without considerable loss of activities in deep beds. The design and validation are the important engineering procedures that prescribe usage of newly developed products and processes. This applies to present study as well making it, therefore, essential to theoretically model physical and biological phenomena. The model should act as tool for validation of new designs in various scenarios. A two-phase heat and moisture transfer model coupled to biological phenomena of fungal growth is developed. Model successfully predicts temperature dynamics concomitant with the observed trends and it outlines the effect of these gradients on growth and viability of fungal cells as well. Applicability of model simulations is extended to include the effect of critical process parameters on bioreactor design and operation.

In Chapter 6 whole work is summarized and, finally conclusions and future aspects of this study are discussed in Chapter 7.

References

[1] Holker U, Hofer M, Lenz J. Biotechnological advantages of laboratory scale solid state fermentation with fungi. Appl Microbiol Biotechnol 2004;64:175-186.

[2] Esterbauer H, Steiner W, Labudova I, et al. Production of *Trichoderma* cellulase in laboratory and pilot scale. Bioresource Technol 1991;36:51-65.

[3] Raimbault M. General and microbiological aspects of solid substrate fermentation. Elect J Biotechnol 1998;27:498-503.

[4] Cen P, Xia L. Production of cellulase in solid state ferementation. In: Scheper T, editor. Recent progress in bioconversion of lignocellulosics. Advances in Biochemical Engineering/Biotechnology. vol. 65. Berlin: Springer; 1999. p. 69.

[5] Stockton BC, Mitchell DJ, Grohmann K, et al. Optimum β-D glucosidase supplementation of cellulase for efficient conversion of cellulose to glucose. Biotechnology Lett 1991;13:57-62.

[6] Duff SJB, Cooper DG, Fuller OM. Effect of media composition and growth conditions on production of cellulase and β-glucosidase by a mixed fungal fermentation. Enzyme Microbiol Technol 1987;9:47-52.

[7] Grajek W. Hyperproduction of thermostable beta-glucosidase by *Sporotrichum* (*Chrysosporium*) thermophile. Enzyme Microbiol Technol 1987;9:744-748.

[8] Botella C, Diaz AB, Wang RH, Koutinas A, Webb C. Particulate bioprocessing: A novel process strategy for biorefineries. Process Biochem 2009;44(5):546-555.

[9] Thibault J, Pouliot K, Agosin E, Perez-Correa R. Reassessment of the estimation of dissolved oxygen concentration profile and K(L)a in solid-state fermentation. Process Biochemistry 2000;36:9-18.

[10] Rahardjo YSP, Jolink F, Haemers S, Tramper J, Rinzema A. Significance of bed porosity, bran and specific surface area in solid-state cultivation of Aspergillus oryzae. Biomolecular Engineering 2005;22:133-139.

[11] Acebal C, Castillon MP, Estrada P, Mata I, Costa E, Aguado J, Romero D, Jimenez F. Enhanced cellulase production from trichoderma-reesei qm-9414 on physically treated wheat straw. Applied Microbiology and Biotechnology 1986;24:218-223.

[12] Evans ET, Wales DS, Bratt RP, Sagar BF. Investigation of an endoglucanase essential for the action of the cellulase system of trichoderma-reesei on crystalline cellulose. Journal of General Microbiology 1992;138:1639-1646.

[13] Rajagopalan S, Modak JM. Heat and mass-transfer simulation studies for solid-state fermentation processes. Chemical Engineering Science 1994;49:2187-2193.

[14] Raghava Rao KSMS, Gowthaman MK, Ghildyal NP, Karanth NG. A mathematical model for solid state fermentation in tray bioreactors. Bioprocess Eng 1993;8:255-262.

[15] Rathbun BL, Shuler ML. Heat and mass-transfer effects in static solid-substrate fermentations - design of fermentation chambers. Biotechnology and Bioengineering 1983;25:929-938.

[16] Smits JP, van Sonsbeek HM, Tramper J, Knol W, Geelhoed W, Peeters M, Rinzema A. Modelling fungal solid-state fermentation: the role of inactivation kinetics. Bioprocess Engineering 1999;20:391-404.

[17] Mitchell DA, Krieger N, Stuart DM, Pandey A. New developments in solid state fermentation II. Rational approaches to design, operation and scale-up of bioreactors. Process Biochemistry 2000;35:1211-1225

Figure 1.1 Solid state fermentation as particulate bioprocessing (*Adapted from [8]*)

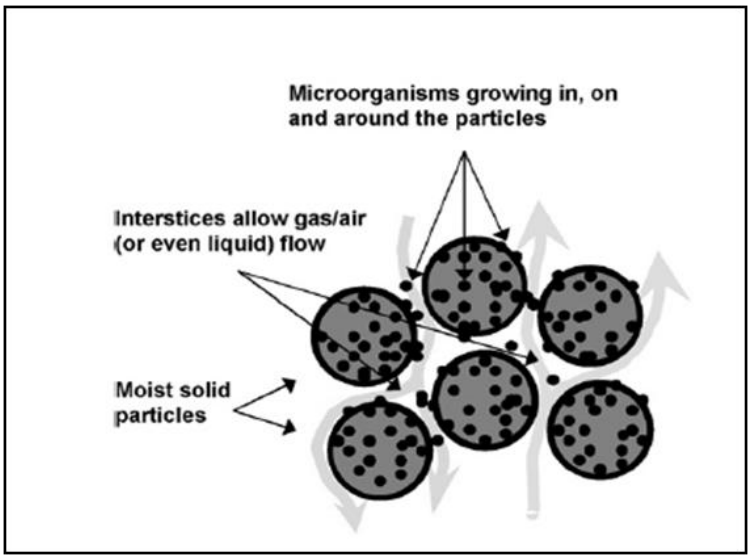

Figure 1.2 Phenomena occurring in bioreactor witnessing fungal growth (*Adapted from [17]*)

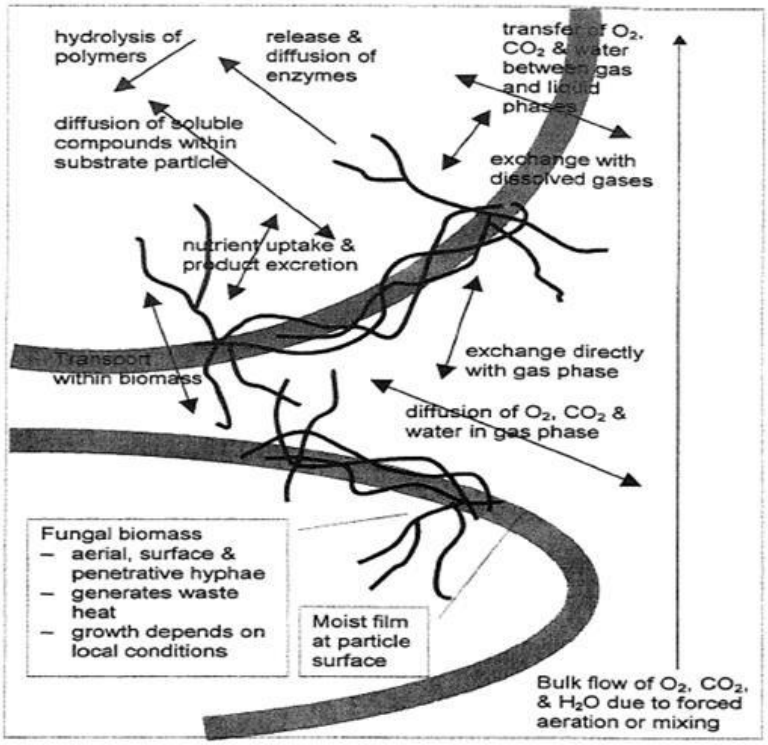

Figure 1.3 Macro-scale phenomena of heat and mass transfer in a deep bed bioreactor (*Adapted from [17]*)

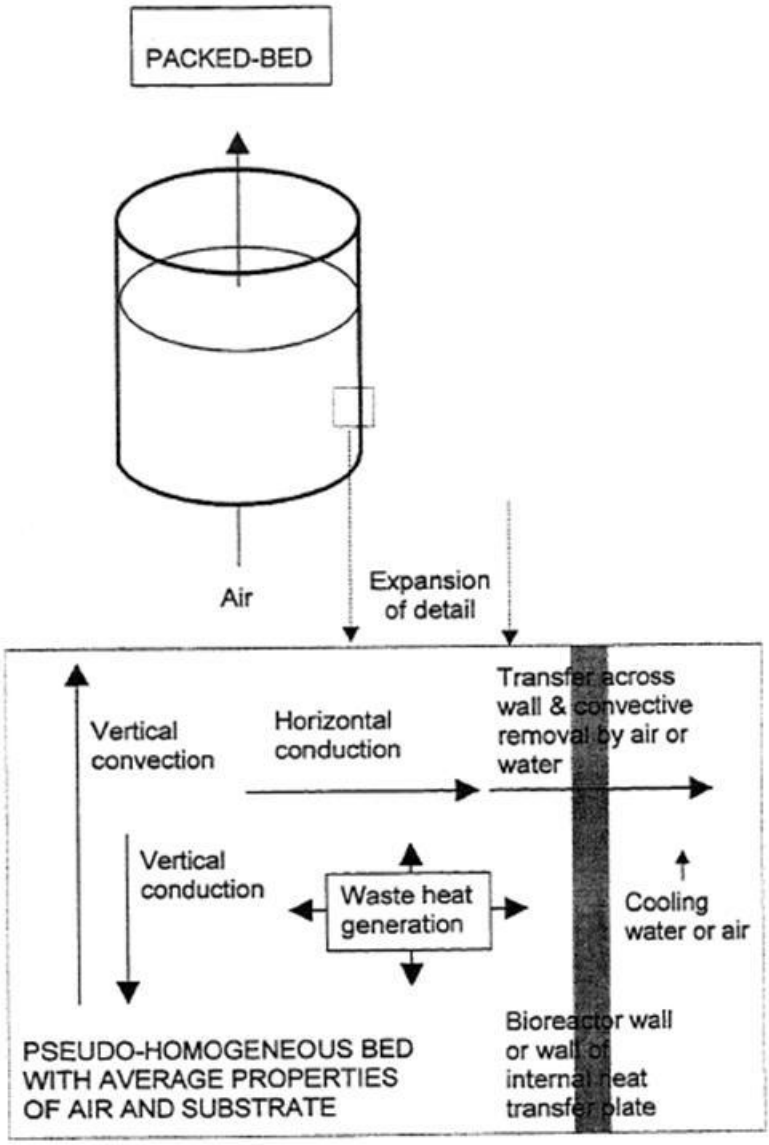

Chapter 2 - Production of a Cellulolytic Enzyme System in Mixed-Culture Solid-State Fermentation of Soybean Hulls Supplemented with Wheat Bran[1]

Abstract

Solid-state fermentation of soybean hulls supplemented with wheat bran using a co-culture of *Trichoderma reesei* and *Aspergillus oryzae* was performed. Three parameters— initial moisture content, incubation temperature, and initial pH— were optimized in culture flasks using response surface methodology. Parameter optimization was carried out with respect to filter paper activity and β-glucosidase activity in the culture. Temperature of 30 °C, pH of 5, and moisture content of 70% were found to be optimum. Optimized parameters were used for laboratory scale-up in static tray fermenters. The maximum filter paper activity of 10.7 FPU/g-ds and β-glucosidase of 10.7 IU/g-ds were obtained after 96 hour incubation period in static tray fermenters in agreement with optimized activities at shake flask level. The results of static tray fermentation also highlighted the importance of mixed culture fermentation. Both enzyme activities and volumetric productivities of enzyme produced were significantly higher in mixed culture fermentation as compared to mono culture static tray fermentation. Expression profile of cellulase system was characterized using SDS-PAGE. The SDS PAGE pattern of cellulase system indicated the presence of all the five major activities corresponding to β-glucosidase, CBH I, CBH II, EG I and xylanase. Enzyme broth was centrifuged and concentrated in an ultrafiltration cell. The concentrate was used for enzymatic saccharification of pretreated wheat straw and the potential of an indigenously developed enzyme concoction was reported in terms of saccharification efficiency. Pretreatment using both acid and alkali was carried out, and

[1] This Chapter is accepted as Brijwani et al. (2010) /Process Biochemistry, 45 (1), 120-128.

differences in sugar yield due to differences in composition as a result of pretreatment were reported. Results showed that alkali treatment generated higher sugars as compared to acid pretreatment. This was due to lignin removal and concentration of the cellulosic fraction. Present work showed that solid-state fermentation in a static tray bioreactor is a valuable technique for producing a system of enzymes with balanced activities that can efficiently saccharify lignocellulosic biomass like wheat straw.

Key words: response surface methodology, *Trichoderma reesei*, *Aspergillus oryzae*, mixed culture, SDS-PAGE, acid and alkali pretreatment

1. Introduction

A cellulolytic enzyme system is a complex system of enzymes composed of endoglucanase (endo-1, 4-β-D--glucanase, EC 3.2.1.4), exoglucanase (1,4-β-D-glucan-cellobiohydrolase, EC 3.2.1.91), and β-glucosidase (β-D-glucoside glucanohydrolase, cellobiase, EC 3.2.1.21) that acts synergistically to degrade cellulosic substrate [1,2]. Cellulolytic enzymes are central to biomass processing for production of fuel ethanol and bioproducts. High cost of these enzymes, however, presents a significant barrier to commercialization of ethanol and chemicals. Due to the heterogeneity and complexity of lignocelluosic biomass, bioconversion requires multiple enzyme activities. An efficient and cost-effective enzyme system should contain balanced activities of cellulases (both endo- and exo-glucanse), β-glucosidase, and xylanase, and such a system should also have high titer of these activities to offset the cost of ethanol production. Solid-state fermentation (SSF) presents many advantages including high volumetric productivity and relatively high concentration of the enzymes produced. Also, it will involve a lower capital investment and lower operating cost [3].

Another important feature of SSF is that it utilizes heterogeneous products of agriculture (mainly agricultural residues) and by-products of agro-based industries [4]. In solid-state fermentation of cellulase production, cellulosic substrate acts as both the carbon source and as an inducer for cellulase production [3]. Both bacteria and fungi can use cellulose as a primary carbon source. Most bacteria, however, are incapable of degrading crystalline cellulose since their cellulase systems are incomplete. On the other hand, cellulolytic enzymes produced by some fungi generally involve all three types of enzymes, so are very useful in the saccharification of renewable pretreated lignocellulosic materials. Fungal strains that produce cellulases are mainly comprised of *Trichoderma, Aspergillus*, *Penicillium*, and *Fusarium* genera. *Trichoderma reesei* is the most widely employed fungus for production of cellulolytic enzymes and has been extensively studied [5]. Strains of *Trichoderma* can accumulate high activities of endo and exo-glucanase, but are poor in β-glucosidase [6], whereas the strains of *Aspergillus* are high in β- glucosidase activity [7]. Cellulolytic fungus *Trichoderma reesei* has been widely investigated for its cellulase production from various cellulosic materials such as wood [8], wheat bran [9], and wheat straw [10]. Use of soybean hulls supplemented with wheat bran in a co-culture fermentation using *T. reesei* and *A. oryzae* has not been investigated so far. Soybean hulls and wheat bran are by-products of the soybean and wheat processing industry and are commonly available in the state of Kansas, USA, and thus have potential as industrial fermentation substrates. Soybean hulls have a rich cellulosic composition containing 40-45% cellulose and 30-35% xylan on a dry basis. Wheat bran is a good source of nitrogen and has been used for the production of cellulases with sugar cane bagasse as solid media [11].

The static tray bioreactor, also known as a koji bioreactor, is the commonly used bioreactor for SSF. In a tray bioreactor, the substrate is placed in trays and incubated in a

controlled-atmosphere room or chamber [12]. Several factors are responsible for limiting the growth of microorganisms. Operating conditions like temperature, pH, and moisture content are very important for microbial growth and efficient cellulolytic enzyme system production during solid-state fermentation [13]. Also, successful scale-up strategy demands optimization of critical parameters that influence microbial growth and product formation. Often optimization of multiple parameters is an arduous and time consuming task. Response surface methodology (RSM) can be used to evaluate the significance of several factors especially when interactions exist among factors and are complex to determine [14]. In addition the whole process can be completed in a reasonable time scale.

In this context, the aim of the present work was to demonstrate efficacy of solid-state fermentation systems, like a static tray bioreactor employing mixed cultures of *T. reesei* and *A. oryzae* with soybean hulls and wheat bran as solid media under optimal process conditions in production of balanced and low-cost celluloytic enzyme systems that can efficiently hydrolyze lignocellulosic biomass for bioethanol and bioenergy.

2. Materials and methods

Soybean hulls and wheat bran were obtained from Archer Daniels Midland, Salina, Kan. Both substrates were ground in a laboratory mill and sieved, using a Ro-Tap sieve sifter (Laval Lab Inc., Canada), to particle-size fractions of 500-1000 μm for use as substrate for fermentation. All dehydrated media were procured from Difco, BBL, USA, and the analytical grade chemicals were procured from Fisher Scientific, USA.

2.1. Microorganisms and their propagation

Trichoderma reesei (ATCC 26921) and *Aspergillus oryzae* (ATCC 12892) were obtained from American Type Culture Collection (ATCC), Virginia, USA, in lyophilized form. *T. reesei*

(ATCC 26921) is a mutant of QM 9123 (ATCC 24449) also referred as QM 9124. It produces 1.5-2.0 times more cellulase on cellulose medium than QM 9123 (ATCC 24449). *A. oryzae* (ATCC 12892) is an Aspergillus strain isolated from moldy bran. A portion of cultures from lyophilized vials was transferred aseptically to 150-ml Erlenmeyer flasks containing 50-ml sterilized potato dextrose broth (PDB) in a P-II biosafety cabinet (Labconco, USA); the flasks were incubated at 30 °C in an incubator shaker (Innova 4000) at 100 rpm for 48 h. Inoculum of 10 ml for both the organisms from each of the prepared flasks was transferred to 250-ml Erlenmeyer flasks containing sterilized 100 ml PDB supplemented with 0.1 ml Tween -80. The flasks were incubated at 30 °C for five to six days under static conditions until a mycelial mat was observed. To prepare the spore suspension, fungal cells from the above medium were cultured on PDB agar plates for five days to attain high density of conidia. Spores were collected from the plates by gentle washing with Mandels media [15] to obtain spore suspension of 10^7 spores/ml. Spore suspension was stored at 4 °C until used.

2.2. Cellulolytic enzyme system production in flasks

Soybean hulls and wheat bran were mixed in a 4:1 ratio. In our initial studies, we noticed that a ratio of 4:1 was ideal to have a balanced proportion of cellulase and β- glucosidase (unpublished data). We also observed that a 96 hour incubation period is ideal, as beyond 96 hours there was no appreciable increase in enzyme activities. Five grams of mixed substrate were adjusted to different moisture contents using Mandels media [15] at a particular pH. The initial pH of Mandels media corresponding to different runs in RSM was adjusted using either 2.5 M sodium hydroxide or 2.5 M hydrochloric acid. Contents were sterilized at 121°C for 30 minutes at 15 psi before inoculation with the fungal inoculum. All flasks for RSM experiments were inoculated with 10% (v/v) of 1:1 *T. reesei* and *A. oryzae* spore suspension containing 10^7 spores/

ml. Since moisture content was one of the parameters used for optimization, moisture from the inoculum was considered during moisture adjustments. Moisture measurements were carried out using a Denver Infrared Moisture Analyzer, Model IR35 (Fisher Scientific, USA). The ratio of cultures in the inoculum was maintained at 1:1 since we found that the equal ratio of two cultures is conducive for balanced production of a cellulolytic enzyme system (unpublished data) and similar observations can be noticed elsewhere [16].

2.3. Experimental design and optimization

Evaluation and optimization of fermentation parameters were carried out using RSM. A three-factor and two-level central composite rotatable design (CCRD), consisting of 20 experimental runs for both cellulase and β-glucosidase, was employed. For cellulase, filter paper units were used for optimization of parameters. Because the hydrolysis of lignocellulosic biomass is due to synergistic action of endo- and exo-glucanase, they are collectively referred to as filter paper units [17] and are considered as a good indicator of balanced production of endo- and exo-glucanse. The design consisted of 2^3 CCD factorial points having six replicates at the central point and six axial points (α). The design space consisted of three independent variables: temperature (X1, °C), initial pH (X2), and moisture content (X3, %). Response variables were cellulase activity (Y1, FPU/g) and β-glucosidase activity (Y2, IU/g). The temperature varied between 21.59 and 38.41°C; pH varied between 3.66 and 5.34; and moisture content varied between 44.89 and 70.11%. Actual values and corresponding values of three independent variables, X1, X2, and X3, are given in Table 2.2. Cellulase and β-glucosidase activity for all 20 runs was analyzed in duplicate and the average of the measurements is shown in Table 2.3.

Experimental data from the CCD was analyzed using RSM algorithm Design Expert 7.1 (Stat-ease, Minn. USA) and fitted according to Eq. (1) as a second-order polynomial equation including main effects and interaction effects for each variable:

$$y = \beta_o + \sum_{i=1}^{3} \beta_i x_i + \sum_{i=1}^{3} \beta_{ii} x_i^2 + \sum_{i=1}^{2} \sum_{j=i+1}^{3} \beta_{ij} x_i x_j \qquad (1)$$

where, y = predicted response, β_o = constant coefficient, β_i= linear coefficient, β_{ii}= quadratic coefficient, and β_{ij}= interaction coefficient.

Analysis of variance (ANOVA) and contour plots were generated using Design Expert 7.1. Optimized values of three independent variables for maximum activities were determined using a numerical optimization package of Design Expert 7.1. Numerical optimization searches the design space using a fitted model to find the optimized values of independent variables that maximize cellulase and β-glucosidase activities.

2.4. Cellulolytic enzyme system production in static tray bioreactor

Soybean hulls and wheat bran in a 4:1 ratio were adjusted to optimized initial moisture and pH, and sterilized at 121 °C for 15 minutes at 15 psi. Sterilized substrate of about 100 g was inoculated with *T.reesei* and *A. oryzae* spore suspension (10^7 spores/ml) in the ratio of 1:1, then aseptically spread in a tray to achieve a depth of approximately 1 cm. Trays were incubated in controlled chamber maintained at an optimized temperature of 30 °C and 90-95% relative humidity by blowing sterile, humidified air. Experiments were carried with two replicates for each incubation time. Trays were harvested for different incubation periods, and enzymes were extracted from the trays. Crude enzyme filtrate from the cultured trays was prepared by the addition of 600 ml of citrate buffer (50mM, pH 5) to the contents of each tray and shaking the contents at 150 rpm for 30 minutes. Enzyme broth was filtered using coarse filter paper (Fisher

Scientific, P-8 coarse grade) and filtrate obtained was centrifuged at 10,000g for 15 minutes at 4^0C (Sorvall RC-2B, Thermo Scientific, USA). Crude enzyme extract obtained was analyzed for various enzyme activities. Crude extract from the 96 hour fermentation was concentrated in an ultrafiltration cell (Amicon Stirred Cell model no. 8400, Millipore Inc., USA) using a 30 KDa cut-off membrane (Biomax, Millipore Inc., USA). Crude extract was immediately used for SDS-PAGE and enzymatic saccharification of dilute-acid and alkali-pretreated wheat straw.

2.5. Enzymatic saccharification of acid- and alkali-pretreated wheat straw

Wheat straw of particle size less than 1mm was suspended in a dilute sulfuric solution of 2% (w/v) for acid pretreatment or dilute sodium hydroxide solution of 1 % (w/v) strength for alkali pretreatment to achieve solid loading of 10% on a dry basis. Pressure cooking was carried out in a vertical sterilizer for 30 minutes at 121°C at 15 psi. Following treatment, the liquor was separated from the residual solid mass. The solid mass was washed several times with distilled water to achieve a pH of 4.8-5. The solid residue was dried overnight at 50 °C for compositional analysis and enzymatic hydrolysis.

2.5.1. Enzymatic saccharification

Concentrated crude enzyme extract was used for enzymatic saccharification. In particular, acid- or alkali-treated wheat straw from the above process was suspended in a sodium citrate buffer pH 5.0 to achieve 5% solid loading. Crude and concentrated enzyme extract was added to the above slurry at the rate of 15 filter paper units per gram of dry solids to initiate saccharification. Saccharification was carried in a water bath shaker at 150 RPM and maintained at 50°C. Aliquots for sugar analysis were collected at 24, 48, 72, and 96 hours, respectively. Aliquots were analyzed for glucose, xylose, and arabinose as major sugars using a Phenomenex

RPM monosaccharide column (300 x 7.8 mm; Phenomenex, Calif.) in a Shimadzu CBM-20A HPLC system connected to a Shimadzu RID-10A refractive index detecter.

2.6. Analytical methods

2.6.1. Compositional analysis

The lignocellulosic composition of soybean hulls and wheat bran was determined using an ANKOM 200 Fiber Analyzer (ANKOM Technology, USA). Neutral detergent fiber (NDF), acid detergent fiber (ADF), and acid detergent lignin (ADL) were analyzed per procedure specified by the manufacturer (www.ankom.com). The values of ADF, NDF, and ADL were used to obtain cellulose, hemicellulose, and lignin content of soybean hulls and wheat bran. Protein content (N x 6.25) was determined by the kjeldahl method after digestion and distillation using an autoanalyser from Leco, FP-2000. Moisture and ash content of soybean hulls and wheat bran were measured using a forced-draft oven and muffle furnace from Fisher Scientific, USA. Lignocellulosic composition of untreated, acid-treated and alkali-treated wheat straw (wheat straw (PS< 1000 µm) was measured per the protocol NREL/TP-510-42618 (www.nrel.gov/biomass/pdfs/42618). All measurements were carried out in triplicate and were reported as mean with corresponding standard deviation.

2.6.2. Enzyme assay

Crude cellulases from the cultured media were extracted by an addition of 50 ml of citrate buffer (50mM, pH 5) to each flask and shaking the contents at 150 rpm for 30 minutes. Contents were filtered using coarse filter paper (Fisher Scientific, P-8 coarse grade) and filtrate obtained was centrifuged at 10,000g for 15 minutes at 4^0C (Sorvall RC-6, Thermo Scientific, USA). The supernatant was analyzed for cellulase and β-glucosidase activity. Cellulase activity was reported in filter paper units per g of dry substrate (FPU/g) using Ghose methodology [18].

β-glucosidase activity was determined using 5 mM, 4-Nitrophenyl β-D- glucopyranoside (pNPG) and the reaction was stopped by using cold 1% sodium carbonate per Kubicek's method [19] and reported as IU (International Units)/g dry substrate. Endoglucanase activity was determined according to Ghose [18] using 1% carboxymethyl cellulose in a pH 5 sodium citrate buffer. Xylanase activity was measured by the method of Bailey et al. [20] using oat spelt xylan. One unit of enzyme was defined as the amount of enzyme required to release 1 µmol of product (glucose equivalents for FPU and CMC, p-nitrophenol for β-glucosidase, and xylose for xylanase) from the appropriate substrates per minute under assay conditions. All colorimetric observations were recorded using the multiprocessor-based UV-Vis Spectrophotometer (UV-1650 PC, Shimadzu , Japan).

2.6.3. SDS-PAGE for expression profile of cellulolytic enzyme system

SDS PAGE of crude enzyme was carried out in a bio-rad mini Protean gel electrophoresis system (Bio-Rad Laboratories, Inc., USA), according to the procedure of Laemmli [21]. Along with crude enzyme concentrate, the three commercial enzymes, Celluclast 1.5L (Sigma, USA), Novozym 188 (Sigma, USA), and commercial xylanase from *A. niger*, a kind gift from Novozymes Inc., USA, were also analyzed and compared with the crude enzyme concentrate. Briefly, samples were diluted to 1 mg/ml protein and mixed with an equal volume of sample buffer [10mM tris HCl, pH 8, containing 1mM EDTA, 2.5% (w/v) SDS, 5% (w/v) 2-mercaptoethanol and traces of bromphenol blue] and boiled for 10 minutes. Electrophoresis was conducted with 10% separating gel and a 4% stacking gel. The gel was run at ambient temperature and a constant 200V power supply. Upon completion of electrophoresis, the bands were analyzed by developing a zymogram. The gel was washed with distilled water and stained with coomassie blue. It was destained for a couple of hours using a destaining buffer comprising

of 45% glacial acetic acid and 55% methanol. Bands appeared as clear dark zones against white background.

3. Results and discussion

3.1. Cellulosic composition of soybean hulls and wheat bran for production of cellulolytic enzymes

The chemical composition of soybean hulls and wheat bran is presented in Table 2.1. Half of the chemical composition of soybean hulls is cellulose and hemicelluloses. Notably higher cellulosic composition is ideal for good growth of fungal cultures and cellulase production. An important requirement in solid-state fermentation is the ratio between carbon and nitrogen (C: N). The ratio of C/N is most crucial for a particular process to obtain specific product [22]. Wheat bran is a good source of nitrogen, due to the protein content, and when added to soybean hulls improves the C/N, presenting ideal conditions for fungal growth and cellulase production. Moreover, it is also a good source of hemicellulose (Table 2.1) rich in arabinans [23], thus contributing a good source of soluble sugar like arabinose apart from xylose and glucose. Also, hemicellulose as a whole is also a good inducer of cellulolytic enzyme system [24]. In our current study, we noticed that supplementation of one part of wheat bran with four parts of soybean hulls was conducive for higher cellulase and β-glucosidase activities (unpublished data) in the mixed-culture solid-state fermentation using *T. reesei* and *A. oryzae* cultures of soybean hulls. A similar study by Camassola and Dillon [11] on mixed-culture fermentation of sugar cane bagasse supplemented with wheat bran strengthened our argument of wheat bran addition. Addition of Mandels media provided a basal salt medium for fungal growth and cellulase production.

3.2. Optimization of process parameters for cellulase and β-glucosidase production at flask level

Optimization of process parameters temperature, moisture, and pH to maximize cellulolytic enzyme system production in mixed-culture fermentation was carried out using response surface methodology. As cellulase and β-glucosidase are the lead activities needed for efficient hydrolysis of lignocellulosic biomass, optimization was carried out with respect to cellulase and β-glucosidase. Notably, not only is their high titer important for improved hydrolysis but the balance of two activities is essential as well. It has often been suggested in the literature that a ratio of 1:1 cellulase and β-glucosidase is recommended for efficient biomass hydrolysis by enzymes [25,26]. Thus for the present optimization work, filter paper activity (representing complete cellulase enzyme, as discussed above) and β-glucosidase activity were used as indicator activities for optimization of process parameters for improved production of a cellulolytic enzyme system.

Experimental results as a function of temperature, pH, and moisture content for both cellulase as measured in filter paper units and β-glucosidase are shown in Table 2.3. Maximum cellulase activity (10.55 FPU/g of dry substrate) was observed at pH 4.5, moisture content of 70%, and temperature of 30°C. For β-glucosidase activity (IU/g), maximum response (8.13 IU/g of dry substrate) occurred at 70% moisture content at a pH of 4.5 and incubation temperature of 30°C. The overall second-order polynomial equation for cellulase activity as measured in terms of FPU (filter paper units)/g dry substrate was

$$Y = 7.95 + 0.76X_1 + 0.34X_2 + 2.97X_3 + 0.21X_1X_2 + 0.82X_1X_3 – 0.026X_2X_3 – 2.56X_1^2 - 0.40X_2^2 – 1.10X_3^2$$

β-glucosidase data was fitted to a quadratic model as well with the following equation:

$$Y = 4.90 + 0.25X_1 - 0.33X_2 + 1.73X_3 + 0.69X_1X_2 + 1.03X_1X_3 + 0.42X_2X_3 - 1.32X_1^2 - 0.24X_2^2 - 0.41X_3^2$$

The ANOVA of the fitted quadratic model is shown in Table 2.4. The lower p-value and insignificant lack of fit suggests the good fit of the quadratic model. A higher coefficient of regression suggests that there was good agreement between predicted and estimated cellulase activity under different conditions of temperature, pH, and moisture content. Surface plots for both total cellulase (FPU/g) and β-glucosidase were made as a function of temperature and pH, moisture content and temperature, and pH and moisture content (Figures 2.1 and 2.2). The plots had elliptical contours enclosing the region of maximum activity within the experimental range investigated. Plots of moisture and temperature at constant pH showed significant effects of moisture, temperature, and their interaction. As temperature and moisture were changed from their optimum values, both filter paper and β-glucosidase activity decreased significantly. The Maximum filter paper and β-glucosidase activity occurred in the vicinity of 30 °C and 70% moisture (Figures 2.1a and 2.2a). Importantly, but in accord with our expectation, it was observed that changes in pH had little effect on filter paper and β-glucosidase activity within the experimental range. From surface plots 2.1b and 2.2b, it could be envisaged that temperature had more influence on cellulase and β-glucosidase production than pH when moisture was held constant. A similar observation can be made from plots 2.1c and 2.2c where moisture showed a more profound effect on the levels of cellulase and β-glucosidase production than initial pH at constant temperature. Robustness against changes in pH from its initial value during enzyme production would be beneficial in shielding any effect on enzyme activities due to varying pH during production. In other words, total cellulase and β-glucosidase from mixed-culture solid-

state fermentation of *T. reesei* and *A. oryzae* could be simultaneously maintained at higher levels by providing appropriate conditions of temperature, moisture and optimum initial pH.

Using Design Expert 7.1, numerical optimization subroutine design space was explored with a fitted quadratic model to arrive at optimum temperature, moisture, and pH conditions. The optimized variables were found using a desirability objective function that assigns relative importance to the responses. Solutions with higher desirability gave an optimum temperature of 30 °C, pH of 5, and moisture content of 70%. Further, with optimized conditions, the cellulase (10.55 FPU/g) to β-glucosidase (8.13 IU/g) ratio of 1:0.8 was achieved, which is close to the recommended 1;1. Based on the above analysis, temperature of 30 °C, pH of 5, and moisture content of 70% were selected as operational parameters for the production of a cellulolytic enzyme system in a static tray bioreactor.

3.3. Production of cellulolytic enzyme system in static tray bioreactor

Kinetics of a cellulolytic enzyme system production during mixed-culture solid-state fermentation of soybean hulls and wheat bran in a static tray bioreactor are shown in Figure 2.3. Trends for total cellulase activity as measured in filter paper units, β-glucosidase activity, endocellulase activity, and xylanase activity, were in a similar pattern and showed increase in levels with an increase in incubation period. Enzymatic activities increased significantly until 96 hours and reached a plateau thereafter. There was no significant difference between 96-hour and 120-hour growth periods for all reported activities. Maximum filter paper activity was 10.7 FPU/g-ds, maximum β-glucosidase was 10.7 IU/g-ds, maximum endoglucanase reached 108 IU/g-ds, and maximum xylanase reached 505 IU/g-ds. Both maximum filter activity and β-glucosidase activity were in accord with activities as optimized at shake flask level. The 96-hour incubation seemed to be the optimal incubation period as we have discussed and observed

previously. This is also in agreement with observations made elsewhere [11,27]. Notably the most significant feature of fermentation in a static tray bioreactor was that total cellulase activity (FPU units) and β-glucosidase activity reached a 1:1 ratio after 96 hours of incubation, the desired ratio for efficient biomass hydrolysis. Another interesting feature of mixed-culture fermentation was higher levels of xylanase production. Xylanase activity, as measured using oat spelt xylan, was essentially endoxylanase activity. The xylanase activity might also have been induced by the presence of cellulose, though both of the substrates (soybean hulls and wheat bran) had appreciable xylan (hemicelluloses) content. According to Olsson et al. [28], *T. reesei* produces high levels of endoxylanase when grown in cellulose; and also as per Aro et al. [29], the presence of cellulose induces not only cellulose production but also xylanases, because a cellulase regulator, ACEII, also influences xylanase regulation. The production of xylanases sometimes can be viewed as a favorable aspect of SSF because side activities like xylanase can be very helpful during complete biomass hydrolysis that has appreciable levels of xylan content, for instance wheat straw. As we shall see later good xylanase activity comes in handy when hydrolyzing alkali-treated wheat straw.

As we commented earlier, we noticed that *T. reesei* and *A. oryzae* when grown as a 1:1 mixed culture performed better than mono cultures at flask level. A particular observation, in line with the literature studies, was that *T. reesei* was a poor producer of essential enzyme β-glucosidase and the deficit of β-glucosidase was overcome when *T. reesei* was co-cultured with *A. oryzae*. We were also interested in the trend in a static tray bioreactor and to satisfy our curiosity, we harvested trays after 96-hour incubation that were inoculated with 10% culture of *T. reesei* and *A. oryzae* separately. All other conditions were maintained the same as the mixed culture trays. The results are presented in Table 2.5, where activities of various enzymes and

volumetric productivity in mixed-culture trays and mono-culture trays after 96 hours of incubation period are featured. Appreciably, we noticed the expected outcome. It was confirmed that lower β-glucosidase activity in *T. reesei* cultures was boosted by co-cultering it with *A. oryzae*. We also observed that *A. oryzae* is a good producer of β-glucosidase activity, and in fact, most of the *Aspergillus* spp produced higher amounts of β-glucosidase activity [7,27,13]. Volumetric productivity of different enzyme activities were calculated taking into account the initial moisture content of solid media, enzyme activity of the broth and initial solid content. Volumetric productivities also followed a similar trend as that of enzymatic activities. Volumetric productivity for enzyme activities in a mixed culture after 96 hours of incubation was significantly higher than volumetric productivity of enzyme activities in a mono culture. Again volumetric productivity of β-glucosidase enzyme in *A. oryzae* was significantly greater than volumetric productivity of β-glucosidase in *T. reesei*. Interestingly, there was no significant difference in the activity of xylanase and its volumetric productivity between mono and mixed cultures. The results presented here have demonstrated that with proper optimization of operational parameters exploiting the symbiotic association of fungal cultures, solid-state fermentation can be a valuable technology to produce a cellulolytic enzyme system not only with higher titers but also with balanced enzyme activities.

3.4. SDS PAGE profiles of a cellulolytic enzyme system produced in a static tray bioreactor

SDS-PAGE profile provides the fingerprint of different activities present in the concoction. For the current work it seems valuable in describing the pattern of cellulolytic enzyme system as a whole and in particular it corroborates the activity analysis carried out earlier. Figure 2.4 represents the profile of a crude enzyme concentrate of 96-hour fermentation in static tray bioreactor with other commercial enzymes. The crude enzyme concentrate had five

bands typically in the range of 40-80 KDa. Comprehensive work in the literature with both commercial and crude enzymes from *Trichoderma and Aspergillus spp [30,31]* suggest presence of 80 KDa protein indicates β-glucosidase; 68 KDa protein represents cellobiohydrolase I (CBH I); 58 KDa protein indicates cellobiohydrolase II (CBH II); and 55 KDa protein suffice endocellulase (EG I). SDS PAGE profile of cellulolytic enzyme system showed the presence of all the four bands (Figure 2.4) in agreement with the activities analyzed against standard substrates. Presence of 80 KDa β-glucosidase is further supported by lane B containing commercial β-glucosidase from *A. niger* that has a prominent band of 80 KDa molecular weight. Though both mono cultures of *T. reesei* and *A. oryzae* produced total cellulase (measured in filter paper units) and endocellulase, it was difficult to identify the contribution of each culture during mixed-culture fermentation in production of CBH I, CBH II and EG I. Nevertheless, mixed culture had significantly higher activities than mono cultures. Analysis on the presence of CBH I, CBH II, and EG I is further supported by looking at the bands of commercial cellulase Celluclast 1.5L that has a prominent band of 58 KDa (CBH II) probably diffused with CBH I (68 KDa) and 55 KDa (EG I). Similar observations for these commercial enzymes can be found elsewhere [31]. The last band, five, appears to be of endoxylanase as confirmed from the prominent band in land D representing commercial xylanase from *A. niger*. The above results highlighted that a cellulolytic enzyme system produced in mixed-culture, solid-state fermentation of soybean hulls supplemented with wheat bran in a static tray bioreactor contained all useful enzyme activities in balanced proportion. Consequently, the enzyme system produced was complete and such a system is expected to efficiently hydrolyze lignocellulosic biomass into sugars for bioethanol and bioenergy. This application is demonstrated in a forthcoming section.

3.5. Enzymatic hydrolysis of acid and alkali treated wheat straw

Figure 2.5 shows the time course of sugar liberation during enzymatic hydrolysis of acid- and alkali-treated wheat straw. Sugar yields increased significantly up to 48 hours of enzymatic reaction and reached a plateau thereafter in both acid-and alkali-treated wheat straw. Alkali-treated wheat straw resulted in a significantly higher yield of about 0.3g sugars per gram of dry substrate as compared to 0.12g of sugar per gram of dry substrate in acid-treated wheat straw after 96 hours of incubation. Alkali-treated wheat straw had significantly higher sugar yields at all incubation periods as compared to acid-treated wheat straw. These differences were attributed to differences in lignocellulosic composition of acid- and alkali-treated wheat straw (Table 2.6). Alkali treatment resulted in a concentration of cellulosic sugars and most importantly removed a considerable amount of lignin that was rather preserved in acid treated wheat straw. Lignin seems to inhibit enzymatic hydrolysis by non-productive binding. This observation has been extensively studied in the literature [32-34]. Total sugars were broken into three corresponding major sugars: glucose, xylose, and arabinose; their yields are shown in Table 2.7. The above argument of lignin inhibition was supported by noticing the differences in glucose production in acid- and alkali-treated wheat straw. For almost the same glucan concentration in acid- and alkali-treated wheat straw (Tables 2.6 and 2.7) glucose yield was almost twice (0.28g/g or 28% conversion of glucan to glucose) that in alkali treated wheat straw as compared to acid-treated wheat straw (0.18g/g or 18% conversion of glucan to glucose). Further, both xylose and arabinose yields were significantly higher than the corresponding acid treatment, owing to the concentration of sugars and lignin removal in alkali-treated wheat straw. The xylose and arabinose yield was close to 0.75g/g in alkali-treated wheat straw, which is a 75% conversion of xylan and arabinan into corresponding sugars. The results suggest that mixed-fungal, solid-state fermentation utilizing soybean hulls supplemented with wheat bran in static tray bioreactor was

an efficient method to produce a cellulolytic enzyme system in an effort towards developing a complete concoction of enzymes in a single process that can efficiently hydrolyze lignocellulosic biomass for bioethanol and bioenergy.

Conclusions

The present study demonstrated for the first time the suitability of mixed-culture, solid-state fermentation in the production of an efficient cellulase enzymes complex from soybean hulls. Laboratory scale-up of mixed-culture, solid-state fermentation of soybean hulls supplemented with wheat bran using cultures of *T. reesei* and *A. oryzae* was conducted in a static tray bioreactor after prior optimization of operational parameters at flask level. Production in a static tray bioreactor with optimized process parameters showed that maximum activities were attained during 96 hours of growth and activities reached plateau thereafter. Maximum filter paper and β-glucosidase activities produced in a tray fermenter were in agreement with activities as optimized at shake flask level using response surface methodology and were present in the balanced proportion as desired. SDS expression profiles of various enzyme activities further validated the completeness of a cellulolytic enzyme system produced in a static tray bioreactor. Saccharification studies by indigenously produced crude enzyme concentrate demonstrated the potential of a cellulase enzyme complex in hydrolyzing pretreated wheat straw. Almost a 30% conversion of glucan to glucose and 75% conversion of xylan and arabinan, to corresponding xylose and arabinose, were reached during 96 hours of enzymatic hydrolysis. Differences in acid- and alkali-treated wheat straw were attributed to compositional disparities and lignin non-productive binding. The study highlighted that solid-state fermentation is a valuable technique for producing a system of enzymes with balanced activities that can efficiently saccharify lignocellulosic biomass like wheat straw. It eliminates the need of producing enzymes separately

and then blending them to form a concoction that adds cost. Also, this fermentation utilizes agro-industrial by-products and does not require elaborate downstream purification, thus minimizing the cost of enzyme production considerably. Further, the different side activities generated during SSF play a major role in hydrolysis of complex substrates like wheat straw. This would have positive repercussions on the economy of bioethanol production. Future studies are aimed at the scale-up operation of static tray bioreactors for cellulase production from soybean hulls, which should be helpful in faster commercialization of the process.

Acknowledgement

The authors wish to thank the Center for Sustainable Energy and Department of Grain Science and Industry, Kansas State University, for funding this project. Authors greatly acknowledge Dr. S Muthukrishnan, Department of Biochemistry, Kansas State University for helpful discussions on SDS-PAGE work regarding enzyme characterization. Author Harinder S. Oberoi acknowledges the Department of Biotechnology, Government of India, for fellowship support for his stay at Kansas State University. This article is contribution no 09-231-J from the Kansas Agricultural Experiment Station, Manhattan, KS 66506.

References

[1] Holker U, Hofer M, Lenz J. Biotechnological advantages of laboratory scale solid state fermentation with fungi. Appl Microbiol Biotechnol 2004;64:175-186.

[2] Esterbauer H, Steiner W, Labudova I, et al. Production of *Trichoderma* cellulase in laboratory and pilot scale. Bioresource Technol 1991;36:51-65.

[3] Cen P, Xia L. Production of cellulase in solid state ferementation. In: Scheper T, editor. Recent progress in bioconversion of lignocellulosics. Advances in Biochemical Engineering/Biotechnology. vol. 65. Berlin: Springer; 1999. p. 69.

[4] Raimbault M. General and microbiological aspects of solid substrate fermentation. Elect J Biotechnol 1998;27:498-503.

[5] Stockton BC, Mitchell DJ, Grohmann K, et al. Optimum β-D glucosidase supplementation of cellulase for efficient conversion of cellulose to glucose. Biotechnology Lett 1991;13:57-62.

[6] Duff SJB, Cooper DG, Fuller OM. Effect of media composition and growth conditions on production of cellulase and β-glucosidase by a mixed fungal fermentation. Enzyme Microbiol Technol 1987;9:47-52.

[7] Grajek W. Hyperproduction of thermostable beta-glucosidase by *Sporotrichum* (*Chrysosporium*) thermophile. Enzyme Microbiol Technol 1987;9:744-748.

[8] Reczey K, Szengyel Z, Eklund R, Zacchi G. Cellulase production by *T. reesei*. Biores Technol 1996;57:25-30.

[9] Smits JP, Rinzema A, Tramper J, van Sonsbeek HM, Knol W. Solid state fermentation of wheat bran by *Trichoderma reesei* QM 9414: substrate compositional changes, C balance, enzyme production, growth and kinetics. Appl Microbol Biotechnol 1996;46:489-96.

[10] Acebal C, Castillon MP, Estrada P, Mata I, Costa E, Aguada J, et al. Enhanced cellulase production from *Trichoderma reesei* QM 9414 on physically treated wheat straw. Appl Microbiol Biotechnol 1986;24:218-23.

[11] Camassola M, Dillon AJP. Production of cellulases and hemicellulases by *Penicillium echinulatum* grown on pretreated sugar cane bagasse and wheat bran in solid state fermentation. J Appl Microbiol 2007;103:2196-2204.

[12] Rathbun BL, Shuler ML. Heat and mass transfer effects in solid state fermentation: Design of fermentation chambers. Biotechnol Bioeng 1983;15:929-938.

[13] Wen Z, Liao W, Chen S. Production of cellulase/β-glucosidase by the mixed fungi culture *Trichoderma reesei* and *Aspergillus phoenicis* on dairy manure. Process Biochem 2005;40:3087-3094.

[14] Liu BL, Tzeng YM. Optimization of growth medium for the production of spores from *Bacillus thuringiensis* using response surface methodology. Bioprocess Biosystem Eng 1998;18:413-418.

[15] Mendels M, Weber J. The production of cellulases. Adv Chem Ser 1969;95:395-414.

[16] Gutierrez-Correa M, Portal L, Moreno P, Tengerdy RP. Mixed culture solid substrate fermentation of *Trichoderma reesei* with *Aspergillus niger* on sugar cane bagasse. Biores Technol 1999;68:173-178.

[17] Chahal DS. Production of *Trichoderma reesei* cellulase system with high hydrolytic potential by solid state fermentation, In: Leatham GF, editor. Enzymes in biomass conversion. ACS Symposium Series. vol. 460. Washington: American Chemical Society; 1991. p. 111-122.

[18] Ghose TK. Measurement of cellulase activities. Pure App Chem 1987;59:257-268.

[19] Kubicek, CP. Beta-glucosidase excretion in *Trichoderma* strains with different cell wall bound beta 1,3-glucanase activities. Can J Microbiol 1983;29:163-169.

[20] Bailey MJ, Biely P, Poutanen K. Interlaboratory testing of methods for assay of xylanase activity. J Biotechnol 1992;23:257-270.

[21] Laemmli UK. Cleavage of structural proteins during the assembly of head of bacteriophage T4. Nature 1970;227:680-685.

[22] Krishna C. Solid state fermentation systems: An overview. Crit Rev Biotechnol 2005;25:1-30.

[23] Lequart C, Nuzillard JM, Kurek B, Debeire P. Hydrolysis of wheat bran and straw by endoxylanase: production and structural characterization of cinnamoyl-oligosaccharides. Carbohydr res 1999;319:102-111.

[24] Babu KR, Satyanarayana T. Production of bacterial enzymes by solid state fermentation. J Sci Ind Res 1996;55:464-467.

[25] Chahal DS, McGuire S, Pikor H, Noble G. Production of cellulase complex by *Trichoderma reesei* RUT-C30 on lignocellulose and its hydrolytic potential. Biomass 1982;2:127-138.

[26] Mandels M, Medeiros JE, Andreotti RE, Bisset FH. Enzymatic hydrolysis of cellulose- effect of physicochemical properties of cellulose on adsorption and rate of hydrolysis. Biotechnol Bioeng 1981;23:2009-2026.

[27] Gutierrez-Coria M, Tengerdy RP. Production of cellulase on sugarcane bagasse by fungal mixed-culture solid-substrate fermentation. Biotech Lett 1997;19:665-667.

[28] Olsson L, Christensen TMIE, Hansen KP, Palmqvist EA. Influence of the carbon source on production of cellulases, hemicellulases and pectinases by *Trichoderma reesei* Rut C-30. Enzyme Microb Technol 2003;33:612–619.

[29] Aro N, Saloheimo A, Ilmen M, Penttila M. ACEII, a novel transcriptional activator involved in regulation of cellulase and xylanase genes of *Trichoderma reesei*. J Biol Chem 2001;276:24309–24314.

[30] Fiechter A, editor. The cellulase proteins of *Trichoderma reesei*: structure, multiplicity, mode of action and regulation of formation. Advances in Biochemical Engineering/Biotechnology. vol. 45. Berlin: Springer; 1992. p. 1.

[31] Kubicek-Pranz EM, Gsur A, Hayn M, Kubicek CP. Characterization of commercial *Trichoderma reesei* cellulase preparations by denaturing electrophoresis (SDS-PAGE) and immunostaining using monoclonal antibodies. Biotechnol Appl Biochem 1991;14:317-323.

[32] Sutcliffe R, Saddler JN. The role of lignin in the adsorption of cellulase during enzymatic treatment of lignocellulosic material. Biotechnol Bioeng Symp 1986;17:748-762.

[33] Palonen H, Tenkanen M, Linder M. Dynamic interaction of *Trichoderma reesei* cellobiohydrolases Cel6A and Cel7A and cellulose at equilibrium and during hydrolysis. Appl Environ Microbiol 1999;65:5229-5233.

[34] Palonen H, Tjerneld F, Zacchi G, Tenkanen M. Adsorption of *Trichoderma reesei* CBH I and EG II and their catalytic domains on steam pretreated softwood and isolated lignin. J. Biotechnol 2004;107:65-72.

Figure 2.1 Contour plots illustrating the effect of a) temperature and pH, b) moisture and temperature, and c) moisture and pH on cellulase activity measured as FPU (filter paper units)/g dry substrate.

a)

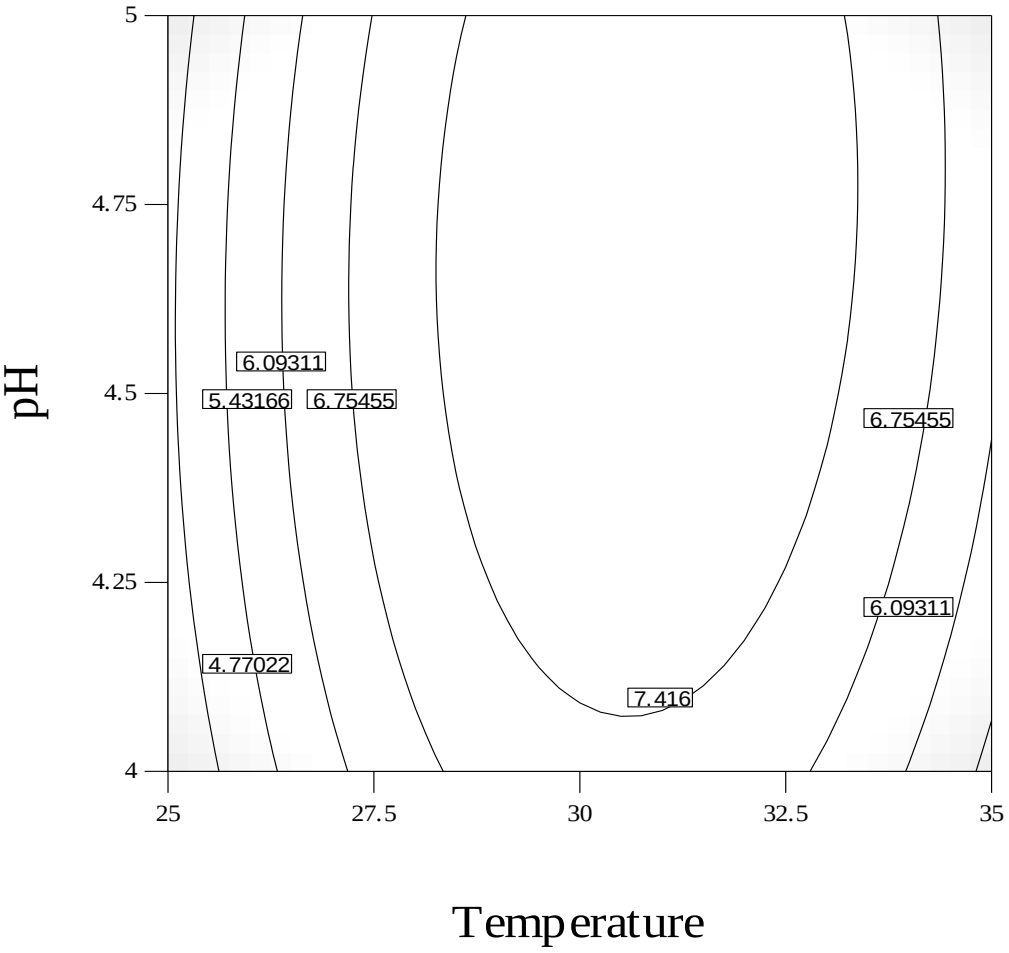

b)

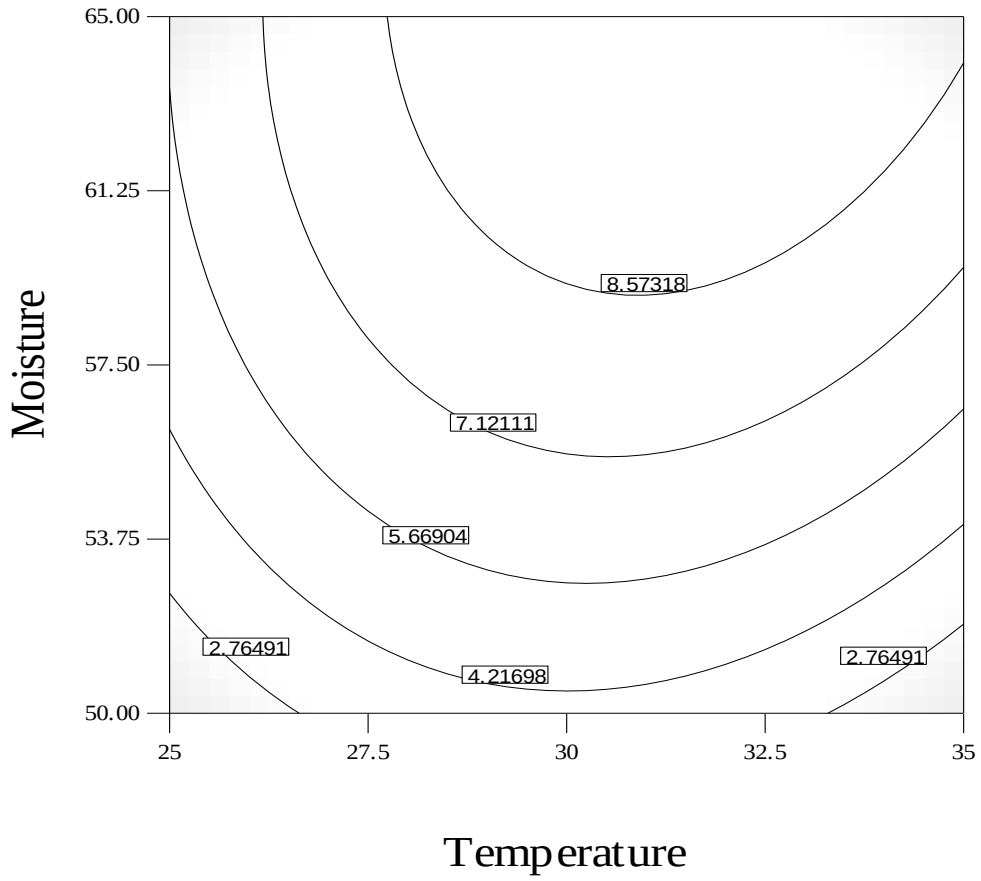
65.00
61.25
57.50
53.75
50.00
Moisture
25
27.5
30
32.5
35
Temperature
8.57318
7.12111
5.66904
4.21698
2.76491
2.76491

c)

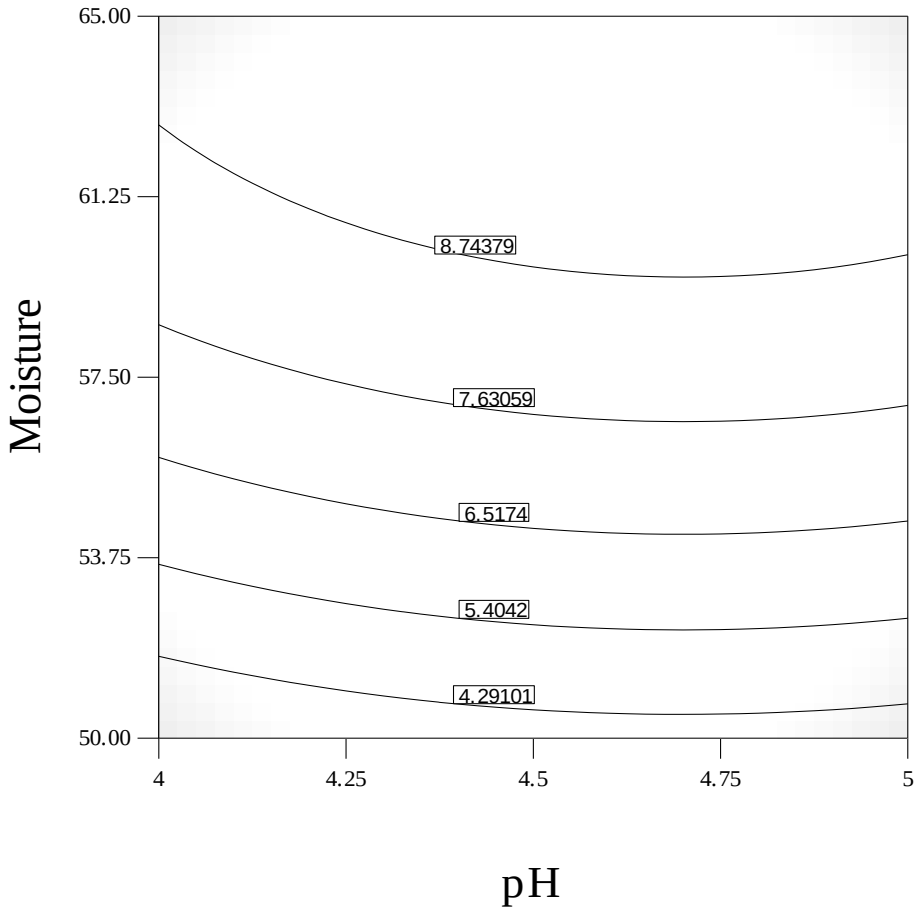
65.00
61.25
57.50
53.75
50.00
Moisture
8.74379
7.63059
6.5174
5.4042
4.29101
4
4.25
4.5
4.75
5
pH

Figure 2.2 Contour plots illustrating the effect of a) temperature and pH, b) moisture and temperature, and c) moisture and pH on β-glucosidase (B-G) activity measured as IU (International Units)/g dry substrate.

a)

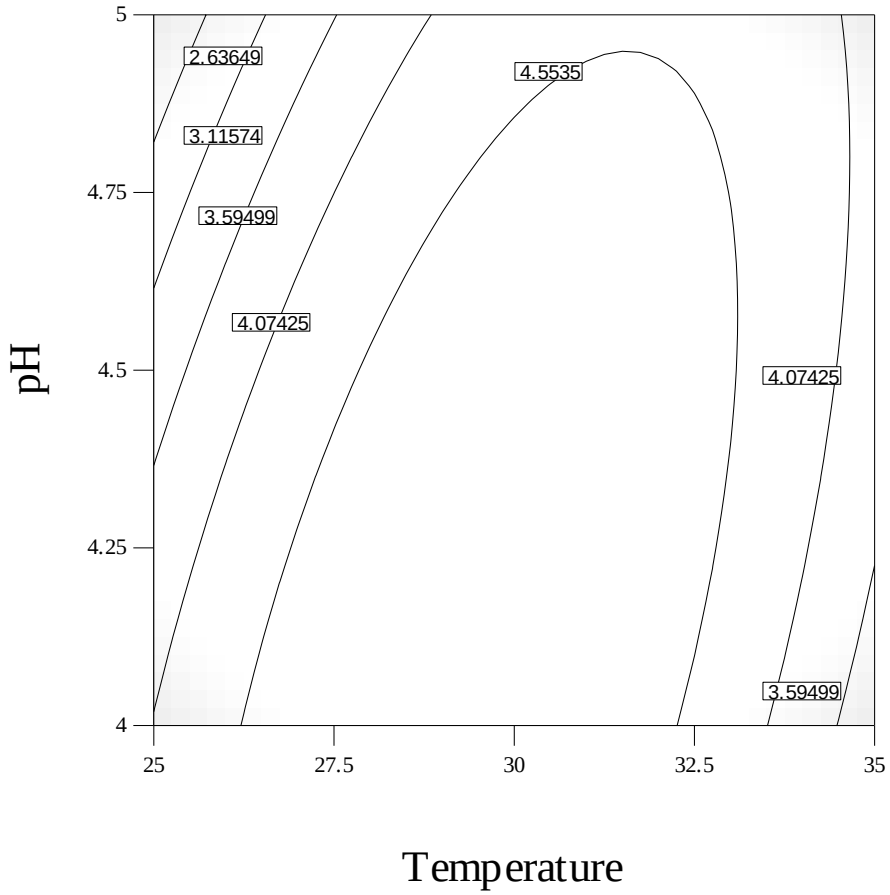

b)

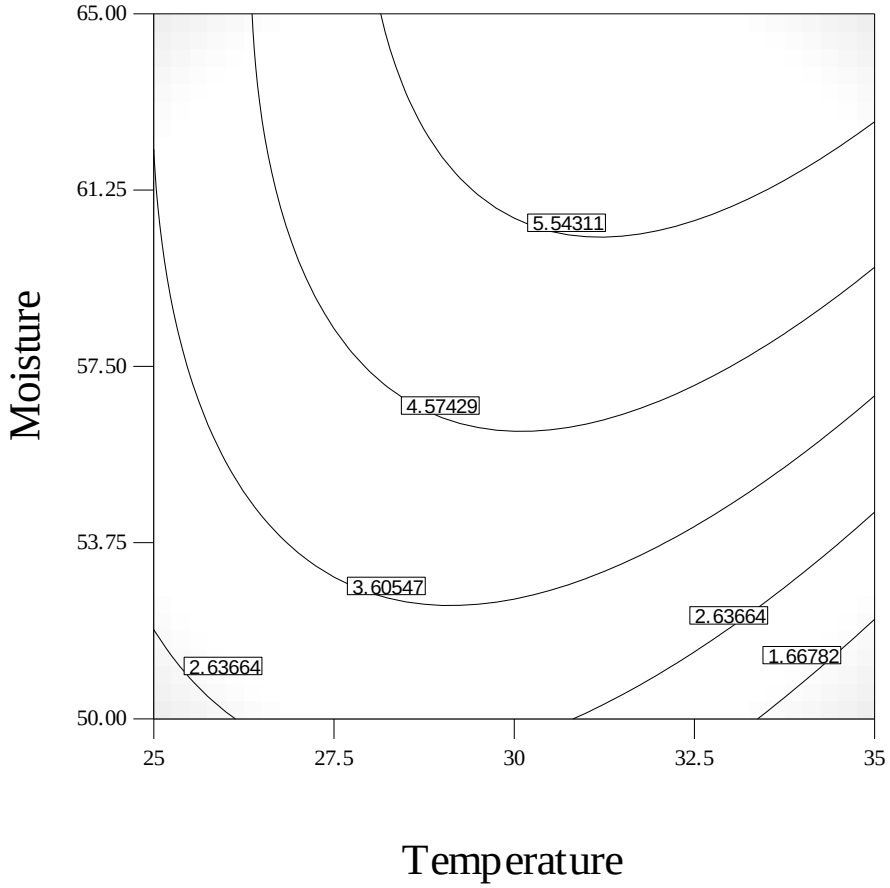
65.00
61.25
57.50
53.75
50.00
Moisture
25
27.5
30
32.5
35
Temperature
5.54311
4.57429
3.60547
2.63664
2.63664
1.66782

c)

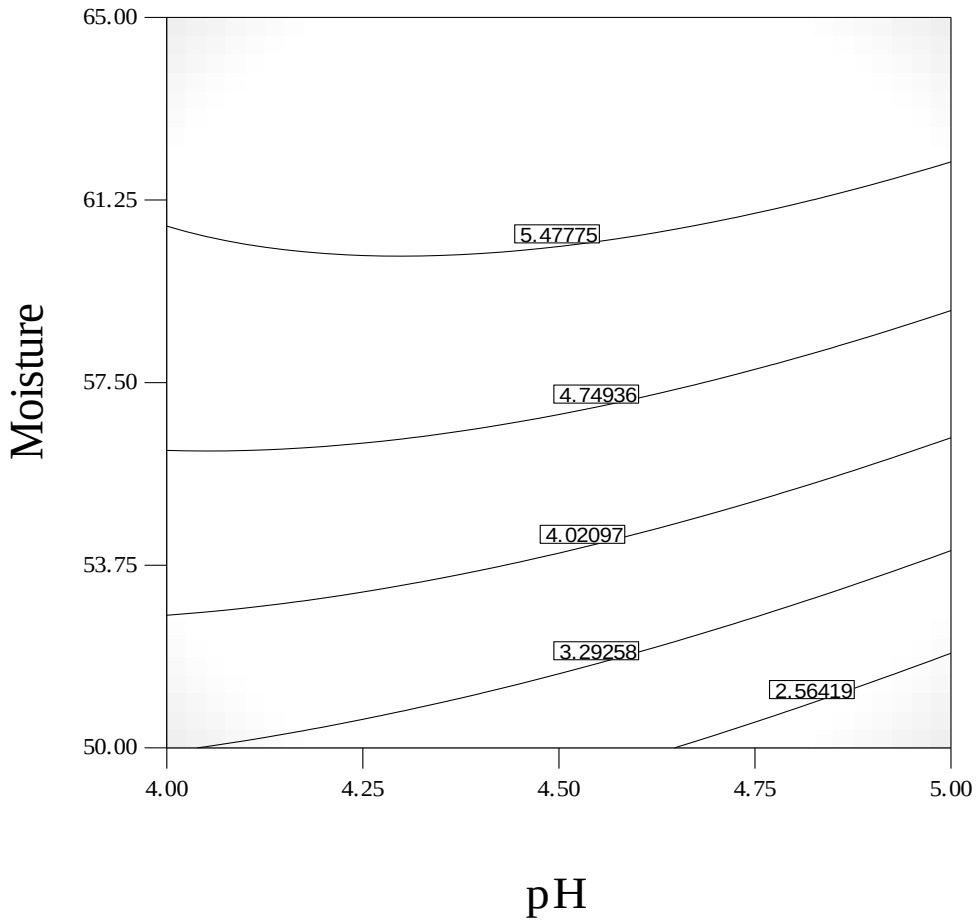
65.00
61.25
57.50
53.75
50.00
Moisture
5.47775
4.74936
4.02097
3.29258
2.56419
4.00
4.25
4.50
4.75
5.00
pH

Figure 2.3 Kinetics of celluloytic enzyme system production during mixed-culture, solid-state fermentation of soybean hulls and wheat bran in static tray bioreactor. All enzymatic activities increased significantly until the 96 hours of growth period. There was no significant difference between the 96-hour and 120-hour growth period for all reported activities. Test of difference of means were conducted using Tukey Kramer HSD at P<0.05.

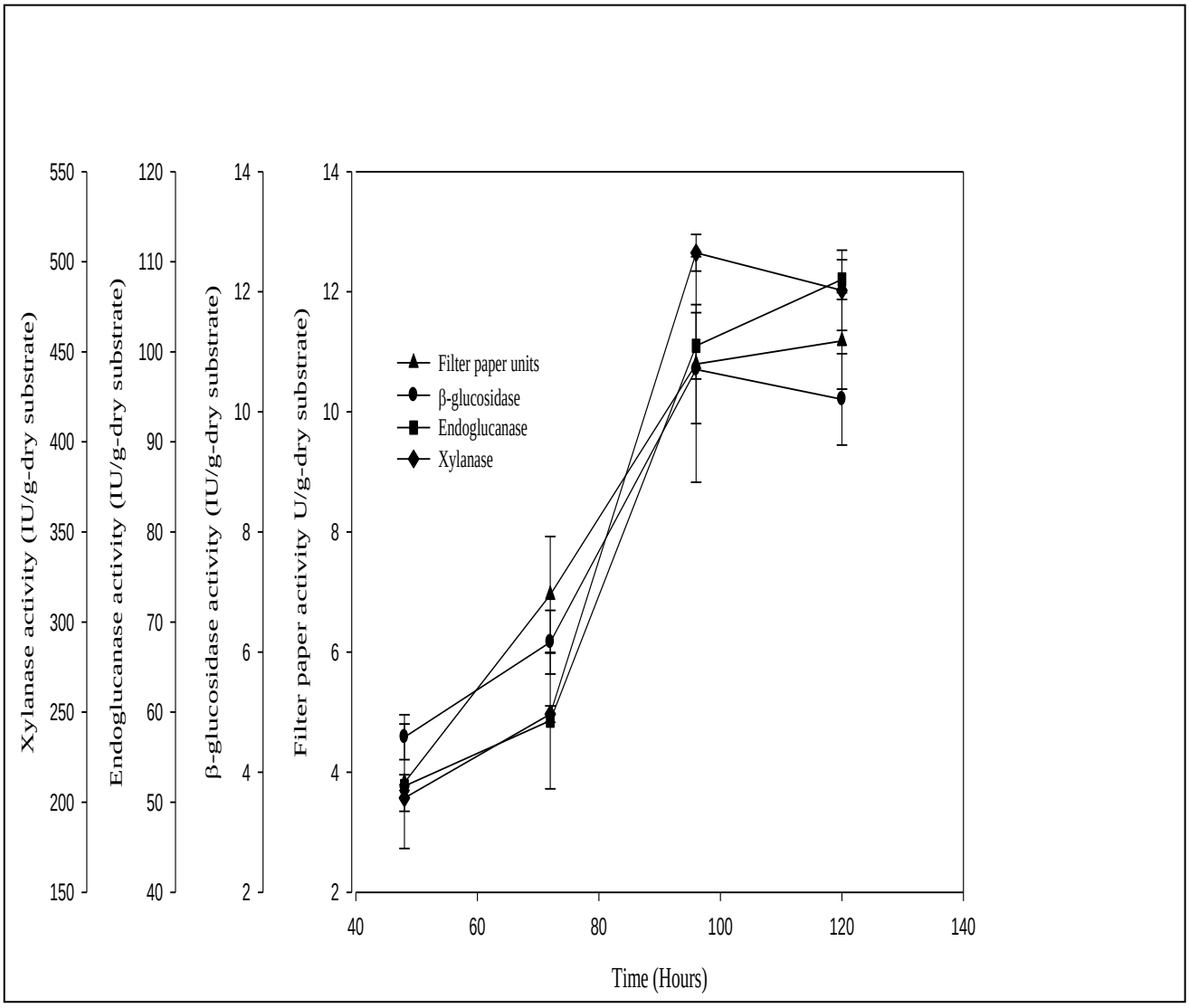

Figure 2.4 Electrophoretic analysis of different cellulase samples by SDS-PAGE. Lane A, Mark 12 Ladder (Invitrogen Inc., USA); Lane B, Celluclast 1.5L; Lane C, Novozym 188, Lane D, Novozyme xylanase; Lane E, Cellulolytic enzyme concentrate from mixed-culture fermentation in static tray bioreactor.

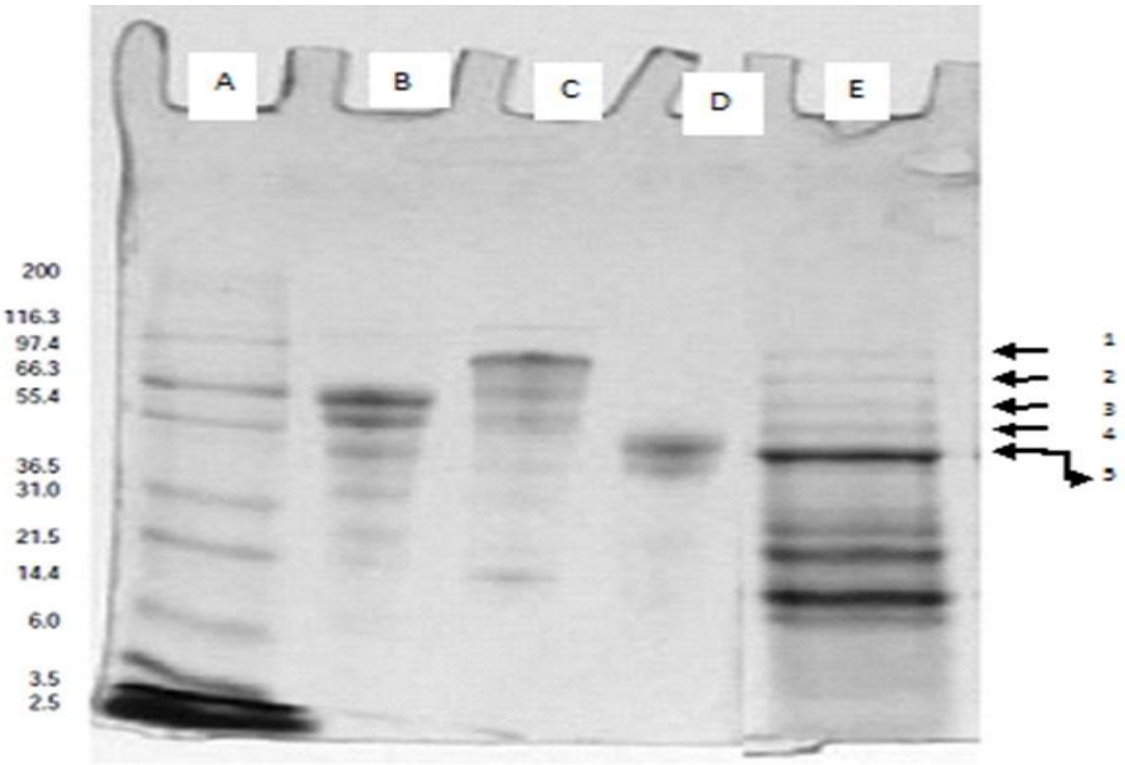

Figure 2.5 Time progress curve of sugar production during enzymatic saccharification of acid- and alkali-treated wheat straw. Values (means) with same letters do not differ significantly for different incubation time during enzymatic hydrolysis. "*" represents significant difference in sugar yields between acid- and alkali-treated wheat straw enzymatic hydrolysis at different incubation periods. Test of difference of means were conducted using Tukey Kramer HSD at P<0.05.

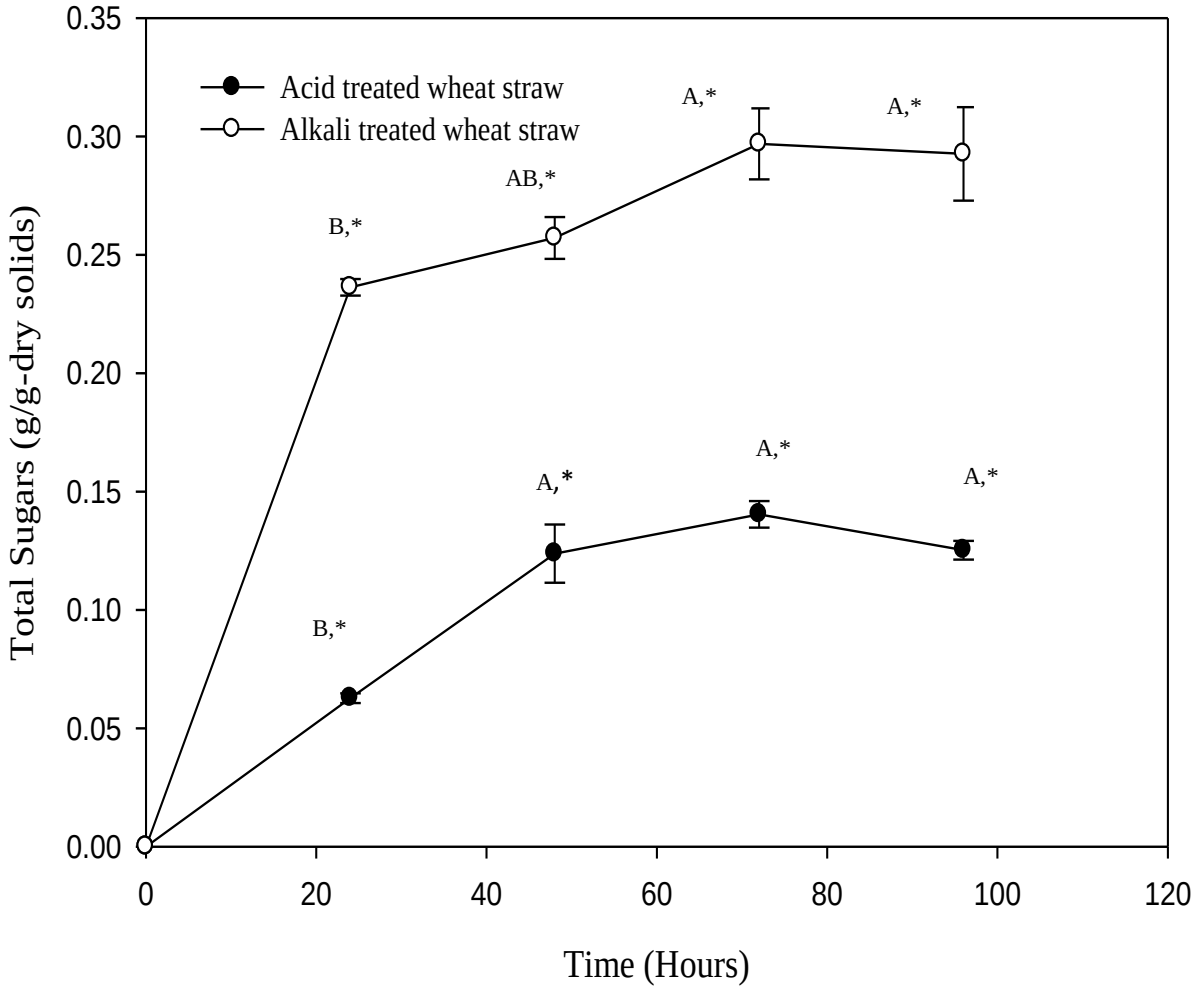

Table 2.1 Cellulosic composition of soybean hulls and wheat bran on dry basis

Type	Cellulose	Hemicellulose	Protein	Lignin	Ash
Soybean hulls	33.49±0.18	17.15±0.04	10.21±0.02	9.88±0.01	4.71±0.07
Wheat bran	7.57±0.17	31.19±0.30	16.29±0.06	4.06±0.09	6.53±0.01

Data is expressed as mean ± S.D. of three replicates

Table 2.2 Independent variables and their coded level chosen for central composite design

Independent variables	Symbol	Coded level				
		1.682 (-α)	-1	0	1	1.682 (α)
Temperature (°C)	X_1	21.59	25	30	35	38.41
pH	X_2	3.66	4	4.5	5	5.34
Moisture content (%)	X_3	44.89	50	57.5	65	70.11

Table 2.3 Cellulase activity (FPU/g dry substrate) and β-glucosidase activity (IU/g dry substrate) under different fermentation conditions

X_1	X_2	X_3	FPU/g	IU/g
1	-1	-1	0.28	0.26
0	0	1.682	10.55	8.13
-1.682	0	0	0.41	0.51
0	0	0	8.04	3.24
-1	1	-1	0.51	0.42
0	-1.682	0	6.62	4.58
0	0	0	8.67	4.10
1	1	1	8.40	4.90
-1	1	1	4.56	2.53
0	0	0	7.49	5.20
0	0	0	6.03	5.03
1.682	0	0	2.59	2.77
1	1	-1	0.69	0.38
0	0	-1.682	0.56	0.27
-1	-1	1	4.83	3.33
1	-1	1	7.48	4.87
0	0	0	8.03	7.10
0	1.682	0	8.49	4.81
0	0	0	9.17	4.57
-1	-1	-1	0.32	4.61

Table 2.4 ANOVA of fitted quadratic model for cellulase activity (FPU/g dry substrate) and β-glucosidase activity (IU/g dry substrate)

Enzyme Activity	Quadratic Model		Lack of Fit	
	Correlation coefficient (R^2)	P-value	F statistic	P-value
Cellulase (FPU/g)	0.9515	<0.0001*	1.04	0.482
β-glucosidase (IU/g)	0.8085	0.0302*	1.26	0.4034

* Significant at P<0.05

Table 2.5 Comparison of cellulolytic enzyme activities and volumetric productivity between mixed and mono cultures after 96 hours of fermentation in static tray bioreactor

Culture	Total cellulase (FPU/g-ds)	β-glucosidase (β-G) (IU/g-ds)	Endocellulase (EC) (IU/g-ds)	Xylanase (XYL) (IU/g-ds)	V_{FPU} $FPUl^{-1}g^{-1}$	$V_{\beta\text{-}G}$ $IUl^{-1}g^{-1}$	V_{EC} $IUl^{-1}g^{-1}$	V_{XYL} $IUl^{-1}g^{-1}$
T. reesei	6.55^{A}	6.30^{A}	60.17^{A}	515.90^{A}	10.91^{A}	10.50^{A}	110.29^{A}	859.83^{A}
A. oryzae	6.70^{A}	9.45^{B}	68.36^{B}	512.16^{A}	11.16^{A}	15.74^{B}	113.93^{A}	853.59^{A}
Mixed	10.78^{B}	10.71^{C}	100.67^{C}	504.98^{A}	17.99^{B}	17.84^{C}	167.78^{B}	841.64^{A}

"A, B, CB indicates significant differences between means within column, i.e. within particular activity of three cultures; means followed by different letters differ significantly." Comparison of pair of means were conducted using Tukey Kramer HSD at $P<0.05$. V followed by subscript represents volumetric productivity for particular enzyme activity.

Table 2.6 Lignocellulosic composition of acid- and alkali-treated wheat straw

Type	Glucan	Xylan	Arabinan	Lignin
Untreated wheat straw	36.70±0.29	26.28±0.18	4.06±0.07	15.82±0.13
Acid treated wheat straw	51.66±0.14	6.56±0.49	1.95±0.01	27.57±0.23
Alkali treated wheat straw	52.59±0.01	24.67±0.25	4.84±0.29	8.85±0.07

Data is expressed as mean ± S.D. of three replicates.

Table 2.7 Sugar yields during enzymatic hydrolysis of acid- and alkali-treated wheat straw

Time of incubation (h)	Acid-treated wheat straw after enzymatic hydrolysis			Alkali-treated wheat straw after enzymatic hydrolysis		
	Glucose yield (g/g-glucan) $Y_{G/S}$	Xylose yield (g/g-xylan) $Y_{X/S}$	Arabinose yield (g/g-arabinan) $Y_{A/S}$	Glucose yield (g/g-glucan) $Y_{G/S}$	Xylose yield (g/g-xylan) $Y_{X/S}$	Arabinose yield (g/g-arabinan) $Y_{A/S}$
24	$0.08^{*,B}$	$0.24^{**,C}$	$0.14^{***,A}$	$0.23^{*,B}$	$0.59^{**,B}$	$0.62^{***,B}$
48	$0.16^{*,A}$	$0.42^{**,AB}$	$0.15^{***,A}$	$0.23^{*,B}$	$0.68^{**,AB}$	$0.74^{***,AB}$
72	$0.18^{*,A}$	$0.44^{**,A}$	$0.19^{***,A}$	$0.27^{*,A}$	$0.74^{**,A}$	$0.78^{***,A}$
96	$0.18^{*,A}$	$0.35^{**,B}$	$0.15^{***,A}$	$0.28^{*,A}$	$0.74^{**,A}$	$0.74^{***,AB}$

"*, **, *** indicates significant differences between means for acid and alkali treatments for yield of particular sugar." "A, B, C, AB indicates significant differences between means for different incubation times for yield of particular sugar; means followed by different letters differ significantly." Comparison of pair of means were conducted using Tukey Kramer HSD at $P<0.05$.

Chapter 3 - Cellulolytic Enzymes Production via Solid-State Fermentation: Effect of Pretreatment Methods on Physicochemical Characteristics of Substrate[2]

Abstract

We investigated effect of pretreatment on the physicochemical characteristics — crystallinity, bed porosity and volumetric specific surface of soybean hulls and production of cellulolytic enzymes in solid-state fermentation of *Trichoderma reesei* and *Aspergillus oryzae* cultures. Mild acid and alkali, and steam pretreatments significantly increased crystallinity and bed porosity without significant change in holocellulosic composition of substrate. Crystalline and porous steam-pretreated soybean hulls inoculated with *T. reesei* culture had 4 Filter Paper Units (FPU)/g-ds, 0.6 IU/g-ds β-glucosidase and 45 IU/g-ds endocellulase, whereas untreated hulls had 0.75 FPU/g-ds, 0.06 IU/g-ds β-glucosidase and 7.29 IU/g-ds endocellulase enzyme activities. In *A. oryzae* steam-pretreated soybean hulls had 47.10 IU/g-ds endocellulase compared to 30.82 IU/g-ds in untreated soybean hulls. Generalized linear statistical model fitted to enzyme activity data showed that effects of physicochemical characteristics on enzymes production were both culture- and enzyme-specific. Study shows a correlation between substrate physicochemical properties and enzyme production.

Keywords: Crystallinity, bed porosity, volumetric specific surface, particulate bioprocessing, *T. reesei*, *A. oryzae*, cellulolytic enzyme complex

[2] This Chapter is accepted as Brijwani K, Vadlani PV (2011)/ Enzyme Research (in press).

1. Introduction

With increasing emphasis on bio-based fuels and chemicals, the cellulase market is expected to increase dramatically [1]. To create a sustainable bio-economy, cellulases need to be produced cost-effectively and possess excellent biocatalytic properties [2]. Solid-state fermentation (SSF) offers a low-cost alternative for producing cellulases using natural polymers derived from agro-industrial residues [3,4].

SSF is defined as a discrete solid phase in which microorganisms grow on the surface of moist, particles as well as inside and between them. The space between particles is occupied by a continuous gas phase [5]. Gas phase in SSF is strongly affected by the size, shape, and tortuosity of a network of gas-filled pores. The air- or gas-filled pores are referred as bed porosity, which is defined as the volume of gas contained in the system at any given time (void fraction) [6]. Availability of spaces between particles ensures availability of oxygen that improves enzyme production in aerobic fungal cultures [7,8,9]. Chutmanop et al. [10] showed that by blending rice bran with wheat bran resulted in substantial improvement in the morphology of rice bran which improved protease production during solid-state culturing of *A. oryzae*. The increase in bed porosity of the substrate could be the reason behind improved production; however, no attempts were made to measure bed porosity to show its relationship to enzyme production. Several authors in the past have suggested the merits of open porous solid beds but no explicit investigation has been conducted yet that relates bed porosity with enzyme production in SSF. In industrial scale SSF processes, bed porosity is essential but not sufficient for complete process control. Other parameters, such as microbial cell physiology, composition of the solid substrate, and substrate reactivity also could influence the productivity of the process [11,12].

Substrate reactivity, especially in case of cellulosic substrates, is influenced by physicochemical characteristics of the substrate at different levels. At microfibril level it is

crystallinity of cellulose, and at fiber level it is specific surface area (characterizing pore size or degree of swelling) [13,14,15]. The increase in cellulase reactivity due to increase in specific surface area is attributed to the creation of surface openings or internal slits, voids, or spaces, by the removal of cell wall components, that enhances the direct physical contact between the enzymes and the substrate [16]. During growth on complex substrates, propagation of fungal mycelium occurs *via* production of enzymes that drive hydrolytic reactions. The hydrolytic reactions are responsible for generation of soluble sugars that facilitate fungal growth. It has been proposed that the hydrolysis occurs efficiently when the pores within the substrate are large enough to accommodate both large and small enzyme components to maintain the synergistic action of the enzyme system [14,17,18]. On the other hand, reduced surface area impede with this synergistic action.

Crystalline cellulose digestion requires concerted action of exo- and endo-glucanases. The crystalline nature of the carbon source used to induce cellulolytic expression in many species of fungi significantly influences the hydrolytic potential of the enzyme preparation [19]. Evans et al. [20] showed that crystalline-cotton-induced cellulolytic complex derived from submerged *T. reesei* cultures exhibited higher potential in hydrolyzing crystalline cellulose than Solka-Floc-induced cellulases. Fungi growing on complex cellulosic substrates are prone to catabolite repression by glucose [21]. The extent of catabolite repression depends on the rate of glucose formation, which in turn depends on the secretion of enzymes that degrade cellulose. Fan et al. [22,23], and, more recently, Ciolacu et al. [24] and Hall et al. [25] have shown that the rate of cellulose degradation is dependent on crystallinity of the cellulosic substrate. In other words, crystallinity of cellulosic sample could alter not only the quality of enzymes (the proportion of various activities with cellulolytic enzyme complex) but also the quantity of enzymes produced.

Thus, studies delineating the effects of crystallinity on enzyme production in SSF are of significant interest.

The growth of fungi in natural substrates is usually slow and this limitation must be overcome by suitable mechanical and chemical pretreatment of the raw substrate [26]. However, pretreatments are known to induce structural changes in cellulosic substrates, which could alter the physicochemical properties of the substrate [2]. The effect of pretreatment methods on physicochemical characteristics of substrate and its repercussions on cellulolytic enzyme productivity in fungal solid state fermentation has not been investigated so far, which is evident from the recent reviews on SSF [3,27]. An in-depth understanding of role of physicochemical characteristics of substrate on cellulase production in SSF would provide a framework for comprehensive analysis of critical design issues that should facilitate cellulase production with enhanced biocatalysis.

The present study aimed to determine the role of pretreatment techniques in altering the physicochemical characteristics– bed porosity, volumetric specific surface and crystallinity of solid state substrate. In addition, the effect of change in physicochemical attributes on enzyme production in fungal solid-state fermentation was studied with respect to type of fungal species and different cellulolytic enzyme activities. The pretreatments were carefully chosen to limit the effect on the chemical compositional changes of solid substrate, which would otherwise diminish the role of physicochemical attributes. Since, crystallinity is critical to this study, new method of measuring crystallinity of complex cellulosic substrate was also discussed.

2. Materials and methods

2.1. Sample Preparation

Untreated ground soybean hulls (purchased from Archer Daniels Midland, Salina, KS, USA), herein referred to as native soybean hulls, had a geometric mean diameter, d_{gw}, of 0.61 ± 0.002 mm. Native soybean hulls were subjected to four different treatments before being used for production of the cellulolytic enzyme system: (1) steam pretreatment, in which a 5% (w/v) slurry of soybean hulls in distilled water was pressure cooked at 121ºC for 60 min; (2) hydrochloric acid pretreatment, in which a 5% (w/v) slurry of soybean hulls in 1N HCl was kept on a gyratory shaker (150 rpm) for 24 h at ambient temperature; (3) sulfuric acid pretreatment, in which a 5% (w/v) slurry of soybean hulls in 1N H_2SO_4 was kept on a gyratory shaker (150 rpm) for 24 h at ambient temperature; and (4) sodium hydroxide pretreatment, in which a 5% (w/v) slurry of soybean hulls in 1N NaOH was kept on a gyratory shaker (150 rpm) for 24 h at ambient temperature. After acid and alkali pretreatments, treated soybean hulls were collected by filtration and extensively washed with distilled water. The pH was adjusted to approximately 5.5. Steam-pretreated soybean hulls were washed once. All treated substrates were dried overnight at 45ºC in a forced-draft oven (Fisher Scientific, USA). Dried substrates were used for compositional analysis, analysis of physicochemical characteristics, and production of enzymes. Treatments were performed in quadruplets.

2.2. SSF for Cellulolytic Enzyme System Production in Native and Pretreated Soybean Hulls

Two fungal cultures *T. reesei* (ATCC 26921) and *A. oryzae* (ATCC 12892) were used for SSF of native and pretreated soybean hulls. Cultures were used as both mono and mixed (1:1). Native and pretreated dried soybean hulls (5 g) were adjusted to 70% (wet basis) moisture

content (mc) by using Mandels media [28] of pH 5 and were sterilized in a vertical sterilizer (121ºC/15 psi gauge) for 30 minutes. Cultures were added as spore suspensions (10^8 spores/ ml-suspension) at the loading of 0.1 ml per gram dry substrate. The propagation, maintenance, and generation of spore suspensions are described in [29]. Flasks containing two cultures in the ratio of 1:1 were labeled as mixed. Flasks were incubated for 5 days at 30ºC. The conditions of temperature, pH, moisture (70%), and incubation days of the SSF process used in this study were optimized previously [29]. Following incubation, enzymes were extracted and analyzed per Section Analytical methods.

2.3. Analysis of Physical Parameters: Bed Porosity

Porosity (ε) of the samples was computed from the values of true density and bulk density by using the relationship described in [30] as follows:

$$\varepsilon = \left(1 - \frac{\rho_b}{\rho_t}\right) \times 100 \quad (1)$$

True density (ρ_t) was determined using a standard liquid pycnometer by determining the volume of the sample at various moisture contents. Volume (V, cm^3) was calculated from the following relationship [31]:

$$V = \frac{(M_{ps} - M_p) - (M_{pts} - M_t)}{\rho_{tol}} \quad (2)$$

where M_t is mass of the pycnometer filled with toluene, M_{ps} is the mass of pycnometer and sample, M_p is mass of the pycnometer, M_{pts} is mass of the pycnometer filled with toluene and sample, and ρ_{tol} is the density of toluene. Knowing V, the true density (g/cc) then can be calculated from the following expression:

$$\rho_t = \frac{(M_{ps} - M_p)}{V} \quad (3)$$

Bulk density (ρ_b) is estimated by weighing the samples (70% mc) after pouring in a vessel of known volume (10 ml) [30].

2.4. Analysis of Physical Parameters: Volumetric Specific Surface (cm^{-1})

Volumetric specific surface is defined as external surface area per unit volume of the samples [32]. Volumetric specific surface of samples was determined from particle size analysis [33]. Samples were sieved using USA standard testing sieves stacked in order of decreasing aperture size above the collection pan placed in Ro-Tap sieve sifter (Laval Lab Inc., Canada). Weight of over-size generated during sieving was used to compute geometric mean diameter (d_{gw}) and geometric standard deviation (S_{gw}) according to the following equations:

$$d_{gw} = log^{-1}\left(\frac{\sum(W_i \log d_i)}{\sum W_i}\right) \quad (4)$$

$$S_{gw} = log^{-1}\sqrt{\left(\frac{\sum[W_i(\log d_i - \log d_{gw})^2]}{\sum W_i}\right)} \quad (5)$$

Where d_i is the diameter of the ith sieve in the stack and W_i is the weight fraction on the ith sieve. Using d_{gw} and S_{gw}, surface area per gram was calculated as [33]:

$$S\ (cm^2/g) = \frac{\beta_s}{\rho\beta_v}\exp(0.5\ ln^2\ S_{gw} - \ln d_{gw}) \quad (6a)$$

Volumetric specific surface (SA, cm^{-1}) can then be obtained from equation (6a) by multiplying it with specific weight (ρ) (g/cm^3) i.e.

$$SA\ (cm^{-1}) = \frac{\beta_s}{\beta_v}\exp(0.5\ ln^2\ S_{gw} - \ln d_{gw}) \quad (6b)$$

Where β_s is the shape coefficient for calculating surface area of particles (fixed at 6) and β_v is the shape coefficient for calculating volume of particles (fixed at 1) [33].

2.5. Analysis of Physical Parameters: Wide-angle X-ray Diffraction

Wide-angle X-ray diffraction (XRG 3100 X-ray generator, Phillips Electronics Instrument Inc., Texas, USA) was used to estimate the crystallinity of native and pretreated soybean hulls. The X-rays from a Cu tube operating at 35 KV and 20 mA were collected by an energy dispersive detector that is able to resolve CuK_{α} line. Counts were collected at a step size of 0.02º at a series of angles between 5º and 40º. Speed of count collection was 0.6º/min.

2.6. Analysis of Physical Parameters: Crystallinity Calculations Using Deconvolution Method

The raw diffractograms were subjected to a fitting procedure using a non-linear least squares numerical procedure. The deconvolution method separate amorphous and crystalline contributions to the diffraction spectrum under curve-fitting process by selecting a shape function [34]. In this method it is very important to understand the major sources that contribute to the shape function of the observed X-ray profile $h(2\theta)$, which is a convolution (Θ) of the intrinsic specimen profile f(2θ) with the spectral distribution (W) and the instrumental function (G) superimposed over the background b [35], as given below:

$$h(2\theta) = [(W\Theta G)\Theta f](2\theta) + b \qquad (7)$$

The Voigt function, which is a convolution of Gaussian and Lorentzian peak functions, would include both Gaussian intrinsic broadening of the specimen along with the Lorentzian instrumental profile that considers the background from amorphous scattering. The Voigt function, therefore, appropriately takes into account the peak broadening due to diffusive scattering [36,35].

Using the Voigt function intensity of the reflection is represented by following equation:

$$f(2\theta) = \frac{a_o \int_{-\infty}^{\infty} \frac{\exp\,(-(2\theta)^2)}{a_l^2 + \left(\frac{x - a_c}{a_g} - 2\theta\right)2} d(2\theta)}{\int_{-\infty}^{\infty} \frac{\exp\,(-(-(2\theta)^2)}{a_l^2 + (2\theta)} d(2\theta)} \quad (8)$$

where a_o is the amplitude of the peak, a_c is the center of the peak, a_l is the width of the Lorentzian component, and a_g is the width of the Gaussian component of the peak. The major reflective planes in cellulosic material from plant sources correspond to the following Miller indices (hkl): 101, $10\bar{1}$, 002, 021, and 040, with 002 as the prominent reflection representing crystalline cellulose (sometimes resolved into 021 plane as well) [37]. X-ray peaks were fitted using Voigt function as profile shape function using Peakfit (SeaSolve Software Inc., MA, USA) program. The program was re-run locking these planes; consequently, five Voigt functions were fitted. The fitted peaks were used to evaluate degree of crystallinity (X_{cr}) of the sample per the equation 9 described by Wada et al. [36].

$$X_{cr}\,(\%) = \frac{I_{002} + I_{021}}{I_{101} + I_{10\bar{1}} + I_{002} + I_{021} + I_{040}} \times 100 \quad (9)$$

Where I followed by a subscript represents the integrated intensity of the particular Bragg plane. Crystallinity, therefore, represents the fraction of α-cellulose represented by planes 002 and 021 present in a particular sample.

2.7. Analytical Methods: Compositional Analysis

The lignocellulosic composition of soybean hulls was determined with an ANKOM 200 Fiber Analyzer (ANKOM Technology, USA). Neutral detergent fiber (NDF), acid detergent fiber (ADF), and acid detergent lignin (ADL) were analyzed per procedure specified by the manufacturer (www.ankom.com). Protein content (N x 6.25) was determined by the Kjeldahl method after digestion and distillation with an autoanalyser (Leco FP-2000, Leco Corporation, MI, USA). All moisture measurements were carried out using Denver Infrared Moisture

Analyzer (Model IR35; Fisher Scientific, USA). Ash content of soybean hulls was measured using muffle furnace from Fisher Scientific.

2.8. Enzyme Assay

Crude cellulases were extracted from various production steps described in section 2.4 by adding 30 ml of citrate buffer (50 mM, pH 5) to each flask and shaking the contents at 150 rpm for 30 minutes. Contents were filtered using coarse filter paper (Fisher Scientific, P-8 coarse grade), and the filtrate obtained was centrifuged at 10,000 ×g for 15 minutes at 4°C (Sorvall RC-6, Thermo Scientific, USA). The supernatant was analyzed for filter paper activity (FPU/g-ds), endocellulase (IU/g-ds), β-glucosidase (IU/g-ds), and xylanase (IU/g-ds) activities. Enzymatic assays were carried out using standard protocols described in Brijwani et al. [29]. Enzyme activities were reported as units per gram of dry substrate (g-ds).

2.9. Statistical Analysis

Statistical analysis was carried out using the GLM procedure in SAS software version 9.1 (SAS Institute, Cary, NC, USA). Multiple comparisons were conducted using Tukey Kramer HSD at $P<0.05$.

3. Results and discussion

3.1. Effect of Pretreatments on Compositional Changes in Soybean Hulls

Effects of various pretreatments on compositional changes in soybean hulls are shown in Table 3.1. Data is represented only to outline holocellulose (cellulose + hemicellulose), lignin, protein and ash content of soybean hulls, and not necessarily reflects the complete composition. Soybean hulls are known to contain appreciable amount of pectin (~15%) and lipids (<4%) as well [38,39]. Both acid and alkali pretreatments enriched the cellulosic fraction and extracted a

small part of the hemicellulosic fraction. Steam-pretreated soybean hulls, on the other hand, had a composition similar to that of native soybean hulls. An interesting finding was that holocellulosic content was fairly constant (no significant difference, $P<0.05$) across the spectrum of treatments used in this study (Table 3.1). Total cellulosic content may be useful to consider since both cellulose and hemicellulose are implicated in induction of cellulolytic enzyme complex [40]. Therefore, subjecting soybean hulls to mild pretreatments preserved the holocellulosic composition of native soybean hulls.

3.2. Effect of Pretreatments on Changes in Physical Attributes of Soybean Hulls: Bed Porosity and Volumetric Specific Surface of Pretreated Soybean Hulls

There was a substantial increase in the bed porosity (Table 3.2), estimated at 70% mc, for pretreated soybean hulls compared with native soybean hulls. The increase in bed porosity is likely due to modification of the internal structure of soybean hulls that led to redistribution and partial solublization of hemicellulose and swelling of the substrate [41]. Volumetric specific surface (cm^{-1}), on the other hand, was similar for pretreated and native soybean hulls. Volumetric specific surface measurements were the outcome of particle size analysis that accounted only for external surface area; however, fibers have lumen characterized by hollow space. It is the interfibrillar space, also referred as "internal porosity" that has capability of accommodating large enzyme molecules, thereby leading to enhanced digestibility. Chemical pretreatment tends to enlarge intermicrofibrillar spaces by dissolution of cell wall capillaries [18]. Finding a simple technique to determine lumen internal surfaces is difficult; volumetric specific surface incorporating external particle diameter is unable to capture the internal specific area, which characterizes microfibrillar spaces [32]. This was evident in the current study when the volumetric specific surface of pretreated and untreated soybean hulls were not significantly

different ($P<0.05$). It is essential to identify or modify current techniques that can easily implement rapid and routine analysis of internal surface area.

3.3. X-ray Crystallinity of Native and Pretreated Soybean Hulls

Wide-angle X-ray diffraction has been used extensively to measure the crystallinity of cellulosic substrates. Crystallinity in the polymeric sample may be measured in several ways from an X-ray diffractogram; the most common is the peak intensity method [42]. The method requires amorphous material to diffract with the same intensity at 18º (~ $10\bar{1}$ plane) and 22º (002 plane), and does not account for peak shifting or overlap. Moreover, the crystallinity values predicted by this method usually are overestimated [25]. This method assumes highest peak (002) as the only determinant of the cellulose crystallinity [34], which is certainly not the case as five planes have been identified responsible for the characteristic reflection. Finally, lignocellulosic substrates contain appreciable amounts of hemicellulose and lignin that lead to diffusive X-ray scattering (reflection), a hallmark of paracrystalline substances [43,44]. Given these drawbacks of the peak intensity method, a sophisticated technique using deconvolution was successfully applied in our studies to X-ray spectra of both native and pretreated soybean hulls for crystallinity measurements. This method is relatively new in the arena of lignocellulosic biofuels research, although it is routinely used in polymer science research [45].

The fitted X-ray diffractograms using Voigt function are shown in Fig. 3.1a–3.1e for both native and pretreated soybean hulls. Fit was assessed using R^2. Almost all diffractograms using this scheme had $R^2>0.95$. Also, featured in the Table 3.2 are adjusted R^2 (Adj. R^2) and root mean square error (RMSE) of the fit. The higher value of adjusted R^2 and lower RMSE further confirmed the goodness of fit. Notice the five peaks corresponding to identified lattice planes and gradual evolution of peaks in pretreated soybean hulls compared to native soybean hulls

indicating increase in degree of crystallinity due to pretreatments. Degree of crystallinity was calculated from equation (9), and the values are listed in Table 3.2. The steam, acid, and alkali pretreatments all resulted in a significant increase in degree of crystallinity compared to native soybean hulls. The pretreated soybean hulls had crystallinity from 57 to 59% (Table 3.2). The enhancement in crystallinity is due to enrichment in the α-cellulose fraction in the pretreated samples due to reduction in the interlocking amorphous cellulosic chains and plausible correction in lattice defects of cellulose during pretreatments [46,47]. The α-cellulose fraction is the crystalline cellulose of plant polymers and is responsible for the characteristic X-ray diffraction. Additionally, due to the mild nature of pretreatments, enrichment in α-cellulose fraction was possible by selective reduction of the amorphous phase. The outcome could have been different if harsh chemical pretreatments (using high temperature and pressure) were employed.

3.4 Effect of Pretreatment Methods on Production of Cellulolytic Enzyme System

Production of a cellulolytic enzyme system was assessed through measurement of four leading activities: filter paper units (FPU/g-ds [dry substrate]), β-glucosidase (IU/g-ds), endocellulase (IU/g-ds), and xylanase (IU/g-ds). Inspection of Fig. 3.2 reveals that enzyme production in both mono and mixed cultures of *T. reesei* and *A. oryzae* was significantly reduced in alkali-pretreated soybean hulls compared to native, and steam- and acid-pretreated substrates. Gossett et al. [48] stated that an important aspect of alkali pretreatment is that biomass itself consumes some of the alkali. As a result, changes brought about by alkali pretreatment can cause solubilization, distribution, and condensation of lignin and hemicellulose and modification of cellulosic structure. These effects can counter the positive effects rendered by alkali pretreatment. Aiello et al. [49] showed that alkali-pretreated sugarcane bagasse in liquid fermentation of *T. reesei* (QM 9414) significantly decreased cellulase yield over untreated

bagasse. Cellulolytic enzyme production in HCl- and H_2SO_4-pretreated soybean hulls was significantly ($P<0.05$) lower for both cultures compared to native and steam-pretreated substrates. Acid pretreatment of lignocellulosics is known to generate inhibitory compounds as result of sugar and lignin degradation during the treatments [50, 51]. Though the acid pretreatment may result in increased digestibility of lignocellulosic substrate, the inhibitory compounds have deleterious effects on enzyme and microbial activity.

Steam pretreatment resulted in significant ($P<0.05$) and substantial enhancement in production of all cellulolytic activities in *T. reesei* culture compared to production in untreated soybean hulls. The production of xylanase, though, was not significantly ($P<0.05$) different. Steam-pretreated soybean hulls had about 4 FPU/g-ds compared with 0.75 FPU/g-ds in native and endocellulase of 45 IU/g-ds compared with 7.29 IU/g-ds in native. β-glucosidase activity also improved significantly ($P<0.05$) in steam-pretreated compared with native soybean hulls. The high activity of enzymes suggest that though native and steam pretreated soybean hulls had compositional similarity (Table 3.1), but have significantly different enzyme production (Fig. 3.2). This is a key indication that in SSF, in which fungal mycelium is in direct contact with the substrate particles, the physicochemical nature of the substrate is important in addition to its composition.

In *A. oryzae* no significant differences ($P<0.05$) occurred in enzyme production between steam-pretreated and native soybean hulls except in endoglucanase levels. In steam-pretreated soybean hulls, *A. oryzae* produced a significantly higher amount of endoglucanase (47 IU/g-ds) compared to that in native substrate (31 IU/g-ds). Mixed culture had similar results as in *A. oryzae*, where production in steam-pretreated soybean hulls was not significantly different ($P<0.05$) compared to native soybean hulls (Fig. 3.2). Steam pretreatment method resulted in

enzymes production disparities, which were both enzyme and culture specific. To relate the trends in enzyme production with physicochemical characteristics of the substrate in the two fungal cultures, *T. reesei* and *A. oryzae*, additional statistical analysis was performed.

3.5. Effect of Interaction between Crystallinity and Porosity on Cellulolytic Enzyme System Production in Pretreated Substrates

The interaction of crystallinity and porosity was modeled using the general linear model of SAS with the following expression:

$$y_{ijk} = \mu + ab_{ij} + \epsilon_{ijk} \quad (10)$$

where y_{ijk} is one of the enzyme activities as the dependent variable, μ is the grand mean (n =4), ab_{ij} is the interaction effect of crystallinity and porosity, and ϵ_{ijk} is random error with mean 0 and experimental error variance as its variance. Both composition (holocellulose) and volumetric specific surface were excluded as they were nearly constant across pretreatments (Tables 3.1 and 3.2). In addition, only native and steam pretreated substrates were considered in our analysis because enzyme production in acid- and alkali-pretreated substrates was lower due to their inhibitory effects on microbial propagation. Crystallinity and porosity were considered together since they were simultaneously altered when substrates were subjected to pretreatments. Also, it is difficult to vary one keeping the other constant. The model represented by equation (10) is more reflective of one-way variance analysis than factorial variance analysis.

Examination of data (Table 3.3) shows that for *T. reesei*, with an increase in crystallinity and porosity due to steam pretreatment, all cellulolytic enzyme activities increased significantly except xylanase. In *A. oryzae* fermentation, significant improvement was noticed only in endoglucanase production, whereas in mixed culture fermentation, significant decrease occurred

in filter paper units at $P<0.01$ and endoglucanase at $P<0.05$ as a result of increased crystallinity and porosity.

Bed porosity ensures oxygen availability between the moist substrate particles. The increased oxygen availability assists in the propagation of fungal cultures and, therefore, affects enzyme production. Rahardjo et al. [8,9] explained this phenomenon by using various model substrates that differed in the amount of open spaces for production of α-amylase in solid-state cultures of *A. oryzae* and explicitly showed that model substrates with more porous structure had better enzyme production compared to less porous substrates. Therefore, decrease in filter paper and endoglucanses activities in mixed culture compared to *T. reesei* could be attributed to another factor i.e. increase in crystallinity. It is apparent from the literature that *T. reesei* cellulases are particularly active towards crystalline cellulose [52,20,53]; however, enzymes from *Aspergillus* spp lack ability to degrade crystalline cellulose [54,55]. In mixed culture fermentation wherein *A. oryzae* was dominant, filter paper and endocellulase activities were reduced due to the inability of *A. oryzae* to digest crystalline substrate. This is further confirmed by observing the data of *A. oryzae* fermentation, where no improvement in cellulolytic activities in steam-pretreated soybean hulls over native substrate was observed except in endoglucanase activity.

Evidently, results highlighted that effect of crystallinity was specific for type of culture as it brought enhancement in cellulolytic activities of *T. reesei*, and this enhancement was not particularly observed in *A. oryzae*. The analysis also showed that within the spectrum of cellulolytic activities studied not all activities got altered on exposure to crystalline substrate. The results are interesting in view of the fact that pretreatments due to their ability to induce

changes in physicochemical attributes resulted in altered enzyme production in fungal SSF of soybean hulls.

4. Conclusions

For the first time, current work demonstrated that mild pretreatment methods could significantly alter the physicochemical attributes of the substrate (soybean hulls) without significant changes in holocellulosic composition. The altered physicochemical attributes due to pretreatment had significant effects on the production of cellulolytic enzyme activities, and these effects were both culture- and enzyme-specific. A sophisticated deconvolution method was used to determine X-ray crystallinity from raw diffractograms of both treated and untreated substrates. This method takes into account diffusive scattering due to paracrystalline nature of celluloses found in plant material, and therefore provides consistent and reliable measurements. Steam-pretreatment significantly increased both porosity and crystallinity of soybean hulls, and production of all the three cellulase activities in *T. reesei* culture (i.e. filter paper, β-glucosidase, and endocellulase) compared to untreated substrate. Xylanase production; however, remained unaltered. While using *A. oryzae* culture, significant improvement was observed only in endocellulase, whereas in the mixed culture fermentation, filter paper and endocellulase activities decreased in steam-pretreated soybean hulls.

Further study of porosity and crystallinity and their effects on enzyme production is necessary if we are to understand fully the effects of physiochemical attributes. Our studies highlighted the effects of pretreatment methods, changes in the physiochemical characteristics of substrates, and choice of fungal culture in SSF on enzyme production. Experimental methods to enhance enzyme production are imperative for the success of the biofuels industry, which uses enzymatic and microbial fermentation platform.

Acknowledgements

The authors are grateful to the Center for Sustainable Energy and the Department of Grain Science and Industry, Kansas State University, for funding this project. Authors gratefully acknowledge Dr. Paul A. Seib, Department of Grain Science, Kansas State University for helpful discussions. This article is contribution no. 10-301-J from the Kansas Agricultural Experiment Station, Manhattan, KS 66506. Authors hereby disclose all conflicts of interest and other potentially conflicting interests, including specific financial interests and relationships and affiliations relevant to use of chemicals, software products, and equipment from the suppliers featured in this study, but not limited to, employment or affiliation, grants or funding, consultancies, honoraria, speakers' bureaus, stock ownership or stock options, expert testimony, royalties, received, pending, or in preparation. This applies to the past 5 years and the foreseeable future.

References

[1] Y.H.P. Zhang, M.E. Himmel, and J.R. Mielenz . "Outlook for cellulase improvement: Screening and selection strategies," *Biotechnology Advances* vol. 24, no. 5, pp. 452–481, 2006.

[2] Y.H.P. Zhang and L.R. Lynd. "Toward an aggregated understanding of enzymatic hydrolysis of cellulose: Noncomplexed cellulase systems," *Biotechnology and Bioengineering* vol. 88, no. 7, pp. 797–824, 2004.

[3] R.R. Singhania, R.K. Sukumaran, A.K. Patel, C. Larroche, and A. Pandey. "Advancement and comparative profiles in the production technologies using solid-state and submerged fermentation for microbial cellulases," *Enzyme and Microbial Technology* vol. 46, no. 7, pp. 541–549, 2010.

[4] S.R. Couto and M.A. Sanroman. “Application of solid-state fermentation to food industry - A review,” *Journal of Food Engineering* vol. 76, no. 3, pp. 291–302, 2006.

[5] C. Botella, A.B. Diaz, R.H. Wang, A. Koutinas, and C. Webb. “Particulate bioprocessing: A novel process strategy for biorefineries,” *Process Biochemistry* vol. 44, no. 5, pp. 546–555, 2009.

[6] T.L. Richard, A.H.M. Veeken, V. de Wilde, and H.V.M. Hamelers. “Air-filled porosity and permeability relationships during solid-state fermentation,” *Biotechnology Progress*, vol. 20, no. 5, pp. 1372–1381, 2004.

[7] Y.Q. Cui, R. van der Lans, and K. Luyben. “Effects of dissolved oxygen tension and mechanical forces on fungal morphology in submerged fermentation,” *Biotechnology and Bioengineering* vol. 57, no. 4, pp. 409–419, 1998.

[8] Y.S.P. Rahardjo, F. Jolink, S. Haemers, J. Tramper, and A. Rinzema. “Significance of bed porosity, bran and specific surface area in solid-state cultivation of *Aspergillus oryzae*,” *Biomolecular Engineering*, vol. 22, no. 4, pp. 133–139, 2005.

[9] Y.S.P. Rahardjo, F.J. Weber, S. Haemers, J. Tramper, and A. Rinzema. “Aerial mycelia of Aspergillus oryzae accelerate alpha-amylase production in a model solid-state fermentation system,” *Enzyme and Microbial Technology*, vol. 36, no. 7, pp. 900–902, 2005.

[10] J. Chutmanop, S. Chuichulcherm, Y. Chisti, and P. Sirinophakun. “Protease production by Aspergillus oryzae in solid-state fermentation using agroindustrial substrates,” *Journal of Chemical Technology and Biotechnology*, vol. 83, no. 7, pp. 1012–1018, 2008.

[11] S. Velkovska, M.R. Marten, and D.F. Ollis. “Kinetic model for batch cellulase production by *Trichoderma reesei* RUT C30,” *Journal of Biotechnology*, vol. 54, no. 2, pp. 83–94, 1997.

[12] F.C. Domingues, J.A. Queiroz, J.M.S. Cabral, and L.P. Fonseca. “The influence of culture conditions on mycelial structure and cellulase production by *Trichoderma reesei* Rut C-30,” *Enzyme and Microbial Technology*, vol. 26, no. 5-6, pp. 394–401, 2000.

[13] L.P. Walker and D.B. Wilson. “Enzymatic-hydrolysis of cellulose - an overview,” *Bioresource Technology*, vol. 36, no. 1, pp. 3–14, 1991.

[14] A.O. Converse, R. Matsuno, M. Tanaka, and M. Taniguchi. “A model of enzyme adsorption and hydrolysis of microcrystalline cellulose with slow deactivation of the adsorbed enzyme,” *Biotechnology and Bioengineering*, vol. 32, no. 1, pp. 38–45, 1988.

[15] S.D. Mansfield, C. Mooney, and J.N. Saddler. “Substrate and enzyme characteristics that limit cellulose hydrolysis,” *Biotechnology Progress*, vol. 15, no. 5, pp. 804–816, 1999.

[16] C.I. Ishizawa, M.F. Davis, D.F. Schell, and D.K. Johnson. “Porosity and its effect on the digestibility of dilute sulfuric acid pretreated corn stover,” *Journal of Agricultural and Food Chemistry*, vol. 55, no. 7, pp. 2575–2581, 2007.

[17] M. Tanaka, M. Ikesaka, R. Matsuno, and A.O. Converse. “Effect of pore-size in substrate and diffusion of enzyme on hydrolysis of cellulosic materials with cellulases,” *Biotechnology and Bioengineering*, vol. 32, no. 5, pp. 698–706, 1988.

[18] A.R. Esteghlalian, M. Bilodeau, S.D. Mansfield, and J.N. Saddler. “Do enzymatic hydrolyzability and Simons' stain reflect the changes in the accessibility of lignocellulosic substrates to cellulase enzymes?” *Biotechnology Progress*, vol. 17, no. 6, pp. 1049–1054, 2001.

[19] M. Meshartree, C.M. Hogan, and J.N. Saddler. “Influence of growth substrate on production of cellulase enzymes by *Trichoderma harzianum* E58.” *Biotechnology and Bioengineering*, vol. 31, no. 7, pp. 725–729, 1988.

[20] E.T. Evans, D.S. Wales, R.P. Bratt, and B.F. Sagar. “Investigation of an endoglucanase essential for the action of the cellulase system of *Trichoderma reesei* on crystalline cellulose,” *Journal of General Microbiology*, vol. 138, pp. 1639–1646, 1992.

[21] N. Hendy, C. Wilke, and H. Blanch. “Enhanced cellulase production using solka floc in a fed-batch fermentation,” *Biotechnology Letters*, vol. 4, no. 12, pp. 785–788, 1982.

[22] L.T. Fan, Y.H. Lee, and D.H. Beardmore. “Mechanism of the enzymatic-hydrolysis of cellulose - effects of major structural features of cellulose on enzymatic-hydrolysis,” Biotechnology *and Bioengineering*, vol. 22, no. 1, pp. 177–199, 1980.

[23] L.T. Fan, Y.H. Lee, and D.H. Beardmore. “The influence of major structural features of cellulose on rate of enzymatic-hydrolysis,” *Biotechnology and Bioengineering*, vol. 23, no. 2, pp. 419–424, 1981.

[24] D. Ciolacu, F. Ciolacu, and V.I. Popa. “Supramolecular structure – a key parameter for cellulose biodegradation,” *Macromolecular Symposia*, vol. 272, pp. 136–142, 2008.

[25] M. Hall, P. Bansal, J.H. Lee, M.J. Realff, and A.S. Bommarius. “Cellulose crystallinity - a key predictor of the enzymatic hydrolysis rate,” *Febs Journal*, vol. 277, no. 6 pp. 1571–1582, 2010.

[26] P. Cen and L. Xia. “Production of cellulase in solid state ferementation.” In: T. Scheper, editor. *Recent progress in bioconversion of lignocellulosics, Advances in Biochemical Engineering/Biotechnology*, vol. 65. Berlin: Springer; 1999, p. 69.

[27] C. Krishna. “Solid-state fermentation systems - An overview.” *Critical Reviews in Biotechnology*, vol. 25, no. 1–2, pp. 1–30, 2005.

[28] M. Mandels and J. Weber. “Production of cellulases.” *Advances in Chemistry Series*, vol. 95, pp. 391–414, 1969.

[29] K. Brijwani, H.S. Oberoi, and P.V. Vadlani. “Production of a cellulolytic enzyme system in mixed-culture solid-state fermentation of soybean hulls supplemented with wheat bran,” *Process Biochemistry*, vol. 45, no. 1, pp. 120–128, 2010.

[30] R. Abalone, A. Cassinera, A. Gaston, and M. A. Lara. “Some physical properties of amaranth seeds,” *Biosystems Engineering*, vol. 89, no. 1, pp. 109–117, 2004.

[31] E. Milani, M. Seyed, A. Razavi, A. Koocheki, V. Nikzadeh, N. Vahedi, M. MoeinFard, and A. GholamhosseinPour. “Moisture dependent physical properties of cucurbit seeds,” *International Agrophysics*, vol. 21, no. 2, pp. 157–168, 2007.

[32] J.Y. Zhu, G.S. Wang, X.J. Pan, and R. Gleisner. “Specific surface to evaluate the efficiencies of milling and pretreatment of wood for enzymatic saccharification,” *Chemical Engineering Science*, vol. 64, no. 3, pp. 474–485, 2009.

[33] S. Baker and T. Herrman. “Evaluating particle size,” Kansas State University Agricultural Experiment Station and Cooperative Extension Service MF-2051, 2002.

[34] S. Park, J.O. Baker, M.E. Himmel, P.A. Parilla, and D.K. Johnson. “Cellulose crystallinity index: measurement techniques and their impact on interpreting cellulase performance,” *Biotechnology for Biofuels*, vol. 3, pp. 10, 2010.

[35] C.J. Garvey, I.H. Parker, and G.P. Simon. “On the interpretation of X-ray diffraction powder patterns in terms of the nanostructure of cellulose I fibres.” *Macromolecular Chemistry and Physics*, vol. 206, no. 15, pp. 1568–1575, 2005.

[36] M. Wada, T. Okano, and J. Sugiyama. “Synchrotron-radiated X-ray and neutron diffraction study of native cellulose,” *Cellulose*, vol. 4, no. 3, pp. 221–232, 1997.

[37] R.G. Liu, H. Yu, and Y. Huang. “Structure and morphology of cellulose in wheat straw,” *Cellulose*, vol. 12, no. 1, pp. 25–34, 2005.

[38] J.R. Mielenz, J.S. Bardsley, and C.E. Wyman. “Fermentation of soybean hulls to ethanol while preserving protein value” *Bioresource Technology*, vol. 100, no. 14, pp. 3532–3539, 2009.

[39] A.C. Schirmer-Michel, S.H. Flores, P.F. Hertz, G.S. Matos, and M.A.Z. Ayub. “Production of ethanol from soybean hull hydrolysate by osmotolerant Candida guilliermondii NRRL Y-2075,” *Bioresource Technology*, vol. 99, no. 8, pp. 2898–2904, 2008.

[40] N. Aro, T. Pakula, and M. Penttila. “Transcriptional regulation of plant cell wall degradation by filamentous fungi,” *FEMS Microbiology Reviews*, vol. 29, no. 4, pp. 719–739, 2005.

[41] P. Kumar, D.M. Barrett, M.J. Delwiche, and P. Stroeve. “Methods for Pretreatment of Lignocellulosic Biomass for Efficient Hydrolysis and Biofuel Production,” *Industrial & Engineering Chemistry Research*, vol. 48, no. 8, pp. 3713–3729, 2009.

[42] L. Segal, J.J. Creely, A.E. Martin, and C.M. Conrad. “An empirical method for estimating the degree of crystallinity of native cellulose using X-ray diffractometer,” *Textile Research Journal*, vol. 29, pp. 786–794, 1959.

[43] N. Kasai and M. Kakudo. “X-ray diffraction by macromolecules.” New York: Springer, 2005, p. 504.

[44] C.G. Vonk. “Computerization of Rulands x-ray method for determination of crystallinity in polymers,” *Journal of Applied Crystallography*, vol. 6, pp. 148–152, 1973.

[45] K. Brijwani and P.V. Vadlani. “Solid state fermentation of soybean hulls for cellulolytic enzymes production.” In: T.B. Ng, editor. *Soybean- Applications and Technology*, in press. Austria: INTECH; ISBN 978-953-307-207-4.

[46] D. Gregg and J.N. Saddler. “A techno-economic assessment of the pretreatment and fractionation steps of a biomass-to-ethanol process,” *Applied Biochemistry and Biotechnology*, vol. 57–8, pp. 711–727, 1996.

[47] H. Palonen, A.B. Thomsen, M. Tenkanen, A.S. Schmidt, and U. Viikari. “Evaluation of wet oxidation pretreatment for enzymatic hydrolysis of softwood,” *Applied Biochemistry and Biotechnology*, vol. 117, no. 1, pp. 1–17, 2004.

[48] J.M. Gossett, D.C. Stuckey, W.F. Owen, and P.L. McCarty. “Heat-treatment and anaerobic-digestion of refuse,” *Journal of Environmental Engineering Division-ASCE*, vol. 108, pp. 437–454, 1982.

[49] C. Aiello, A. Ferrer, and A. Ledesma. “Effect of alkaline treatments at various temperatures on cellulase and biomass production using submerged sugarcane bagasse fermentation with *Trichoderma reesei* QM 9414,” *Bioresource Technology*, vol. 57, no. 1, pp. 13–18, 1996.

[50] A.T.W.M. Hendriks and G. Zeeman. “Pretreatments to enhance the digestibility of lignocellulosic biomass,” *Bioresource Technology*, vol. 100, no. 1, pp. 10–18, 2009.

[51] P.T. Pienkos and M. Zhang. “Role of pretreatment and conditioning processes on toxicity of lignocellulosic biomass hydrolysates,” *Cellulose*, vol. 16, no. 4, pp. 743–762, 2009.

[52] C.P. Kubicek, G. Muhlbauer, M. Klotz, E. John, and E.M. Kubicekpranz. “Properties of a conidial-bound cellulase enzyme-system from *Trichoderma reesei*,” *Journal of General Microbiology*, vol. 134, pp. 1215–1222, 1988.

[53] B. Seiboth, S. Hakola, R.L. Mach, P.L. Suominen, and C.P. Kubicek. “Role of four major cellulases in triggering of cellulase gene expression by cellulose in *Trichoderma reesei*,” *Journal of Bacteriology*, vol. 179, no. 17, pp. 5318–5320, 1997.

[54] N.E. Lee, M. Lima, and J. Woodward. “Hydrolysis of cellulose by a mixture of *Trichoderma reesei* cellobiohydrolase and *Aspergillus niger* endoglucanase,” *Biochimica Et Biophysica Acta*, vol. 967, no. 3, pp. 437–440, 1988.

[55] R.P. de Vries and J. Visser. “*Aspergillus* enzymes involved in degradation of plant cell wall polysaccharides,” *Microbiology and Molecular Biology Reviews*, vol. 65, no. 4, pp. 497–522, 2001.

Figure 3.1 X-ray diffractograms. Gaussian smoothing followed by Voigt function was used to fit the diffractogram output of the instrument. (a) Native soybean hulls. (b) Steam-pretreated soybean hulls. (c) HCl-pretreated soybean hulls. (d) H_2SO_4-pretreated soybean hulls. (e) NaOH-pretreated soybean hulls. Planes corresponding to 2θ are 101 plane (~15º), $10\bar{1}$ (~17º), 021 plane (~20º), 002 plane (~22º), and 040 plane (~34º). (*Adapted from [45]*).

(a)

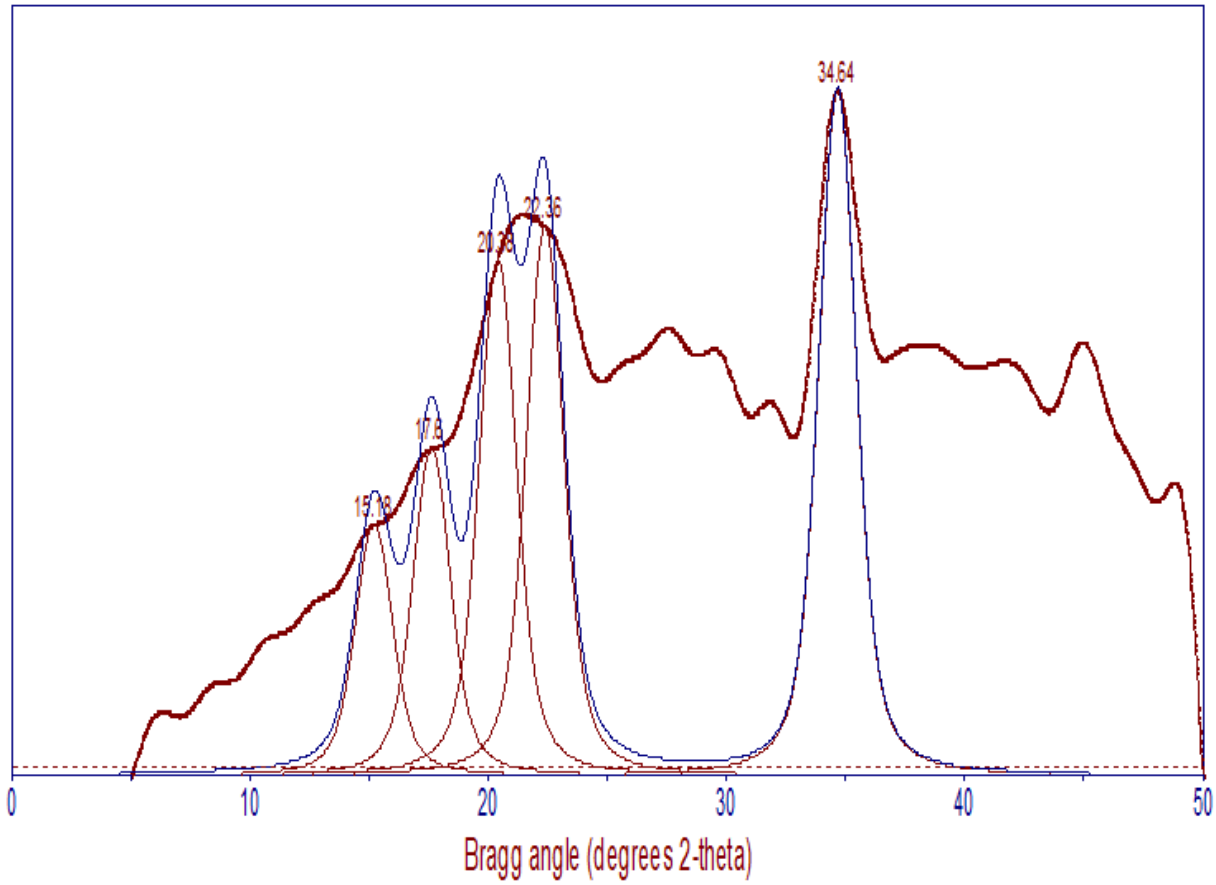

(b)

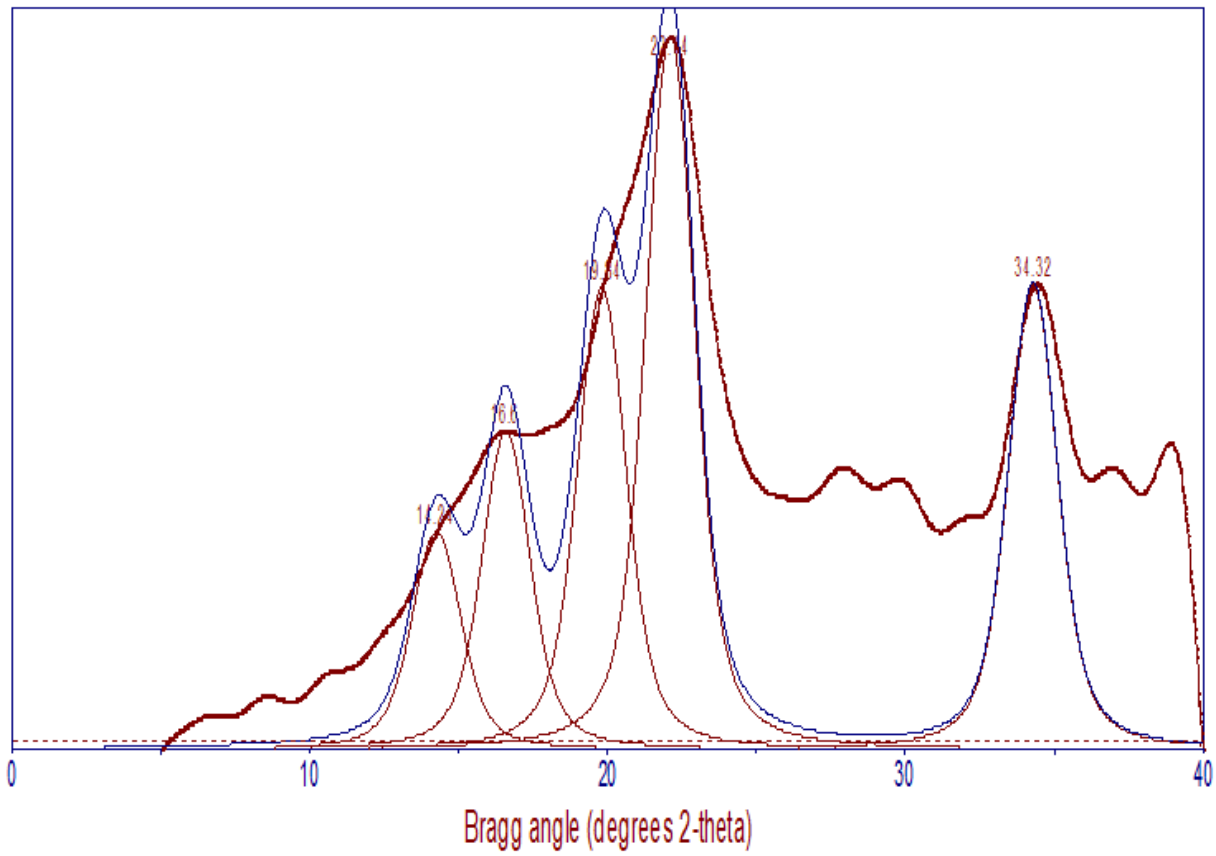

(c)

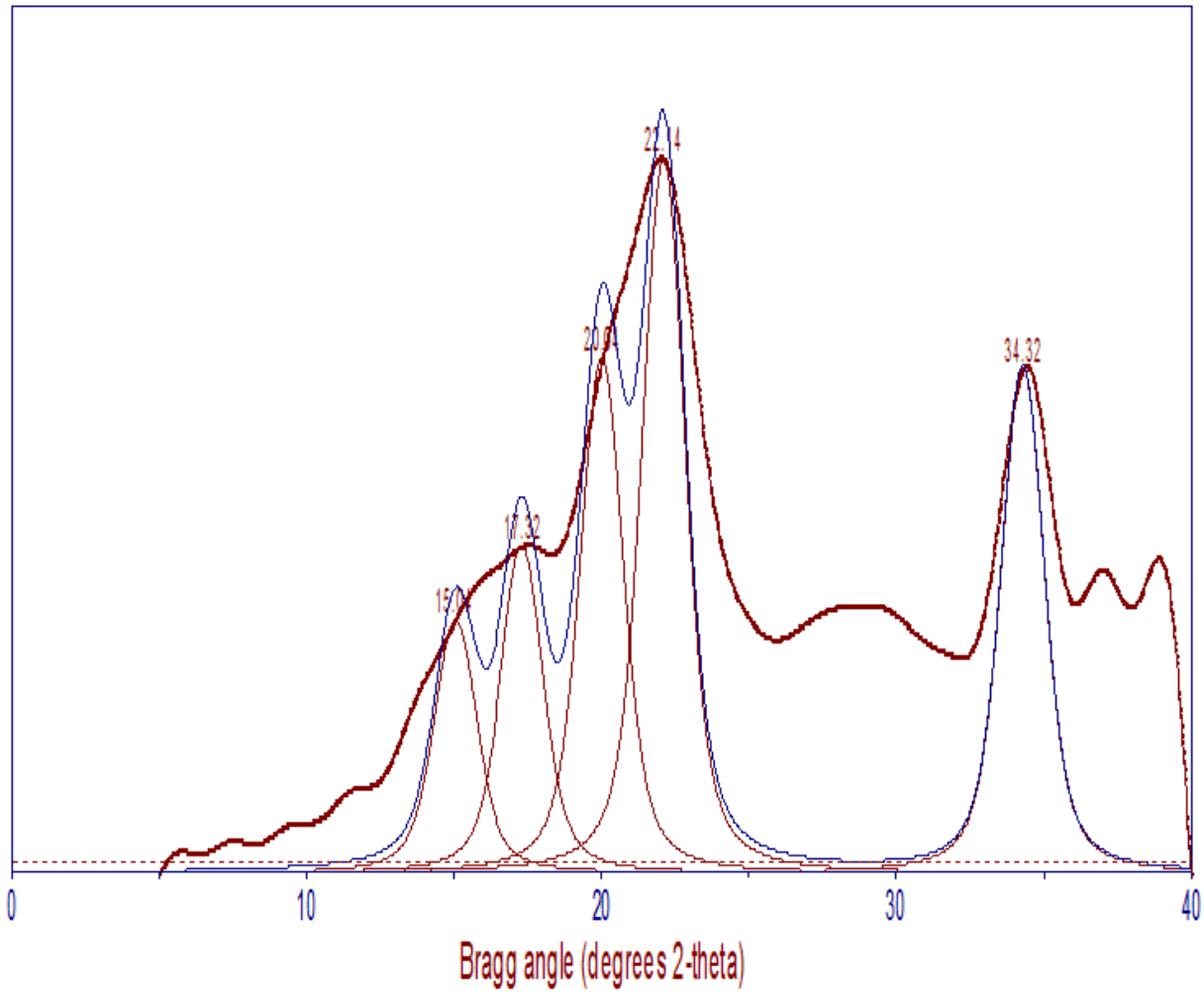

(d)

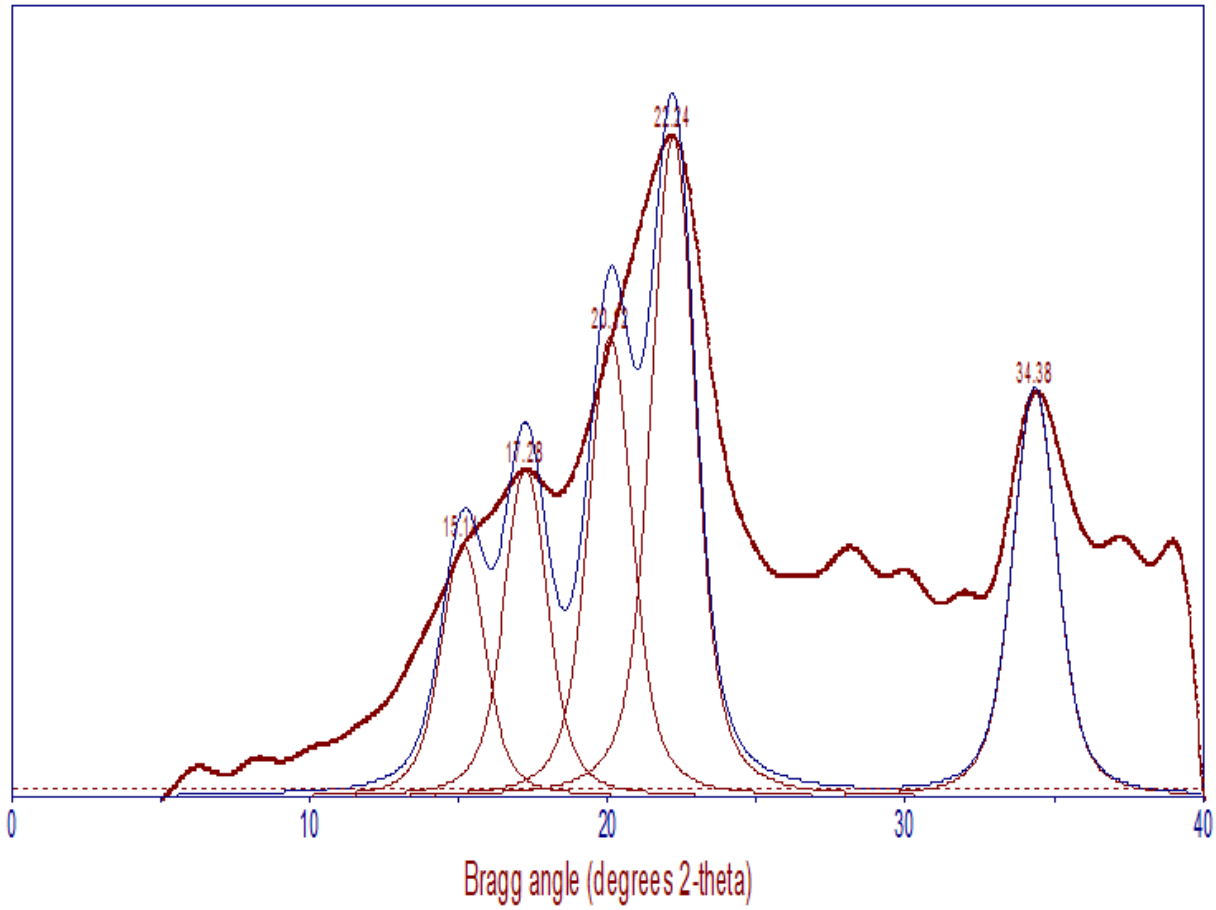

(e)

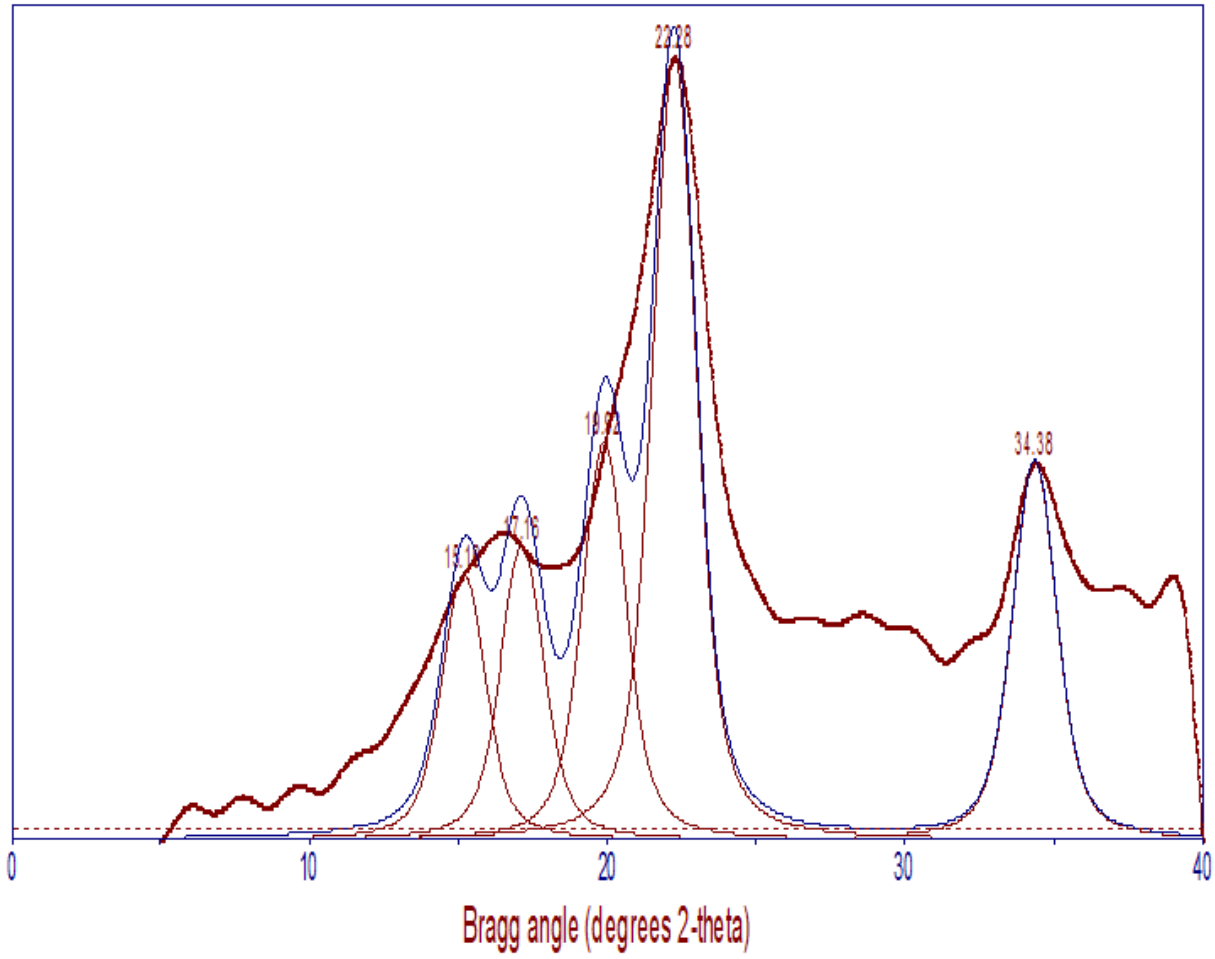

Figure 3.2 Effect of different pretreatments on cellulolytic enzyme production in 5 days grown mono- and mixed cultures of *Trichoderma reesei* and *Aspergillus oryzae*. (a) Filter paper activity. (b) B-glucosidase activity. (c) Endocellulase activity. (d) Xylanase activity. Abbreviations: T.r, *T. reesei*; A.o, *Aspergillus oryzae*; Mix, 1:1 mixture of *T. reesei* and *A. oryzae* cultures; Native, untreated soybean hulls; Steam, steam-pretreated soybean hulls; HCl, hydrochloric acid-pretreated soybean hulls; H2SO4, sulfuric-acid-pretreated soybean hulls; NaOH, sodium hydroxide-pretreated soybean hulls. Refer to text for more details on conditions of pretreatments. Data are expressed as mean ± SE, n=4.

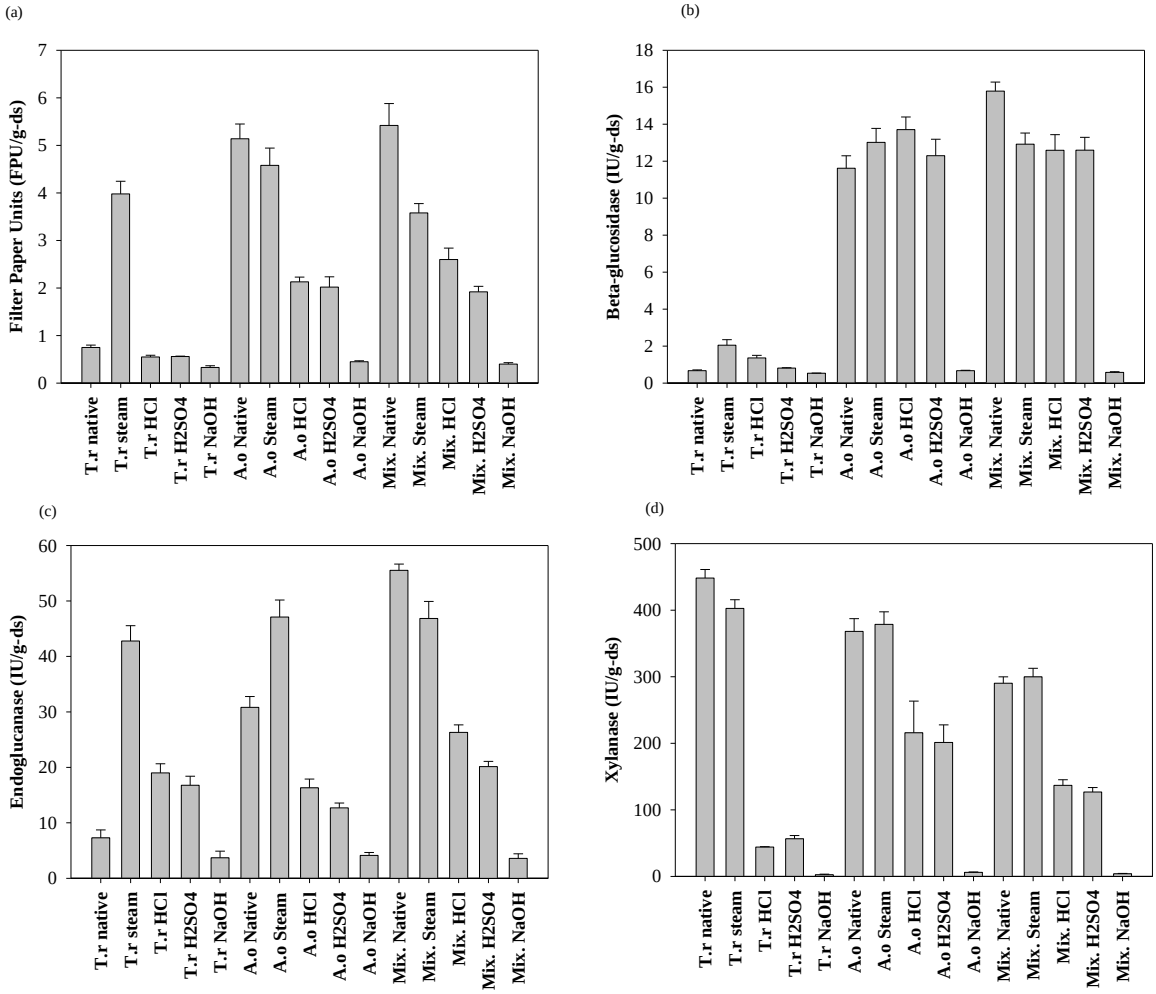

Table 3.1 Composition of various substrates (dry basis)

Sample	Cellulose (ADF-ADL)	Hemicellulose (NDF-ADF)	Holocellulose*	Lignin (ADL)	Protein	Ash
Native soybean hulls	45.90±0.60	19.59±0.57	65.48±1.14^{A}	0.75±0.09	11.96±0.06	5.21±0.01
Steam-treated soybean hulls	49.99±2.67	19.32±0.83	69.31±3.38^{A}	1.19±0.15	10.43±0.07	2.67±0.05
HCl-treated soybean hulls	57.19±0.40	15.33±0.96	72.52±1.08^{A}	1.33±0.07	9.60±0.03	2.55±0.05
H_2SO_4-treated soybean hulls	54.74±0.47	17.39±0.77	72.14±1.23^{A}	1.47±0.19	10.11±0.11	2.78±0.08
NaOH-treated soybean hulls	60.45±1.61	15.66±1.58	76.11±3.15^{A}	1.23±0.03	3.45±0.06	3.26±0.06

*Represents sum of cellulose and hemicellulose; data are expressed as mean ± SE; n=4; means with same letters do not differ significantly. Pairwise comparisons between total cellulosics were tested using Tukey Kramer HSD at $P<0.05$.

Table 3.2 Physical attributes of various substrates

Sample	Degree of crystallinity (%)	Adj. R^2 for X-ray fitting	RMSE for X-ray fitting	Bed porosity (%)	Volumetric specific surface (cm^{-1})
Native soybean hulls	42.56±3.34	0.91	15.06	40.41±1.91	122.28±1.91
Steam-treated soybean hulls	57.16±2.39	0.94	12.48	57.45±0.50	120.41±2.34
HCl-treated soybean hulls	56.29±0.12	0.94	13.40	53.65±0.12	120.28±2.47
H_2SO_4-treated soybean hulls	56.53±0.12	0.95	13.35	50.02±0.68	120.77±2.16
NaOH-treated soybean hulls	59.72±0.43	0.96	11.70	56.77±0.57	128.09±1.84

Data are expressed as mean ± SE; n=4. It should be noted that RMSE values are scaled on y-axis that represents X-ray intensities of various peaks corresponding to Bragg planes. Peak values are usually in the range of 100-500 counts.

Table 3.3 Effect of interaction between crystallinity and bed porosity of substrates on cellulolytic enzyme production in both mono and mixed SSF of *T. reesei* and *A. oryzae*

Interaction	Culture	Cellulolytic enzyme system				Treatments considered
		Filter paper units (FPU/g-ds)	B-glucosidase (IU/g-ds)	Endoglucanase (IU/g-ds)	Xylanase (IU/g-ds)	
Crystallinity × porosity	*Trichoderma reesei*	<0.0001*	0.0388*	<0.0001*	0.0472	Native, steam
Crystallinity × porosity	*Aspergillus oryzae*	0.4629	0.9218	0.0005*	0.9912	Native, steam
Crystallinity × porosity	Mixed	0.0044*	0.0449	0.0257**	0.9061	Native, steam

*Indicates Tukey probability for a particular interaction is significant at 95% confidence. **Indicates significant at P<0.05 but not significant at P<0.01. Model eq. 10 ran in SAS 9.1.
Abbreviations: Native, untreated soybean hulls; Steam, steam-pretreated soybean hulls.

Chapter 4 - Effect of Bed Porosity and Crystallinity of Substrate on Cellulolytic Enzymes Production in Solid State Fermentation

Abstract

Current work demonstrates effect of bed porosity and crystallinity of soybean hulls on cellulolytic enzymes production in fungal solid state fermentation (SSF). By altering moisture content, bed porosity was varied and substrates with higher porosity had significantly higher enzyme production in both *T. reesei* and *A. oryzae* fermentations. Effect of crystallinity was investigated by propagating two cultures on crystalline (avicel and cotton linter) and amorphous (Walseth) forms of celluloses before using them as inoculum. Cotton linter-adapted *T. reesei* had 5.23 FPU/g-ds, 3.8 IU/g-ds beta-glucosidase, and 65.13 IU/g-ds endocellulase activities compared to 3.91 FPU/g-ds, 2.28 IU/g-ds beta-glucosidase, and 55 IU/g-ds endocellulase activities in Walseth-adapted cultures. There was no significant change in xylanase in our experiments. On the other hand, crystalline cellulose adapted *A. oryzae* had significantly reduced cellulolytic enzymes production. This study reinforces role of substrate properties in controlling enzyme production, which should provide a framework for quantitative SSF process design.

Keywords: Soybean hulls, *Trichoderma reesei*, *Aspergillus oryzae*, crystalline cellulose, porosity, X-ray diffraction

1. Introduction

Bioconversion of lignocellulosic biomass has been projected as a sustainable and renewable means to produce liquid transportation fuels *(1)*. Several factors provide impetus to this growing trend; prominent ones are cost and uncertain supplies of fossil fuels, rising level of CO_2 in the atmosphere, and rapid growth in the development of lignocellulosic biomass-based biorefineries *(2)*. Due to complexity and diversity of structural plant cell wall the cost effective

release of fermentable sugars from the lignocellulosic biomass poses largest technological and economic challenge for biomass biorefineries *(3,4)*. For effective biomass hydrolysis multiple enzyme activities collectively called as cellulolytic enzyme complex is required *(3,5)*. A cellulolytic enzyme complex consists of three major activities: exoglucanase (EC 3.2.1.91), endoglucanase (EC 3.2.1.4), and beta-glucosidase (EC 3.2.1.21) *(6)*. Xylanase (EC 3.2.1.8) complements this system; it is needed to elicit complete and efficient hydrolysis of the lignocellulosic biomass, which has appreciable amount of hemicellulose or xylan *(7,8)*. Ostensibly a sustainable bio-economy needs cellulolytic enzyme complex to be produced cost-effectively with excellent catalytic properties *(9)*.

Solid state fermentation (SSF) offers low-cost alternative for producing cellulolytic enzyme complex using natural polymers derived from agro-industrial residues *(10,11)*. In addition, the environment in SSF closely resembles the natural habitat of fungi that can be useful in production of enzyme systems with enhanced catalytic features *(12-14)*. The air phase is important in SSF employing aerobic fungal cultures for enzyme production *(15)*. Air phase not only promotes intra-particle oxygen transfer but also serve as heat transfer fluid for temperature control and excess heat removal *(16-18)*. The air phase in SSF is network of connected pores within substrate matrix characterized by air filled porosity or bed porosity *(15)*. If the pores between the hyphae are filled with water, oxygen diffusion limitation becomes inevitable in fungal pellets *(19)*. On the other hand substrate with large number of air rich pores or higher bed porosity (voidage) will promote higher oxygen transfer and better productivity of the process. Rahardjo et al. *(20,21)* explained this phenomena by employing model substrates that had varying degree of open spaces during production of α-amylase in solid state cultures of *A. oryzae*. Tao et al. *(13)*, and Muniswaran and Charyulu *(22)* proposed the role of bed porosity in

facilitating or promoting better fungal growth and consequently enhanced enzyme productivity. However, in none of these studies bed porosity of the solid substrate was measured to explain the relationship of bed porosity with enzyme production.

In full scale SSF process, in addition to bed porosity other parameters like microbial cell physiology, composition of the solid substrate, and substrate reactivity could influence the productivity of the process *(23,24)*. Substrate reactivity, especially in case of cellulosic substrates, is influenced by crystallinity of cellulose *(25,26)*. In SSF and during cellulolytic enzyme production using any complex cellulosic substrates, the first step is the hydrolysis of substrate to glucose by constitutively expressed enzymes that facilitate fungal propagation. Glucose is known to cause catabolite repression in fungi growing on complex substrates *(27)*. Consequently rate at which glucose is released would influence the production of enzymes in SSF. In fact, Fan et al. *(28,29)* have shown that rate of cellulose degradation is dependent on crystallinity of the cellulosic substrate. This suggests amorphous cellulose would result in faster glucose release leading to stronger catabolite repression or reduced cellulase production. Another aspect of cellulose hydrolysis is that digestion of crystalline cellulose requires the concerted action of both exo- and endoglucanases. Hence, it is foreseeable that cellulolytic enzymes derived from fungi growing on crystalline cellulose would have better catalytic properties towards recalcitrant cellulose. Crystallinity of cellulosic sample, therefore, could not only alter the quantity of enzymes produced but also the quality of enzymes (proportion of various activities within cellulolytic enzyme complex).

The objective of this work is to demonstrate unequivocally the role of bed porosity and crystallinity of solid substrate (soybean hulls) during enzyme production in mono and mixed culture SSF using *Trichoderma reesei* and *Aspergillus oryzae* cultures. To achieve this objective

porosity of the substrate bed (soybean hulls) was altered by varying the initial moisture content and its impact on enzyme production was investigated. Further both cultures were adapted on crystalline cellulose in liquid medium before using them as inoculum for SSF of soybean hulls for enzyme production. It was anticipated that physiological changes induced in fungal cultures due to adaptation on crystalline cellulose would became apparent during cellulolytic enzyme production in SSF. The current work lays the groundwork for an in-depth understanding of process chemistry of SSF that could aid successful adoption of this technology for cellulolytic enzyme production for biofuels and bioproducts.

2. Material and methods

2.1. Materials

Ground soybean hulls were purchased from Archer Daniels Midland, Salina, KS. The crystalline cellulose (avicel PH 101 and cotton linter) and cellobiose were of high purity and procured from Sigma Aldrich, MO. All dehydrated media and the analytical-grade chemicals were purchased from Difco, BBL, NJ and Fisher Scientific, PA.

2.2. Microorganisms and their propagation

T. reesei (ATCC 26921) and *A. oryzae* (ATCC 12892) were obtained from American Type Culture Collection (ATCC), VA, in lyophilized form. Strains were maintained on potato dextrose agar (PDA) and suspensions of spores (10^8 spores/ml) from two strains were generated per methods described in *(8)* and stored at 4 °C until used.

2.3. Cellulolytic enzymes production in soybean hulls of altered bed porosity

Both untreated (native) and steam pretreated soybean hulls (5 g) were adjusted to 60, 65, 70 and 80% initial moisture content (mc) on wet basis using Mandels media *(30)* of pH 5 to alter

the bed porosity. Samples were sterilized in vertical sterilizer (121 ºC/15 psi gauge) and cultures as spore suspensions (10^8 spores/ ml-suspension) at the rate of 10% (v/w) were added. Both fungal species were used as mono and mixed cultures. Mixed culture contained 1:1 ratio of *T. reesei* and *A. oryzae*. Flasks were incubated for 5 days at 30 ºC. Following incubation crude cellulolytic enzymes were extracted and analyzed for filter paper activity (FPU/g-ds), endocellulase (IU/g-ds), β-glucosidase (IU/g-ds), and xylanase (IU/g-ds) activities. Enzymatic assays were carried out using standard protocols described in Brijwani et al. *(8)*. Enzyme activities were reported as units per gram of dry substrate (g-ds). Steam pretreatment was carried out by suspending soybean hulls at 5% (w/v) in distilled water followed by autoclaving at 121 ºC for 60 min. The pretreated samples were washed with distilled water once and dried overnight in forced draft oven at 45 ºC before being used as substrate in SSF as described above.

2.4. Cellulolytic enzymes production in steam-pretreated soybean hulls

2.4.1. Propagation of two cultures on crystalline and amorphous cellulose and on soluble sugar

A loopful of mycelium of two cultures (*T. reesei* and *A. oryzae*) grown in potato dextrose broth was spread on agar plates comprising nutrient medium with crystalline cellulose, amorphous cellulose, or cellobiose as soluble sugar. Two types of crystalline cellulose were used: avicel PH 101 and cotton linter; the amorphous cellulose was Walseth cellulose prepared from cotton linters as described in Hsu and Penner *(31)*. Walseth cellulose was used immediately after preparation without drying. Moisture in Walseth was taken into account during the preparation of nutrient medium containing Walseth cellulose. The nutrient medium used was Czapek-Dox medium as described in Jakubikova et al. *(32)*. The medium had following constituents (g/L): a particular carbon source (crystalline cellulose, amorphous cellulose, or

cellobiose) 10, yeast extract 7, $NaNO_3$ 2, K_2HPO_4 1, KCl 0.5, $MgSO_4$ 0.5, $FeSO_4$ 0.01, agar 25, and distilled water 1 L. pH was adjusted to 6 before sterilization. Agar plates were incubated at 25º C for 7 days approximately until appropriate sporulation (observed visually) was attained. Spores were harvested from the plates by gentle washing with distilled water containing 0.01% Tween 80 to obtain spore suspensions of 10^8 spores/ml. Spore suspensions were stored at 4 °C until used.

2.4.2. Cellulolytic enzymes production in steam-pretreated soybean hulls using adapted cultures

Steam pretreated soybean hulls were adjusted to 70% mc using pH 5 Mendels medium *(30)*. Flasks were sterilized and then inoculated with a 10% (v/w) spore suspension (~10^8 spores/ml) of *T. reesei*, *A. oryzae*, or a 1:1 mix of the two cultures adapted on two crystalline celluloses, one amorphous cellulose, and one soluble sugar. Flasks were eventually labeled as avicel, cotton linter, Walseth, and cellobiose, representing the source of adapted culture inoculated to steam-treated soybean hulls. All flasks were kept at 30 ºC for 5 days. Following incubation, enzymes were extracted and activities were analyzed per Brijwani et al. *(8)*, as mentioned previously.

2.5. Analysis of bed porosity and crystallinity

2.5.1. Bed Porosity

Bed porosity of native and steam pretreated soybean hulls adjusted to different moisture contents was computed from the values of true density (ρ_t) and bulk density (ρ_b) by using the relationship *(33)* as follows:

$$\varepsilon = \left(1 - \frac{\rho_b}{\rho_t}\right) \times 100 \quad (1)$$

True density (ρ_t) was determined using a standard liquid pycnometer by determining the volume of the sample at various moisture contents studied. Volume (V, cm^3) was calculated from the following expression *(34)*:

$$V = \frac{(M_{ps} - M_p) - (M_{pts} - M_t)}{\rho_{tol}} \quad (2)$$

Where M_t is mass of the pycnometer filled with toluene, M_{ps} is the mass of pycnometer and sample, M_p is mass of the pycnometer, M_{pts} is mass of the pycnometer filled with toluene and sample, and ρ_{tol} is the density of toluene. Knowing V, the true density (g/cc) then can be calculated from the following expression:

$$\rho_t = \frac{(M_{ps} - M_p)}{V} \quad (3)$$

Bulk density (ρ_b) is estimated by weighing the samples (of different mc) after pouring in a vessel of known volume (10 ml) *(33)*.

2.5.2. X-ray crystallinity using deconvolution method

Wide-angle X-ray diffraction (XRG 3100 X-ray generator, Phillips Electronics Instrument Inc., Texas, USA) was used to estimate the crystallinity of cellulosic substrates (avicel, cotton linter, and Walseth cellulose). The X-rays from a Cu tube operating at 35 KV and 20 mA were collected by an energy dispersive detector that is able to resolve CuK_α line. Counts were collected at a step size of 0.02º at a series of angles between 5º and 40º. Speed of count collection was 0.6º/min. The raw diffractograms were subjected to deoconvolution method that requires fitting procedure using non-linear least squares numerical procedure. The deconvolution method separate amorphous and crystalline contributions to the diffraction spectrum under curve-fitting process by selecting a shape function *(35)*. Shape function of the observed X-ray

profile h(2θ) is normally the convolution (Θ) of the intrinsic specimen profile f(2θ) with the spectral distribution (W) and the instrumental function (G) superimposed over the background b *(35)*, as given below:

$$h(2\theta) = [(W\Theta G)\Theta f](2\theta) + b \qquad (4)$$

The Voigt function, which is a convolution of Gaussian and Lorentzian peak functions, was used for the deconvolution of the XRD spectra. Voigt function appropriately takes into account the peak broadening due to diffusive scattering *(36,35)*, and thus provides reliable measures of crystallinity *(37,38)*.

Using the Voigt function intensity of the reflection is expressed as follows:

$$f(2\theta) = \frac{a_o \int_{-\infty}^{\infty} \frac{\exp\,(-(2\theta)^2)}{a_l^2 + \left(\frac{x - a_c}{a_g} - 2\theta\right)^2} d(2\theta)}{\int_{-\infty}^{\infty} \frac{\exp\,(-(-(2\theta)^2)}{a_l^2 + (2\theta)}\, d(2\theta)} \qquad (5)$$

Where a_o is the amplitude of the peak, a_c is the center of the peak, a_l is the width of the Lorentzian component, and a_g is the width of the Gaussian component of the peak. Five crystalline peaks correspond to following Miller indices (hkl): 101, 10$\bar{1}$, 002, 021, and 040 have been identified in celluloses from plant material; 002 is the prominent reflection representing crystalline cellulose (sometimes resolved into 021 plane as well) *(39)*. These five X-ray peaks were fitted using Voigt function as profile shape function using Peakfit™ (SeaSolve Software Inc., MA, USA) program and degree of crystallinity (X_{cr}) of the sample was calculated per the equation 6 described by Wada et al. *(36)*.

$$X_{cr}\,(\%) = \frac{I_{002} + I_{021}}{I_{101} + I_{10\bar{1}} + I_{002} + I_{021} + I_{040}} \times 100 \qquad (6)$$

Where I followed by a subscript represents the integrated intensity of the particular Bragg plane. Crystallinity, therefore, represents the fraction of α-cellulose represented by planes 002 and 021 present in a particular sample.

2.6. Statistical analysis

Statistical analysis was carried out using the GLM procedure in SAS software version 9.1 (SAS Institute, NC, USA). Multiple comparisons were conducted using Tukey Kramer HSD at $P<0.05$.

3. Results and discussion

3.1. Effect of bed porosity on the production of cellulolytic enzymes in native and steam treated soybean hulls

Moisture plays an important role in growth of fungi and production of enzymes in SSF *(40,41)*. A hallmark of moisture is that it also affects the bed porosity of various agricultural substrates *(33,34)*. Therefore moisture was used as means to vary the bed porosity such that an explicit demonstration of effect of porosity on enzyme production can be evaluated. Soybean hulls were chosen as SSF substrate. Soybean hulls have rich cellulosic composition *(8)* and represent one of the major crop residues available globally including the state of Kansas, and thus have potential for industrial fermentation substrate. **Table 4.1** shows the variation in porosity of native and steam treated soybean hulls with the moisture. Inclusion of steam pretreated soybean hulls stem from our earlier work *(38)* where it was demonstrated that steam pretreatment significantly enhanced the production of enzymes in fungal SSF. Native (untreated) soybean hulls were included for comparison. It is evident that increase in moisture content led to decrease in porosity of substrates **(Table 4.1)**. Steam pretreated soybean hulls had significantly ($P<0.05$) higher porosity at any initial moisture compared to native soybean hulls.

Figures 4.1a-4.1c feature the production of cellulolytic enzyme at various initial moisture contents in both mono and mixed cultures of *T. reesei* and *A. oryzae*. Expectedly and in agreement with *(38)* steam treatment resulted in significant ($P<0.05$) increase in all the three activities: fitter paper, beta-glucosidase and endocellulase activities at all the moisture levels investigated in *T. reesei* SSF **(Figure 4.1a)**. The expression of xylanase, however, remained constant across the moisture levels for both native and steam treated substrates. Filter paper activity in native soybean hulls significantly ($P<0.05$) decreased from 1.43 FPU/g-ds to 0.74 FPU/g-ds on increasing the moisture content from 60 to 80%. Similarly, in steam pretreated soybean hulls, filter paper activity decreased from 4.75 FPU/g-ds at 60% mc to 2.24 FPU/g-ds at 80% mc. Beta-glucosidase activity in native soybean hulls was significantly lower at 80% mc compared to other moisture contents. Steam pretreated soybean hulls also had significant decrease in beta-glucosidase activity from 2.92 IU/g-ds to 0.85 IU/g-ds when moisture was increased from 60% to 80%. Endocellulase activity for both native and steam pretreated soybean hulls were significantly ($P<0.05$) higher at 60-65% mc than at 80% mc **(Figure 4.1a)**. The above discussion clearly indicated that moisture had definite role in the enzyme production system in *T. reesei*. Low moisture tend to produce more porous substrate bed **(Table 4.1)** that led to enhanced enzyme production in *T. reesei* cultures compared to high moisture that caused decrease in open spaces leading to reduction in the enzyme production. These investigations are supported by research undertaken elsewhere *(13,22)*.

In *A. oryzae* SSF, both filter paper and endoglucansase activities were significantly higher ($P<0.05$) in native soybean hulls compared to steam pretreated soybean hulls at all moisture contents studied. Beta-glucosidase and xylanase activities remained fairly similar (not significantly different) at all moisture levels between the two substrates (**Figure 4.1b**).

Decreased cellulase productivity of *A. oryzae* in steam pretreated soybean hulls was attributed to increased crystallinity of soybean hulls after pretreatment (data not shown). It has been known that *A. oryzae* cellulases are not particularly active toward crystalline cellulose as compared to *T. reesei* cellulases, which explains the reason for the observed trend. Additional details on pretreatment effects on cellulolytic enzyme production in SSF performed in authors lab is explained in *(38)*. Inspection of **Figure 4.1b** revealed that all the activities including xylanase in both native and steam pretreated soybean hulls peaked at 70% mc and decreased on either side of it.

In mixed culture of two fungi, trend similar to *A. oryzae* was observed. This was plausibly attributed due to dominant nature of *A. oryzae* over *T. reesei*. As a result native soybean hulls had significantly ($P<0.05$) higher enzyme production than steam pretreated soybean hulls (**Figure 4.1c**). Similar to the observations in **Figure 4.1b** the activities peaked at 70% mc and reduced on either side of it. It is evident that both *A. oryzae* and mixed cultures were more sensitive to changes in moisture content. Though moisture played an important role, however when optimum moisture was maintained, enzyme production did show dependence on porosity. This was evident by comparing the results between 70% and 80% mc (**Figures 4.1b-4.1c**). At 80% mc, moisture was more than optimum, however, all the activities of cellulase system i.e. filter paper, beta-glucosidase and endocellulase in both *A. oryzae* and mixed cultures were significantly ($P<0.05$) lower in both native and steam treated soybean hulls. Clearly reduced porosity **(Table 4.1)** due to excessive moisture impacted the production of enzymes in both the cultures at 80% mc.

To understand the dynamics of bed porosity and its relationship with the enzyme production processes occurring at micro-scale within SSF have to be investigated. At micro-

scale, SSF involves a discrete phase where microorganisms grow on the moist substrate packing both inside and between them *(42)*. A micro-scale view of SSF is depicted in **Figure 4.2.** Inspection of the schematic reveals that bed porosity is necessary to ensure open spaces around the particles where gas exchange could take place. Another aspect of bed porosity is that more porous bed offers less resistance to air flow by decreasing the obstructions to air flow *(15)* or by increasing the permeability. Permeability is defined as ability of fluid to flow through a mutliphase material, and can be quantified using Darcy's law that explains flow of fluids through porous media. For laminar flow, Darcy's law *(43)* relates the pressure drop across the matrix (distance x) to superficial velocity (ϑ), and viscosity (μ) by defining a matrix permeability (κ) as follows:

$$\vartheta = -\frac{\kappa}{\mu}\frac{dP}{dx} \tag{7}$$

Ergun *(44)* related permeability (κ) with the matrix properties and importantly predicted permeability (κ) as a function of bed porosity (equation 8) as follows:

$$\kappa = \frac{d_p}{A}.\frac{\varepsilon^3}{(1-\varepsilon)^2} \tag{8}$$

Equation (8) suggests for any particle size (d_p) of the substrate with A being constant, the resistance to air flow is dependent on bed porosity. High bed porosity leads to increased permeability of the bed and decreased resistance to air flow. In the context of SSF it would translate to better productivity of fungal cultures due to increased oxygen mass transfer. The relationship between bed porosity, and oxygen transfer and fungal growth is not discussed in this study. Nevertheless, bed porosity appears to be a critical design parameter that should be incorporated in SSF process design and optimization.

3.2. Effect of crystallinity on cellulolytic enzymes production in steam-treated soybean hulls

Two pure, crystalline forms of cellulose (avicel and cotton linter), amorphous Walseth cellulose (had no characteristic X-ray pattern unique to crystalline cellulose) prepared from cotton linters, and one soluble sugar cellobiose were used in this study. X-ray crystallinity for avicel and cotton linter was derived from fitted X-ray diffractograms **(Figure 4.3a-4.3b)**, and is shown in **Table 4.2**; the measurement agrees well with previous studies *(45,46)*. Fitted diffractograms had R^2>0.99 for both avicel and cotton linter. This highlighted the validity of current technique in evaluating crystallinity of paracrystalline substances. In paracrystalline materials like cellulosic substrates the interlocking amorphous regions result in diffusive scattering, which refrain separation of crystalline peak from amorphous peak. This makes the analysis non-trivial and inconsistent when using traditional methods like Segal et al. *(47)*. In a fitting procedure as described here the inherent disability is overcome such that accurate measurements of crystallinity can be achieved.

Data for cellulolytic enzyme production are presented in **Figure 4.4** for both mono- and mixed cultures (*T. reesei, A. oryzae*, and a 1:1 mix of the two). In the current work, the two cultures were propagated on standard substrates in a Czapek Dox medium to generate adapted spore suspension. We anticipated that differences in production profiles of the two cultures due to culturing on different substrates could be preserved and that those physiological changes would emerge when the cultures were re-inoculated in pretreated soybean hulls in SSF process. The reason behind prior adaptation was the inability of the two cultures to grow directly on highly crystalline cellulose in solid-state mode (unpublished data). The steam-pretreated substrate was chosen, because, as described earlier, it performed well in terms of enzyme

production in our previous studies *(38)*. A control was also included for comparison (i.e., steam-pretreated soybean hulls inoculated with a PDA-grown spore suspension of the two cultures).

As expected, crystallinity had a definite relationship with enzyme production in *T. reesei* cultures. Cotton-linter-adapted *T. reesei* had significantly higher production of filter paper units, beta-glucosidase units, and endocellulase units than the other treatments (**Figure 4.4a-4.4c**). Xylanase production **(Figure 4.4d)**, however, was significantly lower in both cotton linter and avicel than the control. Avicel adapted cultures on the other hand had expression levels of enzymes lower than cotton linter adapted cultures but similar to other treatments. Also, cellulosic substrate (crystalline and amorphous) performed much better than soluble sugars (cellobiose and glucose in PDA), particularly in endocellulase production **(Figure 4.4c)**.

The effect of crystallinity was interesting in *A. oryzae*; perhaps, its dominant character produced the similar trend observed in the mixed culture. Walseth (amorphous) cellulose had significantly higher production of filter paper, beta-glucosidase, and xylanase enzymes than both crystalline celluloses **(Figure 4.4)**. Endocellulase production in crystalline celluloses was not significantly different from that in other treatments **(Figure 4.4c)**. The PDA- and Walseth-raised cultures had similar levels of expression for all four activities. Culture grown in cellobiose had expressions levels between those of PDA and Walseth cultures. It is apparent from the literature that *T. reesei* cellulases are particularly active towards crystalline cellulose *(48,49)*; however, enzymes from *Aspergillus* spp lack ability to degrade crystalline cellulose *(50,51)*. Conspicuously, the cellulase enzyme production in both *A. oryzae* and mixed culture underwent a significant decrease when used as inoculum in SSF due to exposure to crystalline cellulose. The study also demonstrated that physiological traits induced in both the cultures during

adaptation on crystalline and amorphous celluloses, and soluble sugars were preserved and emerged during cellulolytic enzyme production in SSF of steam pretreated soybean hulls.

Another interesting result was the dramatic reduction in xylanase production in *A. oryzae* culture grown on crystalline cellulose (avicel and cotton linter). As compared to other cellulolytic activities, the xylanase almost vanished from *A. oryzae* adapted on crystalline cellulose **(Figure 4.4d)**. In other words, a hyper-producer of xylanase had its genes repressed when grown on crystalline cellulose. From a production standpoint, crystalline-cellulose-adapted *A. oryzae* could be used for production of cellulases in applications that do not require xylanase presence. This is an important development and requires further attention.

In conclusion, bed porosity and X-ray crystallinity of substrate played an important role in maneuvering the enzyme production in SSF. These two attributes could be used as a tool for process design and optimization for producing tailor made cellulolytic enzyme concoctions that take into consideration the inherent nature of lignocellulosic biomass. By changing these characteristics, designer can alter the proportion of various activities within the complex to arrive at specific product targeting particular biomass. In fact, this work highlights the simplicity of the nature of SSF and the ways it can be controlled such that this technology can be practiced at small scale employing readily available agro-industrial residues.

Acknowledgement

Authors gratefully acknowledge Dr. Paul Seib, Emeritus Professor, Department of Grain Science & Industry, Kansas State University for his useful insights and discussions.

Funding information

Authors are grateful to the Center for Sustainable Energy and the Department of Grain Science and Industry, Kansas State University, for funding this project. This article is

contribution no: 11-245-J from the Kansas Agricultural Experiment Station, Manhattan, KS 66506.

References

(1) Himmel, M. E.; Ding, S. Y.; Johnson, D. K.; Adney, W. S.; Nimlos, M. R.; Brady, J. W.; Foust, T. D., Biomass recalcitrance: Engineering plants and enzymes for biofuels production. *Science* **2007,** *315*, 804-807.

(2) Orts, W. J.; Holtman, K. M.; Seiber, J. N., Agricultural chemistry and bioenergy. *Journal of Agricultural and Food Chemistry* **2008,** *56*, 3892-3899.

(3) Karboune, S.; Geraert, P. A.; Kermashat, S., Characterization of selected cellulolytic activities of multi-enzymatic complex system from *Penicillium funiculosum*. *Journal of Agricultural and Food Chemistry* **2008,** *56*, 903-909.

(4) Moxley, G.; Zhu, Z. G.; Zhang, Y. H. P., Efficient sugar release by the cellulose solvent-based lignocellulose fractionation technology and enzymatic cellulose hydrolysis. *Journal of Agricultural and Food Chemistry* **2008,** *56*, 7885-7890.

(5) Esteghlalian, A. R.; Srivastava, V.; Gilkes, N. R.; Gregg, D. J.; Saddler, J. N. An overview of factors influencing the enzymatic hydrolysis of lignocellulosic feedstocks. In *Glycosyl Hydrolases in Biomass Conversion*; Himmel, M. E., Baker, J. O., Saddler, J. N., Eds.; ACS Symposium Series 769; American Chemical Society: Washington, DC, 2001; pp 100-111.

(6) Tao, Y. M.; Zhu, X. Z.; Huang, J. Z.; Ma, S. J.; Wu, X. B.; Long, M. N.; Chen, Q. X., Purification and Properties of Endoglucanase from a Sugar Cane Bagasse Hydrolyzing Strain, *Aspergillus glaucus* XC9. *Journal of Agricultural and Food Chemistry* **2010,** *58*, 6126-6130.

(7) Ugwuanyi, J. O.; Obeta, J. A. N., Pectinolytic and cellulolytic activities of heat resistant fungi and their macerating effects on mango and African mango. *Journal of the Science of Food and Agriculture* **1999,** *79*, 1054-1059.

(8) Brijwani, K.; Oberoi, H. S.; Vadlani, P. V., Production of a cellulolytic enzyme system in mixed-culture solid-state fermentation of soybean hulls supplemented with wheat bran. *Process Biochemistry* **2010,** *45*, 120-128.

(9) Zhang, Y. H. P.; Lynd, L. R., Toward an aggregated understanding of enzymatic hydrolysis of cellulose: Noncomplexed cellulase systems. *Biotechnology and Bioengineering* **2004,** *88*, 797-824.

(10) Singhania, R. R.; Sukumaran, R. K.; Patel, A. K.; Larroche, C.; Pandey, A., Advancement and comparative profiles in the production technologies using solid-state and submerged fermentation for microbial cellulases. *Enzyme and Microbial Technology* **2010,** *46*, 541-549.

(11) Couto, S. R.; Sanroman, M. A., Application of solid-state fermentation to food industry - A review. *Journal of Food Engineering* **2006,** *76*, 291-302.

(12) Rathbun, B. L.; Shuler, M. L., Heat and mass-transfer effects in static solid-substrate fermentations - design of fermentation chambers. *Biotechnology and Bioengineering* **1983,** *25*, 929-938.

(13) Tao, S.; Li, P.; Liu, B.; Liu, D.; Li, Z., Solid state fermentation of rice chaff for fibrinolytic enzyme production by Fusarium oxysporum. *Biotechnology Letters* **1997,** *19*, 465-467.

(14) Oostra, J.; le Comte, E. P.; van den Heuvel, J. C.; Tramper, J.; Rinzema, A., Intra-particle oxygen diffusion limitation in solid-state fermentation. *Biotechnology and Bioengineering* **2001,** *75*, 13-24.

(15) Richard, T. L.; Veeken, A. H. M.; de Wilde, V.; Hamelers, H. V. M., Air-filled porosity and permeability relationships during solid-state fermentation. *Biotechnology Progress* **2004,** *20*, 1372-1381.

(16) Rajagopalan, S.; Modak, J. M., Heat and mass-transfer simulation studies for solid-state fermentation processes. *Chemical Engineering Science* **1994,** *49*, 2187-2193.

(17) Smits, J. P.; Rinzema, A.; Tramper, J.; Schlosser, E. E.; Knol, W., Accurate determination of process variables in a solid-state fermentation system. *Process Biochemistry* **1996,** *31*, 669-678.

(18) Nopharatana, M.; Howes, T.; Mitchell, D., Modelling fungal growth on surfaces. *Biotechnology Techniques* **1998,** *12*, 313-318.

(19) Cui, Y. Q.; van der Lans, R.; Luyben, K., Effects of dissolved oxygen tension and mechanical forces on fungal morphology in submerged fermentation. *Biotechnology and Bioengineering* **1998,** *57*, 409-419.

(20) Rahardjo, Y. S. P.; Jolink, F.; Haemers, S.; Tramper, J.; Rinzema, A., Significance of bed porosity, bran and specific surface area in solid-state cultivation of *Aspergillus oryzae*. *Biomolecular Engineering* **2005,** *22*, 133-139.

(21) Rahardjo, Y. S. P.; Weber, F. J.; Haemers, S.; Tramper, J.; Rinzema, A., Aerial mycelia of *Aspergillus oryzae* accelerate alpha-amylase production in a model solid-state fermentation system. *Enzyme and Microbial Technology* **2005,** *36*, 900-902.

(22) Muniswaran, P. K. A.; Charyulu, N., Solid substrate fermentation of coconut coir pith for cellulase production. *Enzyme and Microbial Technology* **1994,** *16*, 436-440.

(23) Velkovska, S.; Marten, M. R.; Ollis, D. F., Kinetic model for batch cellulase production by Trichoderma reesei RUT C30. *Journal of Biotechnology* **1997,** *54*, 83-94.

(24) Domingues, F. C.; Queiroz, J. A.; Cabral, J. M. S.; Fonseca, L. P., The influence of culture conditions on mycelial structure and cellulase production by *Trichoderma reesei* Rut C-30. *Enzyme and Microbial Technology* **2000,** *26*, 394-401.

(25) Walker, L. P.; Wilson, D. B., Enzymatic-hydrolysis of cellulose - an overview. *Bioresource Technology* **1991,** *36*, 3-14.

(26) Converse, A. O.; Matsuno, R.; Tanaka, M.; Taniguchi, M., A model of enzyme adsorption and hydrolysis of microcrystalline cellulose with slow deactivation of the adsorbed enzyme. *Biotechnology and Bioengineering* **1988,** *32*, 38-45.

(27) Hendy, N.; Wilke, C.; Blanch, H., Enhanced cellulase production using solka floc in a fed-batch fermentation. *Biotechnology Letters* **1982,** *4*, 785-788.

(28) Fan, L. T.; Lee, Y. H.; Beardmore, D. H., Mechanism of the enzymatic-hydrolysis of cellulose - effects of major structural features of cellulose on enzymatic-hydrolysis. *Biotechnology and Bioengineering* **1980,** *22*, 177-199.

(29) Fan, L. T.; Lee, Y. H.; Beardmore, D. R., The influence of major structural features of cellulose on rate of enzymatic-hydrolysis. *Biotechnology and Bioengineering* **1981,** *23*, 419-424.

(30) Mandels, M.; Weber, J., Production of cellulases. *Advances in Chemistry Series* **1969**, 391-413.

(31) Hsu, J. C.; Penner, M. H., Influence of cellulose structure on its digestibility in the rat. *Journal of Nutrition* **1989,** *119,* 872-878.

(32) Jakubikova, L.; Farkas, V.; Kolarova, N.; Nemcovic, M., Conidiation of *Trichoderma atroviride* isolate during submerged cultivation in a laboratory stirred-tank fermenter. *Folia Microbiologica* **2006,** *51,* 209-213.

(33) Abalone, R.; Cassinera, A.; Gaston, A.; Lara, M. A., Some physical properties of amaranth seeds. *Biosystems Engineering* **2004,** *89,* 109-117.

(34) Milani, E.; Seyed, M.; Razavi, A.; Koocheki, A.; Nikzadeh, V.; Vahedi, N.; MoeinFard, M.; GholamhosseinPour, A., Moisture dependent physical properties of cucurbit seeds. *International Agrophysics* **2007,** *21,* 157-168.

(35) Garvey, C. J.; Parker, I. H.; Simon, G. P., On the interpretation of X-ray diffraction powder patterns in terms of the nanostructure of cellulose I fibres. *Macromolecular Chemistry and Physics* **2005,** *206,* 1568-1575.

(36) Wada, M.; Okano, T.; Sugiyama, J., Synchrotron-radiated X-ray and neutron diffraction study of native cellulose. *Cellulose* **1997,** *4,* 221-232.

(37) Park, S.; Baker, J. O.; Himmel, M. E.; Parilla, P. A.; Johnson, D. K., Cellulose crystallinity index: measurement techniques and their impact on interpreting cellulase performance. *Biotechnology for Biofuels* **2010,** *3, 1-10*.

(38) Brijwani, K.; Vadlani, P.V.; Cellulolytic Enzymes Production *via* Solid State Fermentation: Effect of Pretreatment Methods on Physicochemical Characteristics of Substrate. *Enzyme Research (in press).*

(39) Liu, R. G.; Yu, H.; Huang, Y., Structure and morphology of cellulose in wheat straw. *Cellulose* **2005,** *12,* 25-34.

(40) Nagel, F. J.; Van As, H.; Tramper, J.; Rinzema, A., Water and glucose gradients in the substrate measured with NMR imaging during solid-state fermentation with *Aspergillus oryzae*. *Biotechnology and Bioengineering* **2002,** *79*, 653-663.

(41) Nagel, F.; Tramper, J.; Bakker, M. S. N.; Rinzema, A., Model for on-line moisture-content control during solid-state fermentation. *Biotechnology and Bioengineering* **2001,** *72*, 231-243.

(42) Botella, C.; Diaz, A. B.; Wang, R. H.; Koutinas, A.; Webb, C., Particulate bioprocessing: A novel process strategy for biorefineries. *Process Biochemistry* **2009,** *44*, 546-555.

(43) Bear, J., Dynamics of fluids in porous media. Elsevier: New York, 1972.

(44) Ergun, S., Fluid flow through packed columns. *Chemical Engineering Progress* **1952,** *48*, 89-94.

(45) Suzuki, T.; Nakagami, H., Effect of crystallinity of microcrystalline cellulose on the compactability and dissolution of tablets. *European Journal of Pharmaceutics and Biopharmaceutics* **1999,** *47*, 225-230.

(46) Teeaar, R.; Serimaa, R.; Paakkari, T., Crystallinity of cellulose, as determined by CP/MAS NMR and XRD methods. *Polymer Bulletin* **1987,** *17*, 231-237.

(47) Segal, L.; Creely, J.J.; Martin, A.E.; Conrad, C.M., An empirical method for estimating the degree of crystallinity of native cellulose using X-ray diffractometer. *Textile Research Journal* **1959**, *29*, 786-794.

(48) Kubicek, C. P.; Muhlbauer, G.; Klotz, M.; John, E.; Kubicekpranz, E. M., Properties of a conidial-bound cellulase enzyme-system from *Trichoderma-reesei*. *Journal of General Microbiology* **1988,** *134*, 1215-1222.

(49) Seiboth, B.; Hakola, S.; Mach, R. L.; Suominen, P. L.; Kubicek, C. P., Role of four major cellulases in triggering of cellulase gene expression by cellulose in Trichoderma reesei. *Journal of Bacteriology* **1997,** *179*, 5318-5320.

(50) Lee, N. E.; Lima, M.; Woodward, J., Hydrolysis of cellulose by a mixture of trichoderma-reesei cellobiohydrolase and aspergillus-niger endoglucanase. *Biochimica Et Biophysica Acta* **1988,** *967*, 437-440.

(51) de Vries, R. P.; Visser, J., Aspergillus enzymes involved in degradation of plant cell wall polysaccharides. *Microbiology and Molecular Biology Reviews* **2001,** *65*, 497-522.

Figure 4.1 Effect of varying initial moisture of the substrate bed on cellulolytic enzyme system production in both mixed and mono cultures of *T. reesei* and *A. oryzae*. (a) Cellulolytic enzyme system production in *T. reesei*; (b) Cellulolytic enzyme system production in *A. oryzae*; (c) Cellulolytic enzyme system production in mixed culture. Test of significance between the means (as discussed in text) was done using Tukey-Kramer HSD at P<0.05. Abbreviations: Native – untreated soybean hulls; Steam – steam-pretreated soybean hulls. Data are expressed as mean ± S.E., n = 4.

(a)

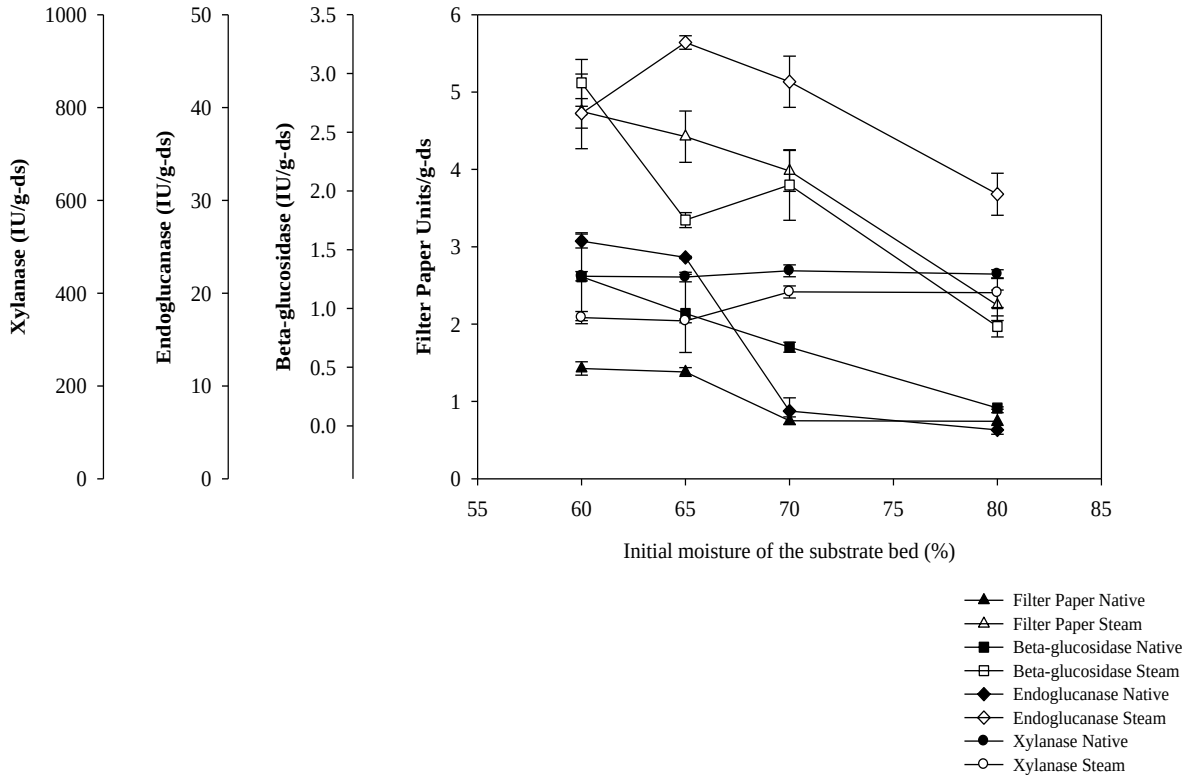

(b)

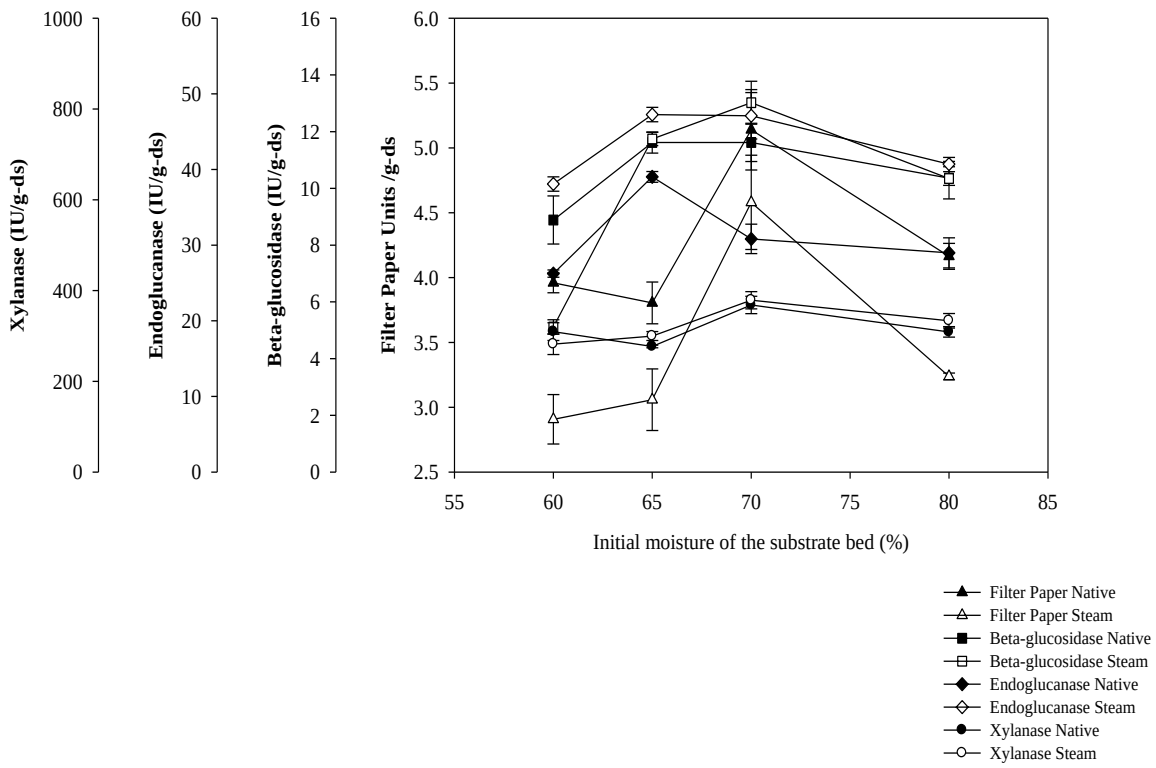
Xylanase (IU/g-ds)
Endoglucanase (IU/g-ds)
Beta-glucosidase (IU/g-ds)
Filter Paper Units /g-ds
Initial moisture of the substrate bed (%)
Filter Paper Native
Filter Paper Steam
Beta-glucosidase Native
Beta-glucosidase Steam
Endoglucanase Native
Endoglucanase Steam
Xylanase Native
Xylanase Steam

(c)

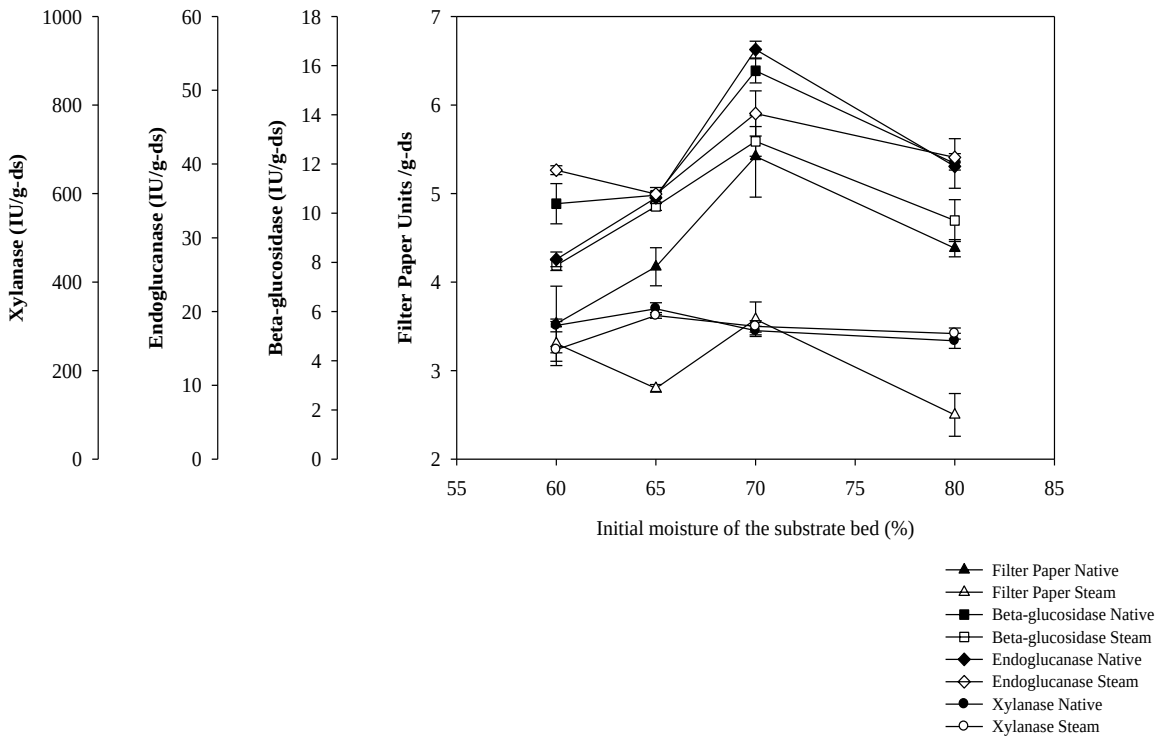
Xylanase (IU/g-ds)
Endoglucanase (IU/g-ds)
Beta-glucosidase (IU/g-ds)
Filter Paper Units /g-ds
Initial moisture of the substrate bed (%)
Filter Paper Native
Filter Paper Steam
Beta-glucosidase Native
Beta-glucosidase Steam
Endoglucanase Native
Endoglucanase Steam
Xylanase Native
Xylanase Steam

Figure 4.2 Schematic of micro-scale view of solid state fermentation

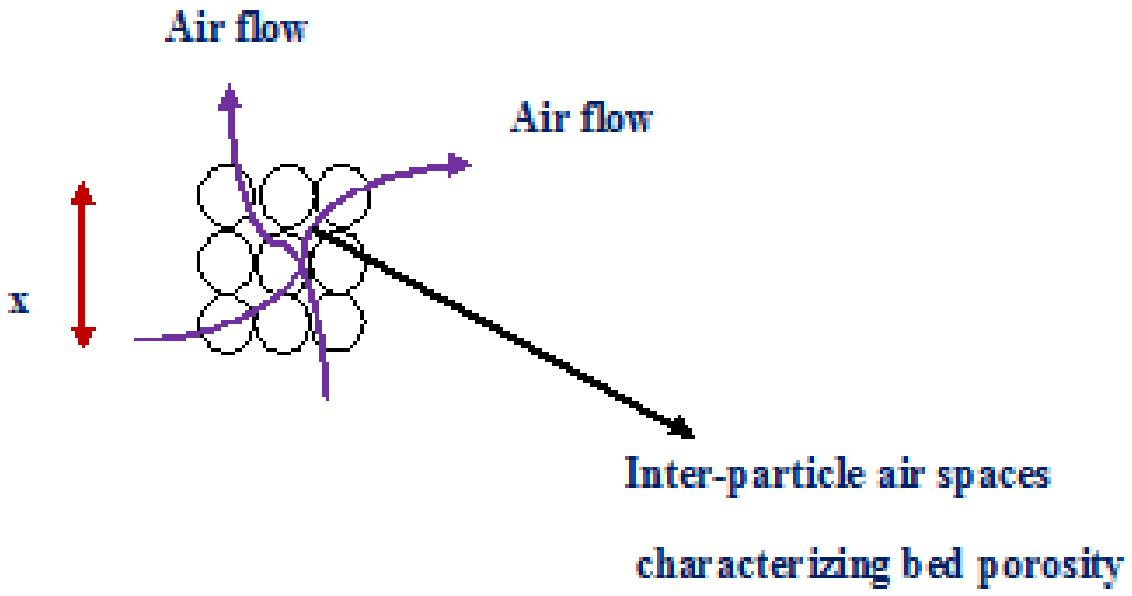

Figure 4.3 X-ray diffractograms. Gaussian smoothing followed by Voigt function was used to fit the diffractogram output of the instrument. (a) Avicel. The characteristic peaks identified were: 2θ = 14.30º (101 plane), 16.52º (10$\bar{1}$), 19.5º (021 plane), 22.42º (002 plane), and 34.38º (040 plane). (b) Cotton linter. The characteristics peaks identified were: 2θ = 14.41º (101 plane), 16.76º (10$\bar{1}$), 19.68º (021 plane), 22.66º (002 plane), and 34.02º (040 plane).

(a)

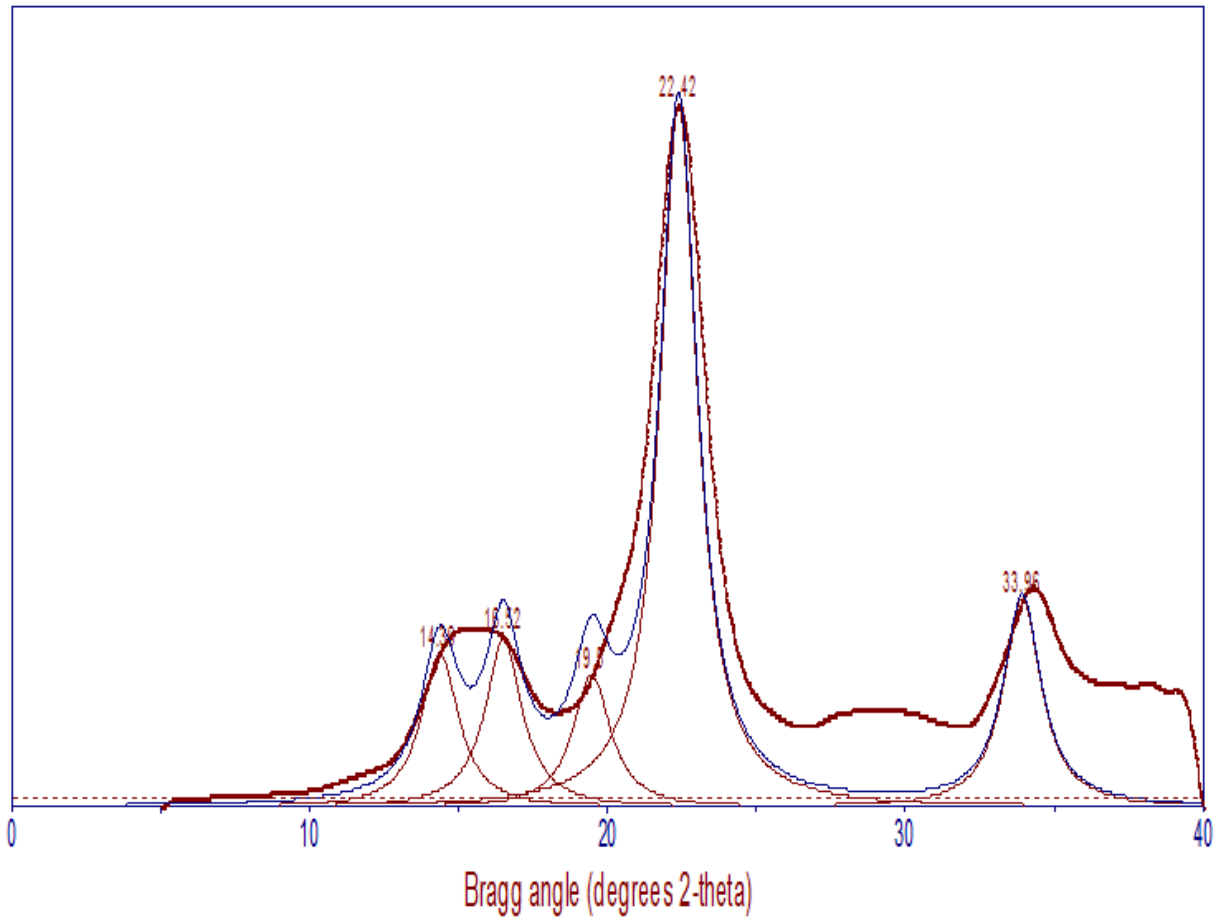

(b)

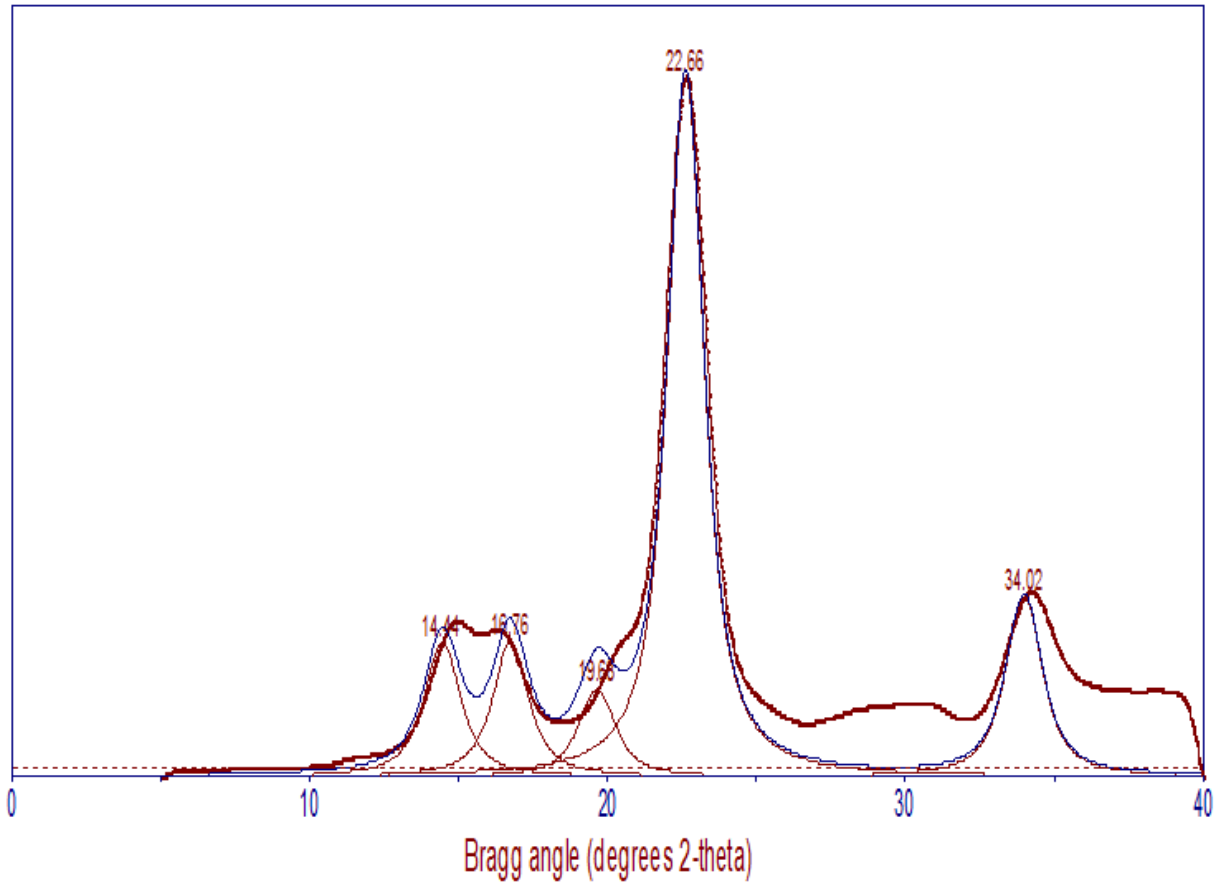

Table 4.1 Effect of initial moisture on the bed porosity of native and steam treated soybean hulls

Substrate type	Initial moisture of the substrate bed (%)	Bed porosity (%)
Native soybean hulls	60	72.29±0.03
Native soybean hulls	65	67.60±1.36
Native soybean hulls	70	40.41±1.91
Native soybean hulls	80	32.62±0.86
Steam-pretreated soybean hulls	60	77.10±2.46
Steam-pretreated soybean hulls	65	69.29±0.38
Steam-pretreated soybean hulls	70	57.45±0.50
Steam-pretreated soybean hulls	80	49.69±1.56

Data is expressed as mean ± S.E.; n =2

Table 4.2 X-ray crystallinity of avicel and cotton linter estimated by fitting Voigt function to raw diffractograms

Sample	Crystallinity (%)
Avicel	67.33±0.18 (65.5%)*
Cotton linter	67.18±0.46 (67%)*

*the parentheses features % crystallinity as reported in *(45,46)* for avicel and cotton linter respectively. Data is expressed as mean ± S.E.; n =2

Chapter 5 - Experimental and Theoretical Analysis of a Novel Deep Bed Solid State Bioreactor for Cellulolytic Enzymes Production

Abstract

A novel deep bed solid state bioreactor was designed and fabricated for cellulolytic enzymes production using mixed fungal cultures. Enhanced heat transfer and better temperature control was achieved through unique bioreactor design made of outer wire-mesh frame with internal air distribution along with a near saturation conditions within the cabinet. Without air flow through the internal distributors, maximum temperatures of 48ºC and 52ºC were observed during half and full capacity operation. These were reduced to 44ºC and 43ºC on resumption of air flow. In terms of cellulolytic enzymes production there was no significant differences in filter paper activity with depth in half capacity operation; however, in full capacity operation, top level filter paper activity (5.39 FPU/g-Solids) was significantly different from middle and bottom level activity. Top level beta-glucosidase, endocellulase and xylanase activities were significantly ($P<0.05$) different from middle and bottom levels in both half and full capacity operation. A two-phase coupled heat and mass transfer model was developed that predicted the experimental trends reasonably well. Model predictions confirmed the cabinet temperature of 30ºC and distributor air flow rate of 3.42 kg h^{-1} during operation for better temperature control, and that distributor air can be supplied at room temperature.

Keywords: *Trichoderma reesei*, *Aspergillus oryzae*, solid-state bioreactor, cellulolytic enzymes, heat and mass transfer, N-tank in series model

1. Introduction

Solid substrate fermentation (SSF) is described as a process in which microorganisms grow on water-insoluble substrates in the absence of free water [1]. The solid substrates are

typically inexpensive agro-industrial residues such as wheat bran, wheat straw, corn stover and other agricultural biomass that offer promise of more cleaner and environmentally benign production of fuels and chemicals via fermentation [2]. SSF processes are more efficient than submerged fermentation in utilization of agro-industrial residues, and therefore are a low cost alternative for production of various microbial products including cellulolytic enzymes [3,4].

However, removal of metabolic heat during SSF is a challenge that could seriously hamper the process productivity and its potential for large scale commercial operation [5,6]. Several bioreactor designs have been proposed to circumvent the heat dissipation problem including trays, packed beds, rotary drums and fluidized beds [7]. Rotary and/ or fluidized bioreactors allow better heat and mass transfer, but are deleterious to mold growth as tumbling action causes mycelium damage as well as agglomeration of substrates [8]. Packed beds in which air is introduced through the packed mass of substrate is another alternative. However, it suffers from higher pressure drop and channeling especially at high flow rates, preventing its use at large scale [9]. Tray bioreactors employ large tray stacks installed in an environmental controlled room referred as “koji” in which humidified air is circulated or in certain cases water is sprayed inside the room to keep the atmosphere near saturation. These bioreactors have simple designs but require large areas, are cumbersome to handle, and their operation is highly labor intensive [10]. As a result the choice of bioreactor for SSF is confined to deep bed systems. Though heat and mass transfer limitations affect deep bed configurations as well, their use is encouraged due to better process management and control compared to tray bioreactors [10,11].

Forced aeration improves growth and productivity of fungal cultures in SSF and also acts as a heat transfer fluid for temperature control and heat removal [12,13]. In addition to forced aeration, several workers have adopted other means to control steep temperature gradients. For

instance, Fernendez et al. [14] controlled temperature gradients (within ±4 ºC) by enhancing evaporative cooling by intermediate addition of water. Other workers [15,16,17] used a water jacket and/ or heat exchanger plates carrying cooling water to contain temperature gradients. These efforts of conductive cooling have resulted in advances in developing systems to control temperature, but they lack scale-up flexibility compared to submerged fermentations [18]. For example, it is difficult to ensure uniform mixing of water added during the process in static deep bed configurations. Water jackets and heat transfer plates offer some help but because of poor conductivity of the bed *per se*, their large scale implementation is a bottleneck [19]. Clearly, aeration remains the most practical way of containing temperature gradients in SSF.

During the design and development phase of new bioreactor prototypes it is imperative that new designs should be subjected to a range of operating parameters to evaluate their performance. While this can achieved by experiments, time and availability of resources is a constraint. Mathematical modeling can substantiate experimental studies and often explain scenarios that may not be possible experimentally. Mathematical models incorporating energy balances have been developed for tray bioreactors [12,20,21] packed bed bioreactors [15,22,23], and rotating drums [24]. In many of these models the pseudo-homogeneous state is assumed, i.e., the solid and inter-particle air phases are not treated separately by supposing thermal and moisture equilibrium between them. Such assumptions are likely in those cases where water is intermittently added during the operation. In deep bed configurations, which are devoid of mixing, the water activity of the substrate changes during the fungal growth [19]. Therefore, mathematical models should treat the solid and gas phases separately, and include the mass transfer of water between them.

The aim of this work was to develop a novel deep bed solid-state bioreactor prototype that allowed for effective temperature control. As convective heat transfer is the best mode for dissipating heat in deep bed systems, a new design with improved convective heat transfer was conceived and tested on cellulolytic enzyme production in mixed fungal SSF of soybean hulls. Along with experimental studies, a comprehensive two phase mathematical model was developed that predicted the performance of the bioreactor for a broad range of operating parameters. It is expected that the model would serve as a valuable tool in studying scale-up of the novel deep bed solid state bioreactor for cellulolytic enzymes production.

2. Materials and methods

2.1 Bioreactor fabrication

Deep bed cubical bioreactor of dimensions 30 cm × 30 cm × 30 cm was fabricated at Advanced Manufacturing Institute, Kansas State University, Manhattan, KS. The outer wire-mesh frame of the bioreactor was made of McNicholSR Quality Perforated Metal, Round Hole, Stainless Steel Type 304, 20 Gauge, Mill Finish, 1/16" Holes on 3/32" (McNichols Inc., Tampa, FL). The inside air distributors were made out of Perforated tubes 1/2" ID .075" holes, 1/8" staggered pattern, 18ga Stainless steel (Perforated Tubes Inc., Ada, MI). The whole bioreactor was placed inside the environmental cabinet (Caron Model 6030, Caron, Marietta, OH) maintained at 30ºC and 95% relative humidity (RH) by blowing a humidified air using air blower. The bioreactor had vertical sliding shutters (width, 7 cm; height, 32 cm) at the front and rear (Fig. 1b) for withdrawing samples from three different bed heights. Temperature at three bed heights were recorded using ACR SmartButton (ACR systems Inc., Surrey, BC, Canada), a miniature size chip based data logger with battery operated assembly. The ACR SmartButton was activated using SmartButton Reader software and it recorded temperature at every 30

minute. After the reactor operation the SmartButtons were removed and stored temperature data were retrieved via cable interfacing with SmartButton Reader. In order to mount SmartButtons at specific positions inside bioreactor, a steel rod (height, 28 cm) carrying three magnets clipped along its vertical dimension (magnets were fastened to heights matching the three different bed heights) was inserted and glued to the base of bioreactor using sticky-clay. SmartButtons were bound to the magnets and wrapped all-around by thin plastic film to prevent moisture seepage.

2.2. Bioreactor operation and experimental set-up

Soybean hulls were purchased in bulk from Manna Pro Products LLC, Chesterfield, MO, and were adjusted to 70 % moisture content (wet basis, wb) and pH 5. Moisture content of 70% (wb) and pH of 5 represented the values optimized previously [25]. Mandels media [26] of pH 5 was used for moisture adjustment. The bioreactor was operated under both half and full capacities. In half capacity operation it was filled to the height of 15 cm with initial dry weight of soybean hulls of 2.51 kg. The bioreactor at this height had a holding capacity of 7.32 kg of moist soybean hulls, which corresponds load of 81.34 kg m^{-2}. The whole height was divided into three levels- top (15 cm from the base), middle (7 cm from the base) and bottom (3 cm from the base). In full capacity operation, it was filled to the height of 25 cm with initial dry weight of 3.51 kg, which corresponds to a working capacity of 10.24 kg of moist soybean hulls, and a load of 113.78 kg m^{-2}. The whole height was divided into three levels- top (25 cm from the base), middle (15 cm from the base) and bottom (3 cm from the base). The wet media after moisture addition was sterilized at 121ºC, 15 psig for 60 minutes followed by cooling to ambient temperature prior to inoculation. The sterilized soybean hulls were inoculated with 1:1 mixed culture (10^8 spores/ml-spore suspension) of *Trichoerma reesei* (ATCC 26921) and *Aspergillus oryzae* (ATCC 12892). Mixed culture was added at 10% (v/w) of dry soybean hulls (moisture from

culture was considered during Mandels media addition). Maintenance of cultures and harvesting the spore suspension was based on our earlier studies [25]. After sterilization, cultured soybean hulls were transferred aseptically to pre-sterilized bioreactor and temperature sensors were activated. The whole bioreactor was transferred to an environmental cabinet maintained at aforementioned temperature and RH. The air distributors were connected to separate hoses that supplied air at 25ºC. Two such bioreactors were fabricated to conduct the experimental studies in replicate.

An estimate of mass flow rate of air through distributors was obtained through macroscopic energy balance per Eq. (1) as described in detail in Rodriguez Leon et al. [27]:

$$F = \frac{0.39\mu_{opt}exp(\mu_{opt}t) - 0.58(T-25)}{0.24(T-25) + 560(H-0.02945)} \quad (1)$$

Where,

F = mass flow rate of dry air (kg-dry air h^{-1})

μ_{opt} = maximum specific growth rate (h^{-1})

t = time since start of fermentation, h

T = maximum temperature reached without air supply through distributors

H = absolute humidity of the inlet air (kg-water kg dry air^{-1})

The specific growth rate of the mixed culture (0.136 h^{-1}) was obtained by taking the average of *T. reesei* (0.123 h^{-1}; [13]) and *A. oryzae* (~0.15 h^{-1}) growth rates estimated under similar experimental conditions. The absolute humidity (0.02945 kg-water/kg-air) of the air inside chamber at saturation was calculated using the Antoine equation [28]. As inlet air was supplied at 25ºC, H was obtained, assuming air to be saturated, as 0.019995 kg-water/kg-air using the Antoine equation. Since the air flow rate was constant over the duration of fermentation, the maximum temperature and time to attain maximum temperature was from non-

aerated experiment. The maximum temperature reached without air through distributors was 53ºC in 44 hours of operation and this gave a mass flow rate of 3.42 kg-dry air h^{-1} or 50 L/min of volumetric flow rate. The air flow rate through distributors was fixed at 50 L/min using Rate-Master Flowmeter (Model no. RMA-150-APF, Dwyer Instruments Inc., Michigan City, IN).

2.3 Analysis

2.3.1 Analytical assays

After the operation for the specified incubation period, the whole bioreactor was removed from the cabinet and samples were withdrawn from three different heights using a sharp cutting knife. Samples were analyzed for moisture content and cellulolytic enzyme activities. Moisture measurements were performed using Denver Infrared Moisture Analyzer (Model IR35) (Fisher Scientific, USA). Crude cellulolytic enzymes were extracted by adding 30 ml of citrate buffer (50 mM, pH 5) to each sample (~10 g) followed by shaking at 150 rpm for 30 minutes. Contents were filtered using coarse filter paper (Fisher Scientific, P-8 coarse grade), and the filtrate obtained was centrifuged at 10,000 ×g for 15 minutes at 4°C (Sorvall RC-6, Thermo Scientific, USA). The supernatant was analyzed for filter paper activity (FPU/g-ds), endocellulase (IU/g-ds), β-glucosidase (IU/g-ds), and xylanase (IU/g-ds) activities. Enzymatic assays were carried out using standard protocols as described in [25]. Enzyme activities were reported as units per gram of dry solids (ds) that included both biomass content and residual substrate.

2.3.2. Statistical analysis

Statistical analysis was performed using the GLM procedure in SAS software version 9.1 (SAS Institute, NC, USA). Multiple comparisons were conducted using Tukey Kramer HSD at $P<0.05$.

3. Two-phase heat and mass transfer mathematical model

A two-phase mathematical model is developed to demonstrate the inherent characteristics of novel deep bed bioreactor. Both energy and mass balances are written separately for solid and air phases. The balance equations described in the model are modified from the earlier studies of Mitchell et al. [29] and Marques et al. [30] to suit the current bioreactor design and operation. In the balance equations terms were normalized as per kilogram solids in the bioreactor. The N-tank-in-series methodology has been adopted to discretize the bioreactor axial space into well mixed tanks such that spatial homogeneity of scalar potentials i.e. temperature and mass within tanks can be ensured. This approach was successfully used in modeling heat and mass transfer in solid state packed bed reactors previously [29,31] and is a well established chemical reaction engineering technique [32]. Other techniques like orthogonal collocation have been used by the previous researchers; however, that needs complex computer codes and becomes computationally intensive as size of bioreactor increase (to have enough collocation points to span the whole bioreactor space). N-tanks series on the other hand, could be easily employed, especially for simple geometries, such as cubic, to map the complete space of bioreactor just by varying the number of tanks.

The transport model is developed based on the design of deep bed bioreactor (Fig. 5.1a-b). The bioreactor is a wire-mesh cubical box of volume L^3 housing internal air distributors. The whole space of the bioreactor is partitioned into well mixed N-tanks arranged axially as shown in Fig. 5.2. The N-tanks are categorized into two types: tanks encompassing air distributors within their space and tanks devoid of air distributors. The bioreactor is kept inside a temperature and humidity controlled chamber. Atmospheric humidified air flows over and below the moist substrate mass filled inside the bioreactor. The whole substrate bed of total dry mass M (including biomass content and residual substrate) is divided into N-equal size well mixed beds

devoid of spatial gradients of temperature, moisture and biomass concentration at any time. The distributor air instantaneously comes in equilibrium with humidity inside the chamber such that its temporal moisture balance is avoided. It is assumed that no pressure drops occur within the bed, radial gradients are neglected due to design and operation of bioreactor, and bed porosity and total mass of dry solids (M kg) are constant. An oxygen mass balance is not written as previous studies have shown that in aerated bioreactors oxygen transfer is not a limiting factor [33,34].

3.1. Mass balance for moisture in the solid phase

The liquid water in the solids (W, kg-water kg-solids^{-1}) is affected by evaporative transfer of water between the solid and gas phase, and metabolic production of water during growth of fungal cells. The mass balance of liquid water for nth tank for both with and without an air distributor is give by the following equation:

$$\frac{M}{N}\frac{dW_{\mathrm{n}}}{dt} = Y_{\mathrm{WX}}\left(\frac{M}{N}\right)\frac{dX_{\mathrm{n}}}{dt} - K_{\mathrm{W}}V(W_{\mathrm{n}} - W_{\mathrm{sat,n}}) \qquad (2)$$

3.2. Mass balance for moisture in the gas phase

The water vapor in the gas phase (H, kg-vapor kg-dry air^{-1}) is affected by the difference in the humidity of the incoming air and humidity at any time, t, within the tank, and also convective flow of water from the solids into air. The mass balance of water vapor for nth tank including an air distributor is give by the following equation:

$$V\varepsilon\rho\frac{dH_{\mathrm{n}}}{dt} = F\left(H_{\mathrm{n\text{-}1}} - H_{\mathrm{n}}\right) + K_{\mathrm{W}}V(W_{\mathrm{n}} - W_{\mathrm{sat,n}}) \qquad (3)$$

For an Nth tank without an air distributor no balance is set.

3.3. Energy balance for the solid phase

The energy balance in the solid phase is a function of four processes – convective heat transfer between the gas from air distributors and solids, heat transfer between the solids and surroundings, evaporative cooling due to moisture migration from solids to surrounding gas phase, and metabolic production of heat due to fungal growth. The heat transfer between solids and surroundings is considered as overall heat transfer that do not takes into account solids to wall and wall to surrounding heat transfer rates. This is conceivable as outer skeleton of bioreactor is made of wire-mesh that facilitates enhanced interface of solids with surroundings. Therefore, the energy balance for nth tank housing an air distributor is as following:

$$\frac{M}{N}(C_{\mathrm{PM}} + W_{\mathrm{n}}C_{\mathrm{PW}})\frac{dT_{\mathrm{sn}}}{dt} = Y_{\mathrm{QX}}\left(\frac{M}{N}\right)\frac{dX_{\mathrm{n}}}{dt} - h_{\mathrm{ov}}A(1-\varepsilon)(T_{\mathrm{sn}} - T_{\mathrm{surr}}) - h_{\mathrm{g}}V(T_{\mathrm{sn}} - T_{\mathrm{gn}}) - K_{\mathrm{W}}V\lambda(W_{\mathrm{n}} - W_{\mathrm{sat,n}}) \quad (4)$$

For an nth tank without an air distributor the third term in the right hand side of Eq. (4) is not included.

3.4. Energy balance for the gas phase

The change in the energy content of the gas is the function of change in the sensible heat of the distributor air flowing from n-1 to n tank, change in the sensible energy of water vapor entering and leaving the bed in the flowing air, convective heat transfer between the solid and gas phase, and overall heat transfer between the gas phase and surroundings. Therefore, the energy balance for the nth tank including an air distributor is:

$$V\varepsilon\rho(C_{\mathrm{PA}} + H_{\mathrm{n}}C_{\mathrm{PV}})\frac{dT_{\mathrm{gn}}}{dt} = F * C_{\mathrm{PA}}\left(T_{\mathrm{g(n-1)}} - T_{\mathrm{gn}}\right) + F * C_{\mathrm{PV}}\left(H_{\mathrm{n\text{-}1}}T_{\mathrm{g(n-1)}} - H_{\mathrm{n}}T_{\mathrm{gn}}\right) + h_{\mathrm{gn}}V(T_{\mathrm{sn}} - T_{\mathrm{gn}}) - h_{\mathrm{ov}}A\varepsilon(T_{\mathrm{gn}} - T_{\mathrm{surr}}) \quad (5)$$

3.5. Biomass production

Fungal biomass production is described by a logistic equation. As the processes within the bioreactor are affected by the transport phenomena of heat and moisture transfer, the specific growth rate is modeled as a function of both temperature and water activity of the solids per the expressions developed by von Meien and Mitchell [19]. In solid state fermentation, the temperature can increase beyond the optimal temperature, causing cell death. Total biomass (X, kg-biomass kg-solids^{-1}), therefore, is comprised of viable cells and dead cells. The total biomass production in an nth tank is written as:

$$\frac{dX_{\mathrm{n}}}{dt} = \mu_{\mathrm{n}} * X_{\mathrm{vn}}\left(1 - \frac{X_{\mathrm{n}}}{X_{\mathrm{M}}}\right) \qquad (6)$$

Viable biomass (X_v, kg-biomass kg-solids^{-1}) for an nth tank is:

$$\frac{dX_{\mathrm{vn}}}{dt} = \mu_{\mathrm{n}} * X_{\mathrm{vn}}\left(1 - \frac{X_{\mathrm{n}}}{X_{\mathrm{M}}}\right) - k_{\mathrm{D}}X_{\mathrm{vn}} \qquad (7)$$

Where, k_D is the specific death rate coefficient (h^{-1}) given by Eq. (8) in Table 1. In order to write the specific growth rate, μ, as a function of environmental variables (temperature and water activity) it has been proposed previously [19] to write μ as the geometric mean of individual fractional specific growth rates i.e.

$$\mu = \mu_{\mathrm{opt}}\sqrt{\mu_{\mathrm{T}}\mu_{\mathrm{W}}} \qquad (9)$$

Where μ_{opt} is the optimal growth rate under ideal conditions, μ_T is the fractional specific growth rate as a function of temperature of solids given by the Eq. (10), Table 1 and μ_W is the fractional specific growth rate as a function of water activity of solids given by Eq. (11), Table 1 respectively.

3.6. Sorption isotherm for water activity measurements

In order to calculate μ_W per Eq. (11), the water activity of the fermenting solids at any time, t, is required. It has been argued in the literature that sorption isotherm for fermenting solids is different from the solids in its natural state. This has been validated for corn [30]. However, authors also used soybean as solid substrate and found predicted bioreactor performance in terms of biomass production was not significantly different when the sorption isotherm for fermenting solids was considered in the same way as the sorption isotherm of soybeans. Thus, to avoid computational complexities in our studies with soybean hulls used as substrate, the sorption isotherm of native soybean [30] has been used for the water activity measurements. Therefore, we have

$$a_W = 1 - \exp(-4.988W^{0.7202}) \qquad (12)$$

Where, W, is the liquid water (kg-water kg-solids^{-1}) at any time, t. Using Eq. (12) a_W is calculated and substituted in Eq. (11) to obtain μ_W. In order to calculate saturation water content (W_{sat}) the expression for water activity of the gas phase (a_{Wg}) is required, which needs saturation vapor pressure data. The saturation vapor function as a function of temperature of gas phase is obtained from the Antoine equation [28], which is then combined in Eq. (13) (Table 1) for the calculation of a_{Wg}. Knowing a_{Wg} saturated water content is obtained from Eq. (14), Table 1.

3.7. Transfer coefficients

The solid to gas convective heat transfer coefficient (h_g, J h^{-1} m^{-3} $^oC^{-1}$) is calculated using Eq. (15), Table 1. The h_g represents heat transfer rate per cubic meter of the bed and is the function of gas temperature T_g and air mass flow rate (F). The correlation (Eq. 15) is adapted from Marques et al. [30]. The correlation uses mass flow rate in kg s^{-1}, therefore appropriate unit conversions were incorporated during calculations, and final h_g was reported as J h^{-1} m^{-3} $^oC^{-1}$

respectively. Similarly, water mass transfer coefficient between the solid and gas phase (K_w, kg-dry solids h^{-1} m^{-3}) is the mass transfer rate per cubic meter of the bed volume. It is a function of both gas temperature (T_g) and water content of the bed (W) (Eq. (16), Table 1). Overall heat transfer coefficient between the bed surface (solids or gas) and surroundings (h_{ov}, J h^{-1} m^{-2} $^oC^{-1}$) is fixed at 54000 [35]. As mentioned earlier, the overall heat transfer coefficient between bioreactor system (solid or gas) and the surroundings means that the bioreactor wall is not treated as a separate subsystem, and this is a reasonable assumption for present design where bioreactor wall is made of thin wire mesh.

3.8. Initial conditions, parameter values, inlet conditions and numerical solution

Table 5.2 lists the initial values of various state variables (H_o, T_{go}, T_{so}, W_o, X_o, and X_{Vo}) that are applied to all N tanks during simulations. Also, are featured the values of distributor mass flow rate of air (F, set-up by the user), total mass of the bed under two different operations (half capacity and full capacity), inlet air temperature and humidity (set equal to T_{go} and H_o) respectively. The inlet humidity (0.027 kg-water vapor kg-dry air^{-1}) is at saturation at 30ºC. The system of differential equations along with supplementary algebraic equations was solved by semi-implicit algorithm due to the stiff nature of the equations. The semi-implicit algorithm is a generalized higher order Runge-Kutta algorithm that uses backward Runge-Kutta method with a fixed order and a variable time step [36].

4. Results and discussion

4.1. Bioreactor design and operation

Mechanical drawings of the bioreactor in third angle orthographic and isometric projections are shown in Fig. 5.1a-b. The outer wire mesh frame design was conceived to allow for a better interface with the environment for enhanced heat conduction within the substrate

bed. The internal air distributors were positioned strategically along the vertical hollow shaft at 6 cm interval with the last one at 6.5 cm from the base. The air distributors had radial spouts each of 7 cm in length that were protruded parallel to the X-Y plane of the bioreactor thereby covering the entire space within the horizontal plane (Fig. 5.1b). The particular design was envisaged keeping in mind that internal air circulation in conjunction with aeration within the environmental cabinet would allow better convective heat transfer. In addition, the near saturation atmospheric conditions inside the cabinet would also restrict excessive evaporative loss of moisture and prevent bed drying.

The aforementioned design characteristics, therefore, exploit advantages of both tray bioreactors as well as packed bed bioreactors. In tray bioreactors, the main mode of heat transfer is conduction; the design suffers from heat transfer, oxygen transfer and moisture transfer limitations [9]. It has been demonstrated previously [10] that a bed height of as little as 8 cm could lead to a temperature rise of as high as 20ºC above optimum in the interiors of the bed. In packed bed operation, the main mode of heat transfer is convection and evaporation [9]. Due to forced aeration the oxygen transfer is not limited; however, temperature control can be a serious problem [33,34]. In previous studies, use of water cooled heat transfer plates have been tried using *T. harzianum* but it was difficult to control temperature during the exponential growth phase by circulating water [16]. Further, excessive water loss especially near the air outlet and the difficulty in replenishing water during operation limits the height of packed bed bioreactors [17,37].

The present design is an effort in the direction that takes full advantage of forced aeration. The design features including the wire mesh skeleton, internal air distributors and use of an environmental cabinet were incorporated to overcome the impediments of poor conduction

(inherent of agricultural substrates), improper convective heat transfer, and excessive moisture loss. The forthcoming sections present the experimental and theoretical studies that have been conducted to benchmark the performance of this innovative bioreactor design.

4.2. Cellulolytic enzymes production in novel deep bed bioreactor

Production of cellulolytic enzymes in both half and full capacity operation is shown in Fig. 5.3a-b. Distributor air flow rate was fixed at 3.42 kg h^{-1} during the operation with inlet air and surrounding temperatures at 25 and 30ºC, respectively. Air flow rate through the distributors was determined using a macroscopic energy balance as discussed, which took into consideration the heat load of the process.

Comparing the data with production of cellulolytic enzymes in static trays (1 cm bed height kept in large humidified room) from our previous study [25] it was evident that the production rate of enzymes in the newly developed bioreactor was quicker and reached optimum within 48-72 hours of operation. In contrast, static tray required 96 hours to reach optimum (data not shown, ref: [25]). The disparity in performance was due to the mode of operation of static tray versus deep bed bioreactor. Lack of forced aeration through substrate bed in static tray and difficulty in maintaining humidity near saturation in the koji room resulted in prolonged fermentation time. The apparent bed drying was also noticeable during fermentation in static trays, and sometimes required sprinkling of water just to prevent desiccation of the bed. On the other hand, the deep bed bioreactor had forced aeration and was placed in the environmental cabinet maintained at saturated conditions, which led to enhanced growth and production rate of enzymes. Comparing the peak enzyme activities in the deep bed bioreactor with laboratory scale flask trials of Brijwani and Vadlani [38], it was evident that peak values of all four enzyme activities (especially of the top level) were well within the range observed during laboratory

studies of mixed culture fermentation of soybean hulls (Table 5.3). Preserving the fermentative potential of cultures for production of enzymes is important for the scale-up of the bioreactor and highlights the significance of the unique design features that were incorporated during its conceptualization and fabrication.

The results of statistical analysis of the peak value of various activities with depth in both half and full capacities operation are listed in Table 5.3. In half capacity operation, there were no significant differences in filter paper activity with depth; however, beta-glucosidase at the top level was significantly different from the middle and bottom levels. Similarly both endoglucanase and xylanase at the top level were significantly different from the middle and bottom levels. Similar trends were also observed during full capacity operation, except that the top level had significantly higher filter paper activity compared to middle and bottom levels. Comparison of activities at corresponding levels between half and full capacity operation revealed that the top level during full capacity operation had significantly higher production of all enzyme activities compared to the top level during half capacity operation. However, filter paper activity was not significantly different (Table 5.3). The middle and bottom levels of both operations had similar filter paper and endoglucanase activities but different beta-glucosidase and xylanase activities. The observed differences in the survival of various enzyme activities at various depths are attributed to the thermo-stability of enzymes, which is a function of evolutionary genetics of enzymes within fungal species. Such observations have been documented, for instance, Chin and Nokes [39] observed no significant differences in xylanase levels with depth even though the maximum temperature reached was 49ºC (middle level) with minimum of 43ºC (bottom level) in their deep bed forced aeration bioreactor. Nevertheless, the optimal performance of the bioreactor during its full capacity is appealing, especially given the

general nature of deep bed operations which are limited in height due to build up of extreme temperature gradients.

4.3. Moisture gradients during half and full capacities operation

The moisture dynamics for both half and full capacities operation is shown in Fig. 5.4. At the top level during half and full capacities operation, the moisture after 96 hours of operation dropped to 65% (wb) and 67% (wb) from an initial value of 70% (wb). At the middle level for both capacities, moisture after 96 hours of operation was around 68% (wb). At the bottom level for both capacities the moisture after 96 hours of operation dropped to 67% (wb) and 68% (wb), respectively. Fortunately, the moisture losses for both operations at all three levels were not significantly different and remained close to optimum (70%, wb). Similar results were also reported by Mazutti et al. [40] where the near saturation atmosphere prevented excessive moisture loss. In contrast to packed bed operation where moisture losses are significant, especially at the air outlet [19,22,41], this innovative bioreactor design inside an environmental cabinet kept moisture loss to a minimum.

4.4. Temperature control and model validation

Temperature profiles without air flow through the distributors in both half and full capacities operation are shown in Fig. 5.5. Inspection of the data revealed that the middle level of the bioreactor under both capacities had a much greater temperature rise compared to the top and bottom levels. Temperatures of 48 and 52ºC were recorded for half and full capacity operation respectively at the middle level during 40 h of operation. Ghildyal et al. [10] reported temperatures of 50 and 52ºC for bed heights of 8 (total height of bed was 16 cm) and 16 (total height of bed was 24 cm) with comparable substrate loads of 88.9 kg m^{-2} and 126.1 kg m^{-2} as used in this study, respectively.

On resuming the air flow at the rate of 3.42 kg h^{-1}, there was a significant drop in peak temperatures at all three levels under both half and full capacity operation (Fig. 5.6a-b). The middle level had a peak temperature of 43ºC (down by 5ºC), the bottom level 44ºC (down by 1ºC), and the top level 40ºC (down by 3ºC) during 40 hours of operation under half capacity. During full capacity operation, temperature dropped by 12ºC at the middle level, and the top level had a peak temperature of 31ºC during 40 h of operation. The low temperature at the top level was due to convective heat dissipation due to sparging of air from distributor and its proximity to the environment above it. The temperature reductions at the bottom level was trivial for both half and full capacity operation because the bottom portion did not encompass the air distributor as the lower most distributor was fabricated at 6.5 cm from the base.

The two-phase mathematical model was validated with observed temperature data from half and full capacity operation. Predicted and observed temperature profiles are shown in Fig. 5.6a-b along with the corresponding root mean square error (RMSE) values. The data is presented for 20 h and beyond as during this period actual growth occurred. The two-phase mathematical model appropriately predicted the observed temperature profiles such that RMSE values for both half and full capacity operation were under 2.5. The model also effectively outlined the role of internal air distribution on temperature control. For both half and full capacity operation, the substrate bed was divided into cubical tanks each of 5 cm height, width and depth. During half capacity operation the total number of cubical tanks was three to map 15 cm of bioreactor space, and in full capacity operation the total number of cubical tanks was five to map 25 cm of bioreactor space. The tank size of 5 cm was chosen considering the observed experimental trends and the design features of the bioreactor. It has been shown in the literature that tank height under 10 cm ensures spatial homogeneity of state variables [29,31], an important

consideration for the N-tank in series methodology. As per the design, the bottom tank was devoid of an air distributor and consequently temperature control was not as effective as with tanks housing air distributor (middle and top levels), a trend correctly captured by the model. One of the challenges in modeling solid state fermentation is synchronizing growth of microorganisms as estimated from kinetic parameters with changes in process conditions with time [42]. No attempt was made to re-estimate some of the model parameters so that a better fit could be obtained. The modeling approach developed here, therefore, represents a first step and would need additional work for in-depth analysis of bioreactor design and operation.

4.5. Simulations to show the effect of different operating conditions on bioreactor performance

The applicability of the model was extended to understand the role of operating conditions on bioreactor performance. Rajagopolan and Modak [12] noted chamber or incubation temperature, and temperature and mass flow rate of the gas as critical parameters in controlling the enzyme production in static bioreactors. Therefore, simulations were carried out where these parameters were varied. Temperature profile of the substrate bed and fungal growth were considered as key indicators in evaluating the bioreactor performance. Enzyme productivity was not modeled because of the lack of available literature data with regard to cellulolytic enzymes production kinetics in fungal cultures. Nevertheless, the predictions in terms of fungal growth can give meaningful insight into the potential efficacy of the enzyme production process.

4.5.1. Effect of simulated cabinet temperature on bed temperature profile and fungal growth

Effect of simulated cabinet temperature on substrate bed temperature profile and fungal growth is shown in Fig. 5.7a-b. Distributor air temperature and mass flow rate were fixed at 25ºC

and 3.42 kg h^{-1}. Inspection of the data revealed that predicted substrate bed temperatures were sensitive to changes in cabinet temperature. At lower cabinet or incubation temperature, substrate bed temperature at all three levels was close to the optimum of 35ºC. As the cabinet temperature was increased beyond 30ºC, the process was no longer at optimum temperature and peak temperatures reached beyond 40ºC at all levels. The severity of the temperature rise was greater at the bottom level due to the absence of air distributors (Fig. 5.7a). At much higher cabinet temperature (~ 40-45ºC) the cooling capacity of the bed was predicted to be completely diminished and the bed temperatures remained above 45ºC throughout the process. Predicted growth was synchronous with the rise in temperature (Fig. 5.7b). At cabinet temperature under 25ºC, fungal growth at all three levels was slow but attained its maximum value of 0.248 kg-biomass/kg-substrate within 60 h of incubation. Due to the slower growth rate, there was a shift in the temperature peak and it took 60 h to reach its maximum (Fig. 5.7a). At 30ºC, fungal growth was quicker and attained its maximum value within 40 h of operation at both the middle and top levels. At the bottom level, however, due to the absence of cooling growth reached 80% of its maximum value within 40 h operation. As expected, when cabinet temperatures were greater than 35ºC, growth almost ceased at all levels (Fig. 5.7b).

It is interesting to note that maintaining the cabinet temperature near the optimum value (~ 35ºC) for fungal cells did not necessarily predicted maximum cell mass yield. As the growth starts, the substrate bed temperature will reach maximum in a very short time due to increased metabolic production of heat. Consequently, fungal growth rate will fall resulting in poor yield. It seems more promising to keep cabinet temperature lower than what is required for optimal fungal growth to prevent temperature build-up within the bed during scale-up. Similar observations have been noted elsewhere [43,12,13].

4.5.2. Effect of predicted distributor air temperature and mass flow rate on bed temperature profile and fungal growth

At constant cabinet temperature of 30ºC variation in distributor air temperature and mass flow rate did not cause any shift in temperature and growth peaks such that their maximum values were reached in 40 h of operation. Hence for the sake of simplicity studying the entire profiles was avoided. Increasing the distributor air temperature from 15 to 55ºC only increased the predicted peak bed temperature for the middle and top levels by 4-5ºC from their initial values at constant air mass flow rate of 3.42 kg h^{-1} (Fig. 5.8a-b).There was no effect observed on the bottom level temperature and fungal growth during simulations due to the absence of air distributors. Fungal growth remained constant for both middle and top levels because bed temperatures remained under 40ºC (Fig. 5.8a) at all air temperatures simulated. Thus no significant change in growth was observed.

When mass flow rate of air was varied at constant distributor air temperature (25ºC) from 0.034 to 34 kg h^{-1}, bed temperatures at both the middle and top levels decreased significantly from non-optimum to near optimum values (Fig. 5.9a-b). When flow rate was increased from 34 to 340 kg h^{-1}, decrease in bed temperatures was more subtle. Fungal biomass reached its peak at 3.4 kg h^{-1} and decreased thereafter because at higher flow rates temperature decreased beyond its optimum.

5. Conclusions

The present work examines the design and testing of novel deep bed solid-state bioreactor that avoided build up of extreme temperature gradients during scale-up. The unique wire-mesh outer skeleton housing internal air distributors and a near saturation environment within a cabinet resulted in enhanced convective heat transfer and effective dispersal of metabolic heat during fugal growth without excessive moisture loss. The cellulolytic enzymes

production was faster compared to conventional static tray operation and reached levels during 48 h of operation that were comparable to those obtained during lab scale trials.

A comprehensive two-phase model was developed to predict the performance of the bioreactor over a broad type of operating parameters. The model predicted the experimental results with reasonably good accuracy. Simulation results indicated that bioreactor performance was more sensitive to changes in cabinet (incubation) temperature and mass flow rate of air through the distributors than distributor air temperature. Within the range of parameters studied cabinet temperature of 30ºC and mass flow rate of 3.4 kg h^{-1} resulted in optimum performance. These values confirmed those chosen for the experimental trials.

Current bioreactor design was benchmarked in terms of cellulolytic enzymes production, which is important for lignocellulosic biomass hydrolysis for fuels and chemicals. The modular design of the bioreactor enables an effective scale-up for production of large quantity of low-cost enzymes for biomass conversion.

Acknowledgements

The authors express their gratitude to the Center for Sustainable Energy and the Department of Grain Science and Industry, Kansas State University for funding this project. Authors are grateful to engineers Taylor Jones and Jared Henry at Advanced Manufacturing Institute, Kansas State University for fabrication of the bioreactor. Authors express their sincere appreciation to Dr. Charles Fahrenholz of Phibro Animal Health Inc. for providing the environmental cabinet for this study and technical assistance during set-up of the bioreactor. This article is contribution no. … from the Kansas Agricultural Experiment Station, Manhattan, Kansas 66506.

References

[1] M. Moo-Young, A.R. Moreira, R.P. Tengerdy, Principles of solid state fermentation, in: J.E. Smith, D.R. Berry, B. Kristiansen (Eds.), The filamentous fungi, vol 4, Edward Arnold, London 1983, pp. 117-144.

[2] C. Webb, R. Wang, Development of a generic fermentation feedstock from whole wheat flow, in: G.M. Campbell, C. Webb, S.L. McKee (Eds.), Cereals: novel uses and processes, Plenum Press, New York and London, 1997, pp. 205-218.

[3] C. Krishna, Solid-state fermentation systems - An overview. Critical Reviews in Biotechnology 25 (2005), 1-30.

[4] R.R. Singhania, R.K. Sukumaran, A.K. Patel, C. Larroche, A. Pandey, Advancement and comparative profiles in the production technologies using solid-state and submerged fermentation for microbial cellulases. Enzyme and Microbial Technology 46 (2010), 541-549.

[5] B. L. Rathbun, M. L. Shuler, Heat and mass-transfer effects in static solid-substrate fermentations - design of fermentation chambers. Biotechnology and Bioengineering 25 (1983), 929-938.

[6] N. P. Ghildyal, M. K. Gowthaman, K. Rao, N. G. Karanth, Interaction of transport resistances with biochemical reaction in packed-bed solid-state fermentors - effect of temperature-gradients. Enzyme and Microbial Technology16 (1994), 253-257.

[7] M. Khanahmadi, R. Roostaazad, A. Safekordi, R. Bozorgmehri, D. A. Mitchell, Investigating the use of cooling surfaces in solid-state fermentation tray bioreactors: modelling and experimentation. Journal of Chemical Technology and Biotechnology 79 (2004), 1228-1242.

[8] B. K. Lonsane, N. P. Ghildyal, S. Budiatman, S. V. Ramakrishna, Engineering aspects of solid-state fermentation. Enzyme and Microbial Technology 7 (1985), 258-265.

[9] D. A. Mitchell, M. Berovic, N. Krieger, T. Scheper, Biochemical engineering aspects of solid state bioprocessing. Advances in Biochemical Engineering Biotechnology; New products and new areas of bioprocess engineering 68 (2000), 61-138.

[10] N. P. Ghildyal, M. Ramakrishna, B. K. Lonsane, N. G. Karanth, M. M. Krishnaiah, Temperature-variations and amyloglucosidase levels at different bed depths in a solid-state fermentation system. Chemical Engineering Journal and the Biochemical Engineering Journal 51 (1993), B17-B23.

[11] A.R. Durand, J. Renaud, J. Maratray, S. Almanza, The INRA-Dijon reactors: designs and applications, in: S. Roussos, B.K. Lonsane, M. Raimbault, G. Viniegra-Gonzalez (Eds.), Advances in solid state fermentation, Kluwer Academic Publishers, Dordrecht, 1997, pp. 71-92.

[12] S. Rajagopalan, J. M. Modak, Heat and mass-transfer simulation studies for solid-state fermentation processes. Chemical Engineering Science 49 (1994), 2187-2193.

[13] J. P. Smits, A. Rinzema, J. Tramper, E. E. Schlosser, W. Knol, Accurate determination of process variables in a solid-state fermentation system. Process Biochemistry 31 (1996), 669-678.

[14] M. Fernandez, J. R. PerezCorrea, I. Solar, E. Agosin, Automation of a solid substrate cultivation pilot reactor. Bioprocess Engineering 16 (1996), 1-4.

[15] G. Saucedo-Castaneda, M. Gutierrez-Rojas, G. Bacquet, M. Raimbault, G. Viniegra-Gonzalez, Heat-transfer simulation in solid substrate fermentation. Biotechnology and Bioengineering 35 (1990), 802-808.

[16] S. Roussos, M. Raimbault, J. P. Prebois, B. K. Lonsane, Zymotis, a large-scale solid-state fermenter - design and evaluation. Applied Biochemistry and Biotechnology 42 (1993), 37-52.

[17] P. Sangsurasak, D. A. Mitchell, Validation of a model describing two-dimensional heat transfer during solid-state fermentation in packed bed bioreactors. Biotechnology and Bioengineering 60 (1998), 739-749.

[18] A. Durand, Bioreactor designs for solid state fermentation. Biochemical Engineering Journal 13 (2003), 113-125.

[19] O. F. von Meien, D. A. Mitchell, A two-phase model for water and heat transfer within an intermittently-mixed solid-state fermentation bioreactor with forced aeration. Biotechnology and Bioengineering 79 (2002), 416-428.

[20] S. Rajagopalan, J. M. Modak, Modeling of heat and mass-transfer for solid-state fermentation process in tray bioreactor. Bioprocess Engineering 13 (1995), 161-169.

[21] J. P. Smits, H. M. van Sonsbeek, J. Tramper, W. Knol, W. Geelhoed, M. Peeters, A. Rinzema, Modelling fungal solid-state fermentation: the role of inactivation kinetics. Bioprocess Engineering 20 (1999), 391-404.

[22] D. A. Mitchell, A. Pandey, P. Sangsurasak, N. Krieger, Scale-up strategies for packed-bed bioreactors for solid-state fermentation. Process Biochemistry 35 (1999), 167-178.

[23] F. J. Weber, J. Tramper, A. Rinzema, A simplified material and energy balance approach for process development and scale-up of *Coniothyrium minitans* conidia production by solid-state cultivation in a packed-bed reactor. Biotechnology and Bioengineering 65 (1999), 447-458.

[24] D. M. Stuart, D. A. Mitchell, Mathematical model of heat transfer during solid-state fermentation in well-mixed rotating drum bioreactors. Journal of Chemical Technology and Biotechnology 78 (2003), 1180-1192.

[25] K. Brijwani, H. S. Oberoi, P. V. Vadlani, Production of a cellulolytic enzyme system in mixed-culture solid-state fermentation of soybean hulls supplemented with wheat bran. Process Biochemistry 45 (2010), 120-128.

[26] M. Mandels, J. Weber, Production of cellulases. Advances in Chemistry Series (1969), 391-413.

[27] J. A. Rodriguez Leon, A. Torres, J. Echevarria, G. Saura, Energy balance in solid state fermentation processes. Acta Biotechnologica 11 (1991), 9-14.

[28] F. D. H. Dalsenter, G. Viccini, M. C. Barga, D. A. Mitchell, N. Krieger, A mathematical model describing the effect of temperature variations on the kinetics of microbial growth in solid-state culture. Process Biochemistry 40 (2005), 801-807.

[29] D. A. Mitchell, L. E. N. Cunha, A. V. L. Machado, L. F. D. Luz, N. Krieger, A model-based investigation of the potential advantages of multi-layer packed beds in solid-state fermentation. Biochemical Engineering Journal 48 (2010), 195-203.

[30] B. C. Marques, M. C. Barga, W. Balmant, L. F. D. Luz, N. Krieger, D. A. Mitchell, A model of the effect of the microbial biomass on the isotherm of the fermenting solids in solid-state fermentation. Food Technology and Biotechnology 44 (2006), 457-463.

[31] A. H. Sahir, S. Kumar, Modelling of a packed bed solid-state fermentation bioreactor using the N-tanks in series approach. Biochemical Engineering Journal 35 (2007), 20-28.

[32] O. Levenspiel, Chemical Reaction Engineering, third ed., John Wiley & Sons Inc., New York, 1999.

[33] M. K. Gowthaman, N. P. Ghildyal, K. Rao, N. G. Karanth, Interaction of transport resistances with biochemical reaction in packed-bed solid-state fermenters - the effect of gaseous concentration gradients. Journal of Chemical Technology and Biotechnology 56 (1993), 233-239.

[34] M. K. Gowthaman, K. Rao, N. P. Ghildyal, N. G. Karanth, Gas concentration and temperature-gradients in a packed-bed solid-state fermenter. Biotechnology Advances 11 (1993), 611-620.

[35] F. Nagel, J. Tramper, M. S. N. Bakker, A. Rinzema, Temperature control in a continuously mixed bioreactor for solid-state fermentation. Biotechnology and Bioengineering 72 (2001), 219-230.

[36] B.A. Finlayson, Nonlinear analysis in chemical engineering, McGraw-Hill Inc., New York, 1980.

[37] M. Gutierrez-Rojas, S. A. A. Hosn, R. Auria, S. Revah, E. FavelaTorres, Heat transfer in citric acid production by solid state fermentation. Process Biochemistry 31 (1996), 363-369.

[38] K. Brijwani, P.V. Vadlani, Cellulolytic Enzymes Production *via* Solid State Fermentation: Effect of Pretreatment Methods on Physicochemical Characteristics of Substrate. Enzyme Research (in press).

[39] M.S. Chin, S.E. Nokes, Temperature control of solid substrate cultivation deep-bed reactor using an internal heat exchanger. Transactions of ASAE 46 (2003), 1741-1749.

[40] M. A. Mazutti, G. Zabot, G. Boni, A. Skovronski, D. de Oliveira, M. Di Luccio, M. I. Rodrigues, H. Treichel, F. Maugeri, Kinetics of inulinase production by solid-state fermentation in a packed-bed bioreactor. Food Chemistry 120 (2010), 163-173.

[41] F. J. Weber, J. Oostra, J. Tramper, A. Rinzema, Validation of a model for process development and scale-up of packed-bed solid-state Bioreactors. Biotechnology and Bioengineering 77 (2002), 381-393.

[42] M. Khanahmadi, R. Roostaazad, D. A. Mitchell, M. Miranzadeh, R. Bozorgmehri, A. Safekordi, Bed moisture estimation by monitoring of air stream temperature rise in packed-bed solid-state fermentation. Chemical Engineering Science 61 (2006), 5654-5663.

[43] M. V. Ramesh, B. K. Lonsane, Solid-state fermentation for production of alpha-amylase by *Bacillus megaterium* 16M. Biotechnology Letters 9 (1987), 323-328.

Figure 5.1 Deep bed bioreactor. a) Third angle orthographic projection; b) isometric projection. All dimensions are in cm.

a)

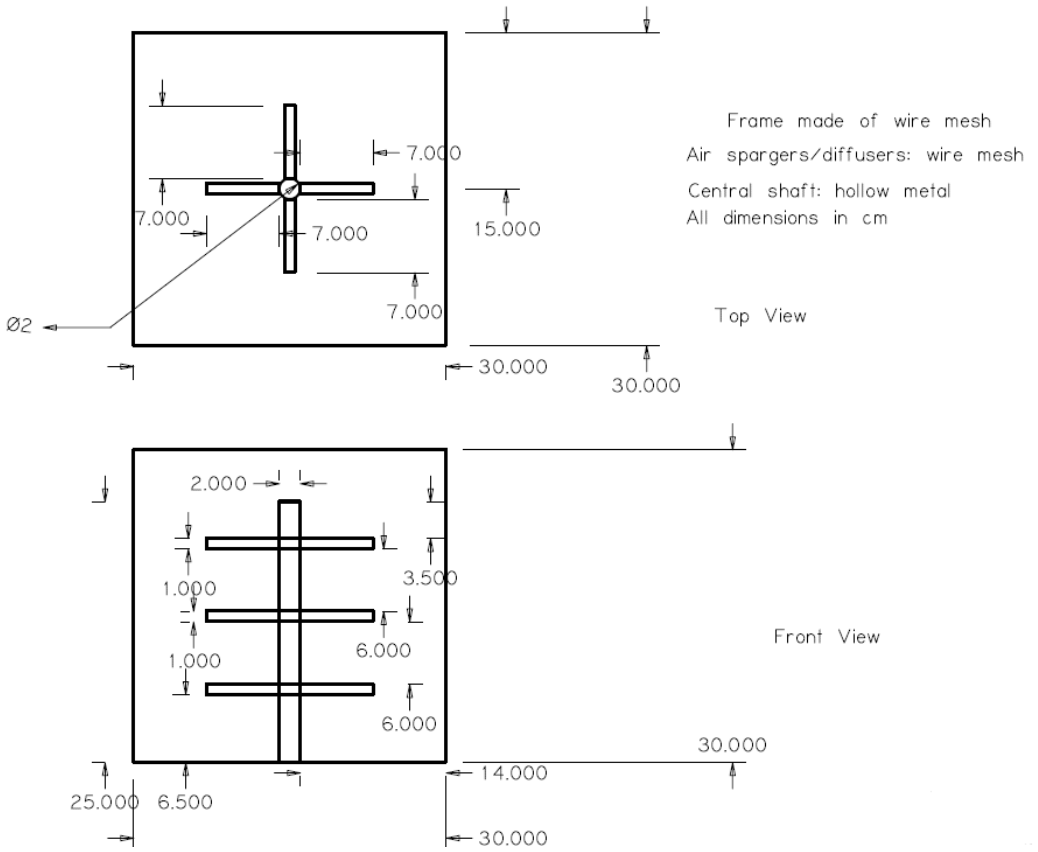

b)

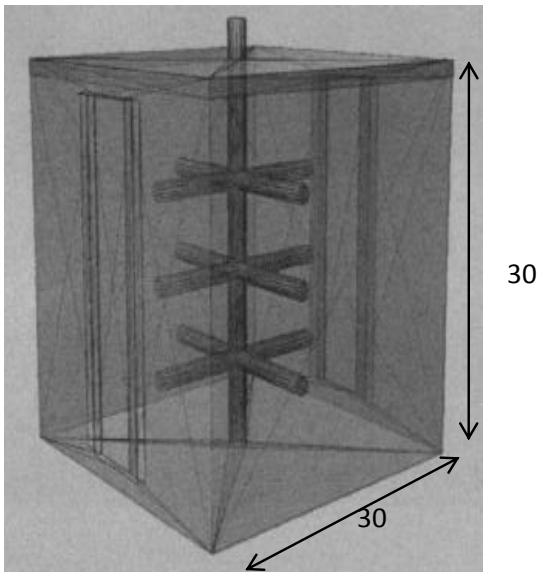

Figure 5.2 Schematic of the bioreactor portioned into N-tanks in series

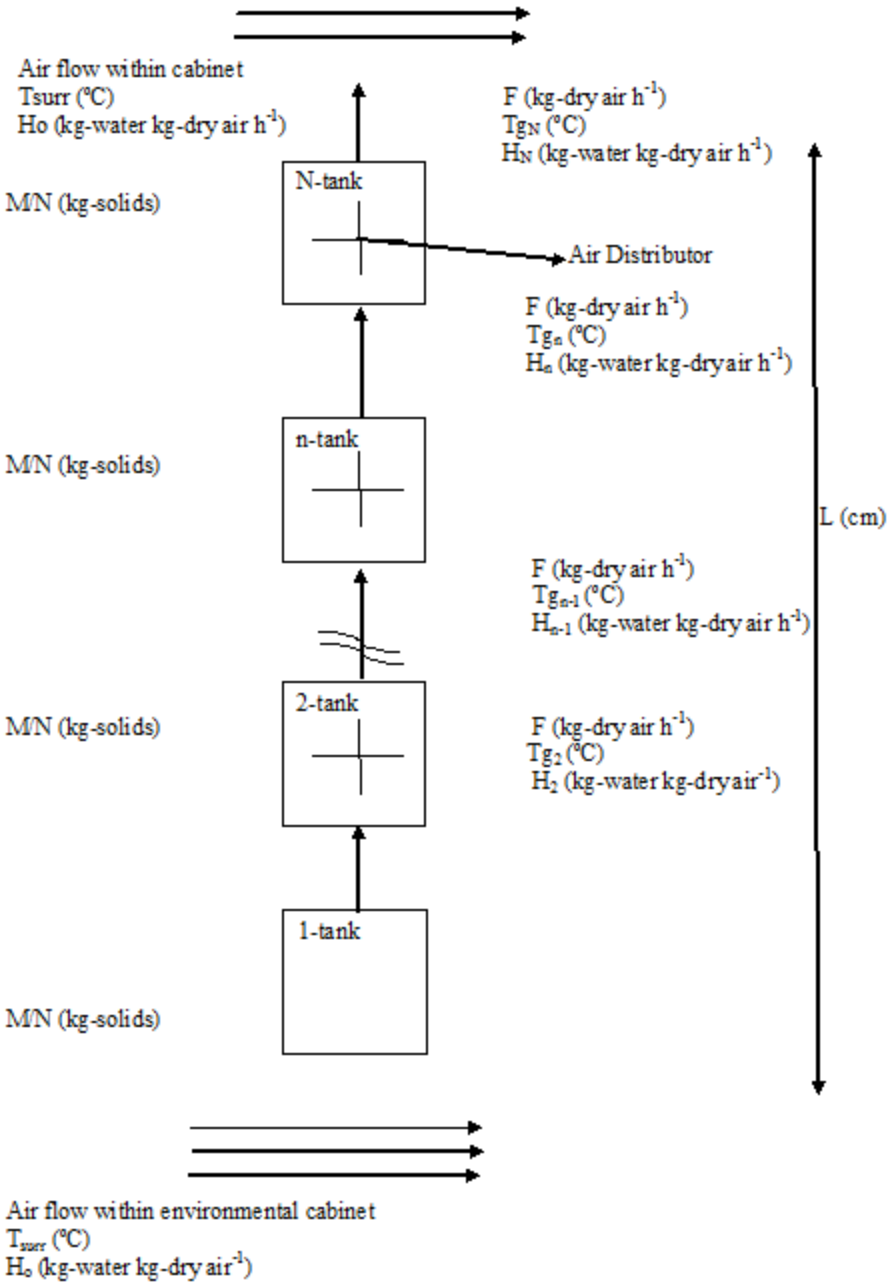

Figure 5.3 a) Cellulolytic enzymes production in half capacity operation. Bottom (3 cm from the base); Middle (7 cm from the base); Top (15 cm from the base). b) Cellulolytic enzyme production in full capacity operation. Bottom (3 cm from the base); Middle (15 cm from the base); Top (25 cm from the base). Distributor air flow rate is 3.42 kg-dry air h^{-1}. Error bars represents standard error of mean for n =4.

a)

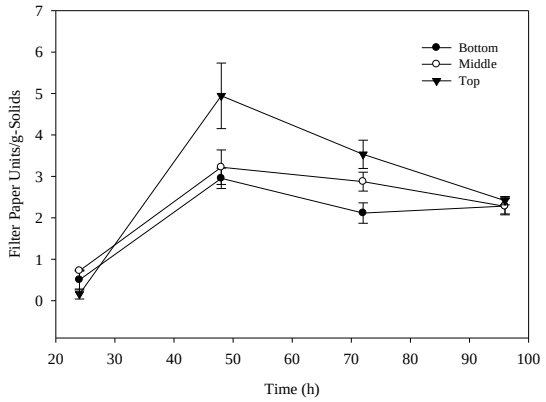
Filter Paper Units/g-Solids
Time (h)
Bottom
Middle
Top

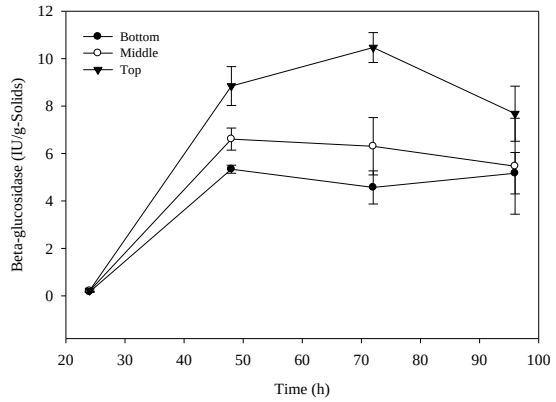
Beta-glucosidase (IU/g-Solids)
Time (h)
Bottom
Middle
Top

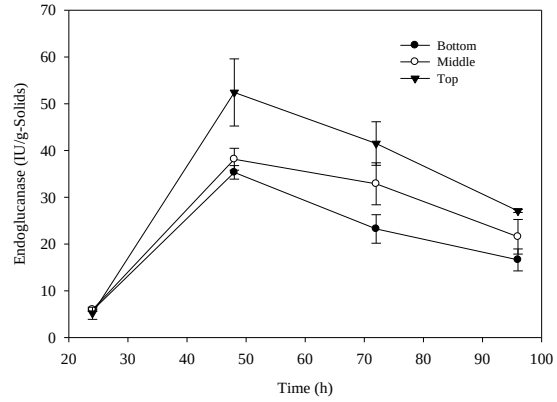
Endoglucanase (IU/g-Solids)
Time (h)
Bottom
Middle
Top

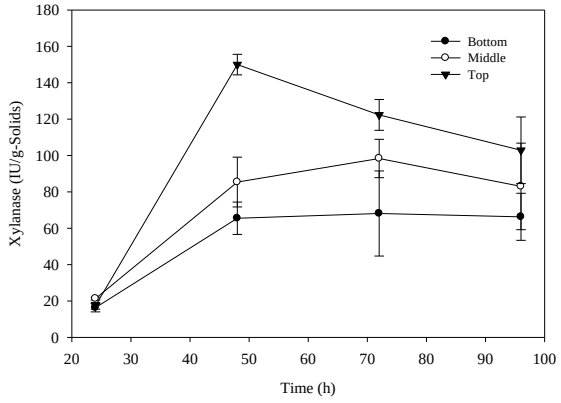
Xylanase (IU/g-Solids)
Time (h)
Bottom
Middle
Top

b)

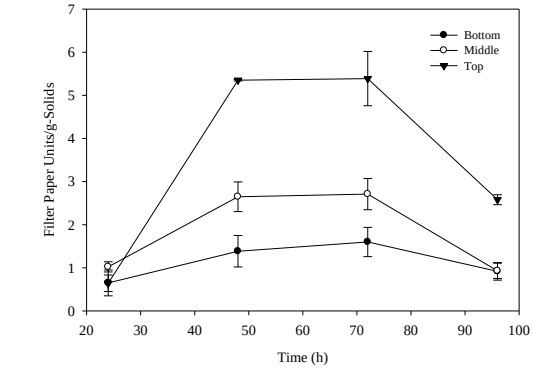
Filter Paper Units/g-Solids
Time (h)
Bottom
Middle
Top

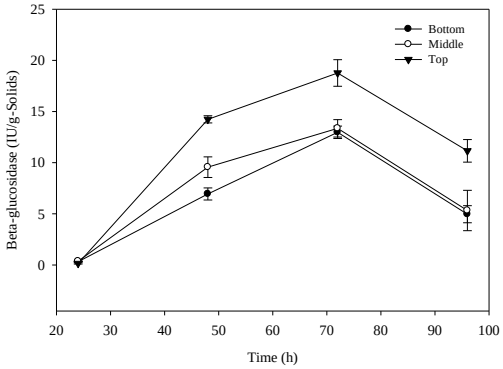
Beta-glucosidase (IU/g-Solids)
Time (h)
Bottom
Middle
Top

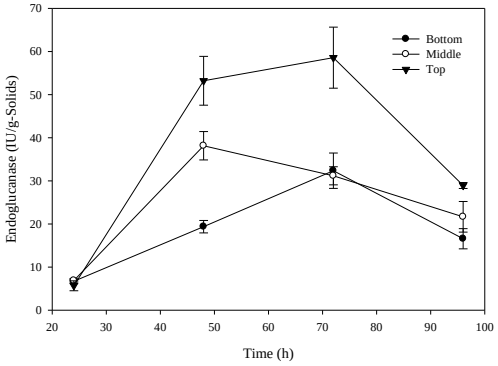
Endoglucanase (IU/g-Solids)
Time (h)
Bottom
Middle
Top

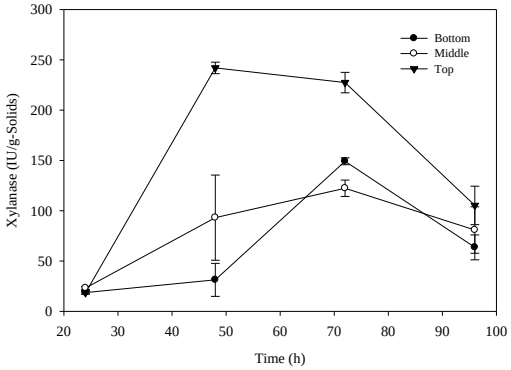
Xylanase (IU/g-Solids)
Time (h)
Bottom
Middle
Top

Figure 5.4 a) Observed moisture profile for half capacity operation with distributor air flow rate of 3.42 kg-dry air h^{-1}. b) Observed moisture profile for full capacity operation with distributor air flow rate of 3.42 kg-dry air h^{-1}. Bottom (3 cm from the base); Middle (7 cm from the base); Top (15 cm from the base) for half capacity operation. Bottom (3 cm from the base); Middle (15 cm from the base); Top (25 cm from the base) for full capacity operation. Error bars represents standard error of the mean for n = 2.

a)

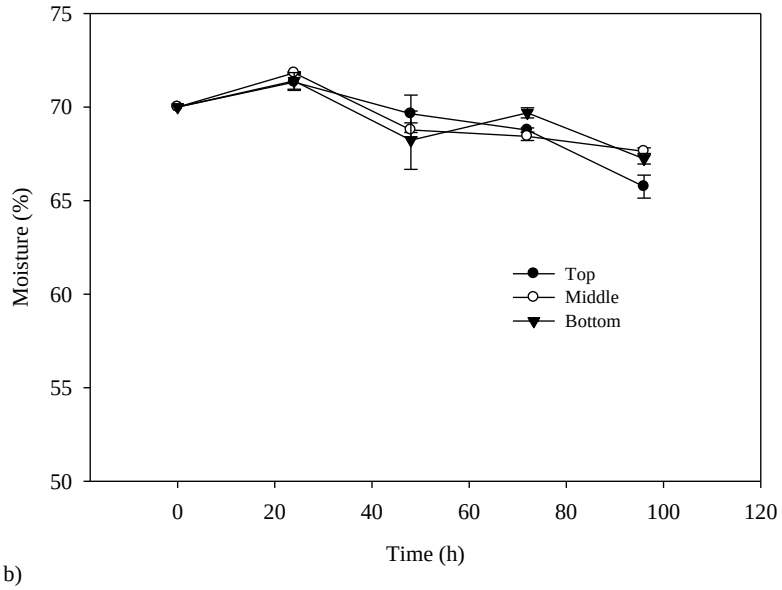

b)

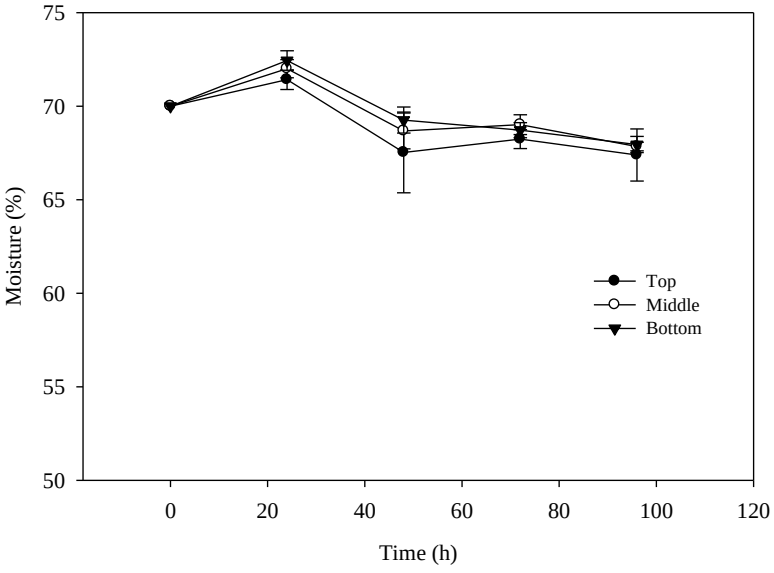

Figure 5.5 a) Observed temperature profile for half capacity operation without air flow through distributors. Bottom (3 cm from the base); Middle (7 cm from the base); Top (15 cm from the base). b) Observed temperature profile for Full capacity operation without air flow through distributors. Bottom (3 cm from the base); Middle (15 cm from the base); Top (25 cm from the base). Error bars represents standard error of the mean for n = 2.

a)

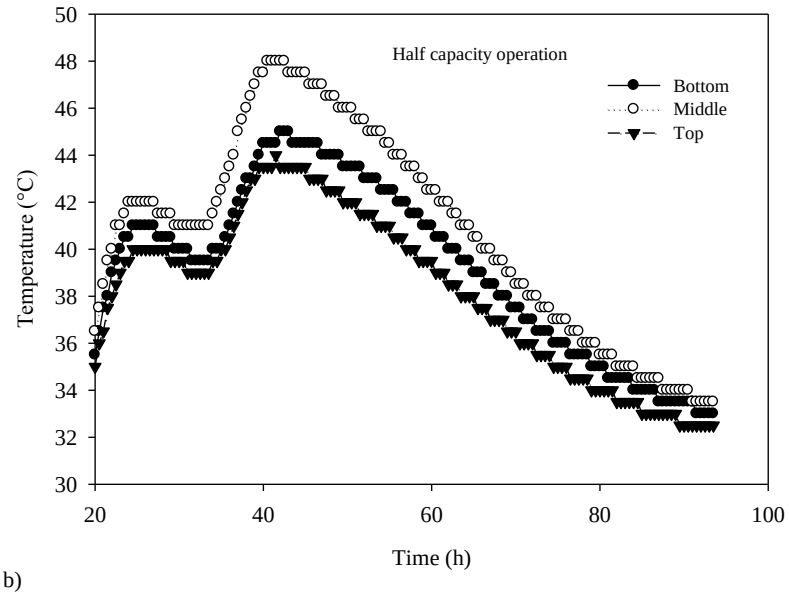

b)

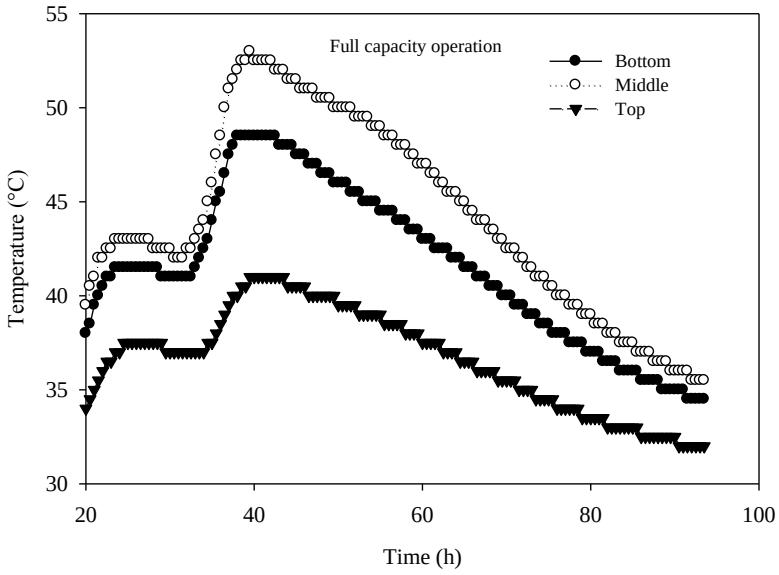

Figure 5.6 a) Observed and predicted temperature profile for half capacity operation with distributor air flow rate of 3.42 kg h^{-1}. Bottom (3 cm from the base); Middle (7 cm from the base); Top (15 cm from the base). b) Observed and predicted temperature profile for full capacity operation with distributor air flow rate of 3.42 kg h^{-1}. Bottom (3 cm from the base); Middle (15 cm from the base); Top (25 cm from the base). Error bars represents standard error of the mean for n = 2.

a)

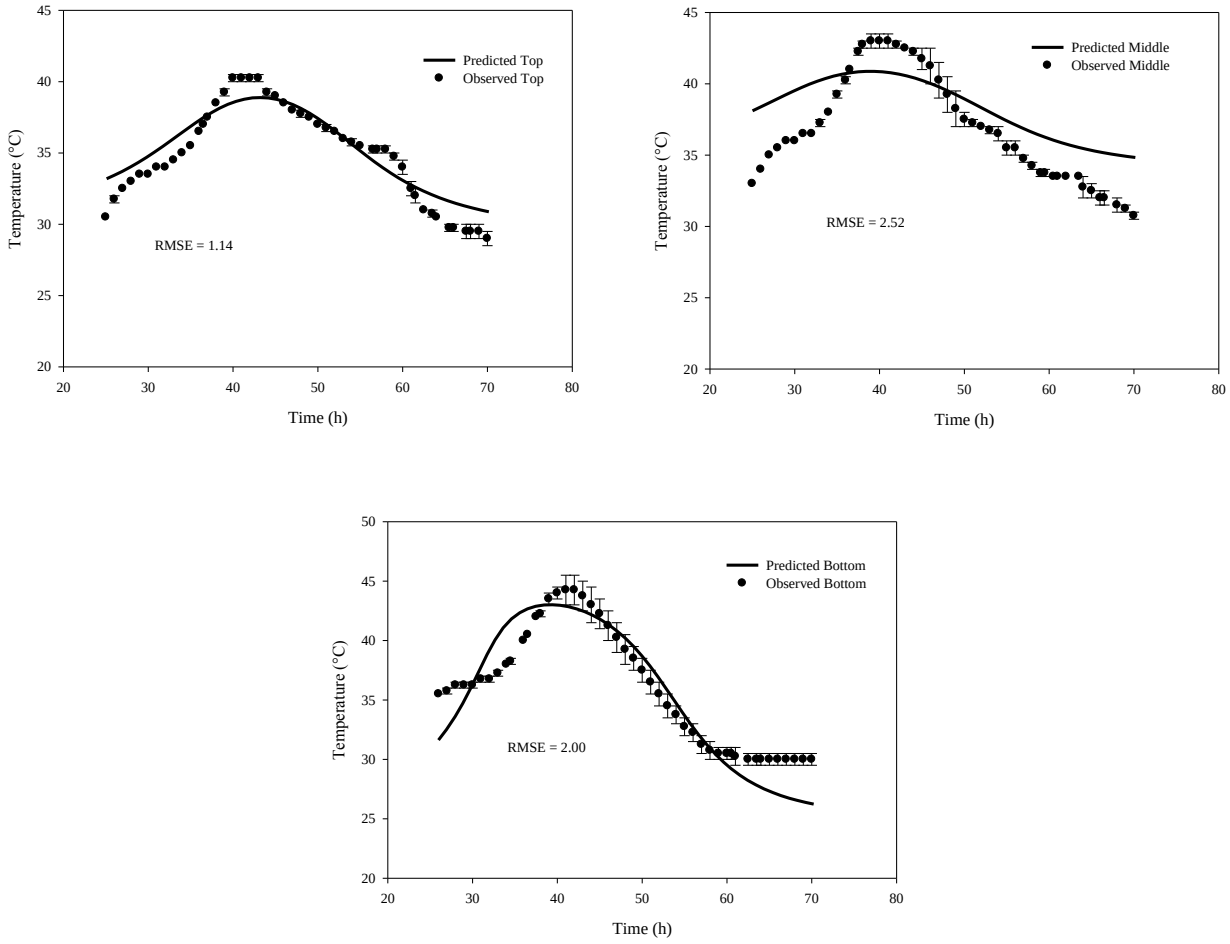

b)

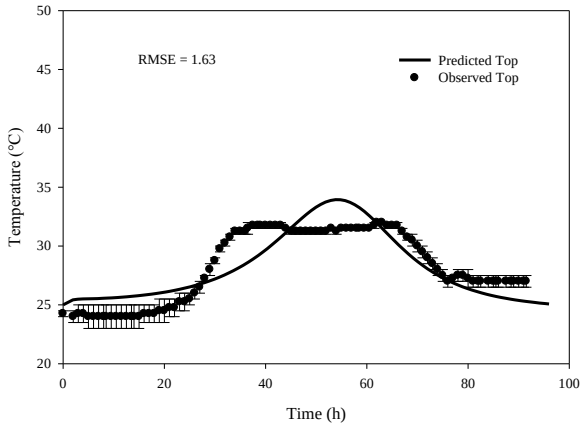
RMSE = 1.63
Predicted Top
Observed Top
Temperature (°C)
Time (h)

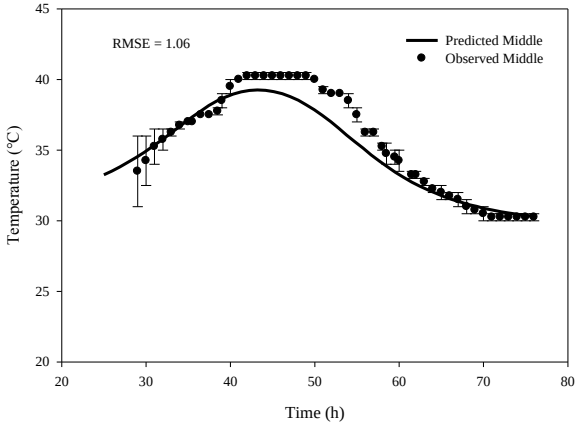
RMSE = 1.06
Predicted Middle
Observed Middle
Temperature (°C)
Time (h)

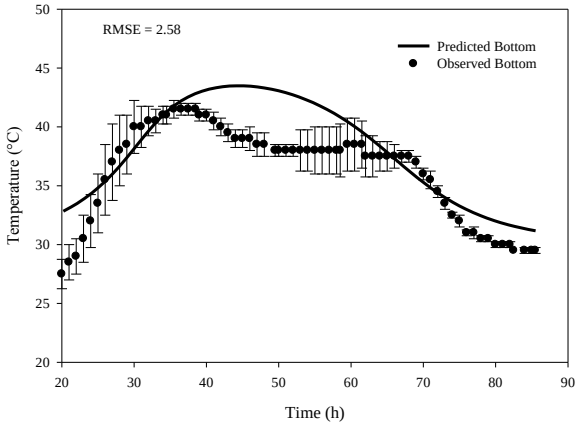
RMSE = 2.58
Predicted Bottom
Observed Bottom
Temperature (°C)
Time (h)

Figure 5.7 Effect of cabinet temperature on bioreactor's performance during full capacity operation. a) Predicted substrate bed temperature profile across the bed height. b) Predicted fungal growth profile across the bed height. Bottom (3 cm from the base); Middle (15 cm from the base); Top (25 cm from the base). Distributor air temperature and flow rate fixed at 25ºC and 3.4 kg h^{-1} during simulations.

a)

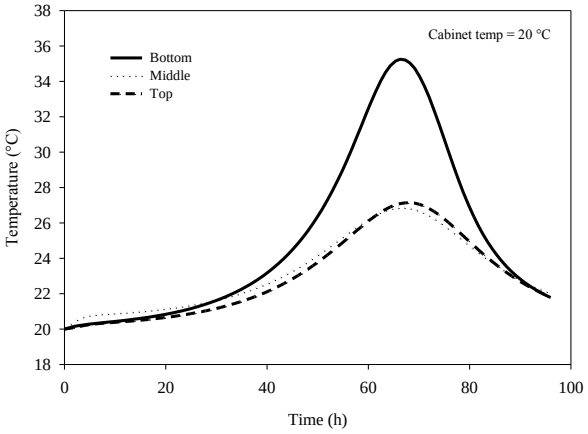
Cabinet temp = 20 °C
Bottom
Middle
Top
Temperature (°C)
Time (h)

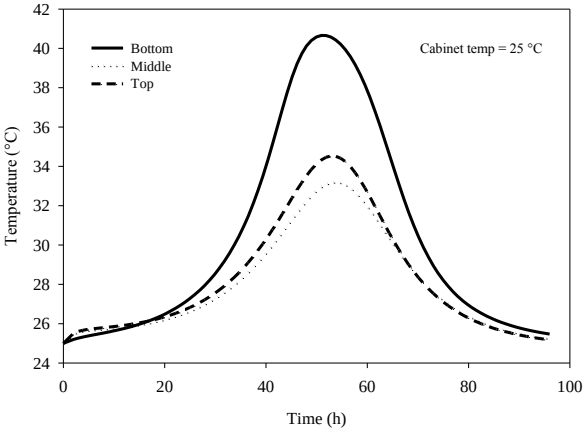
Cabinet temp = 25 °C
Bottom
Middle
Top
Temperature (°C)
Time (h)

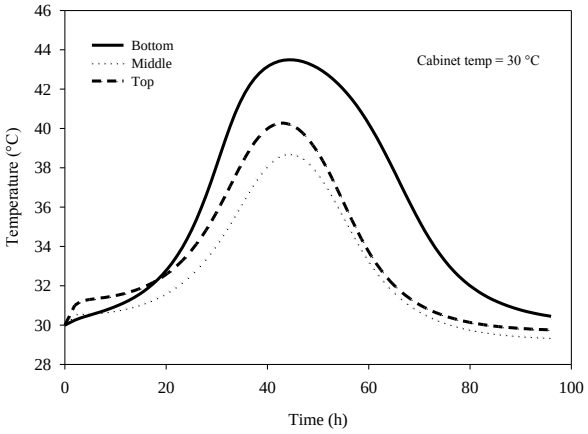
Cabinet temp = 30 °C
Bottom
Middle
Top
Temperature (°C)
Time (h)

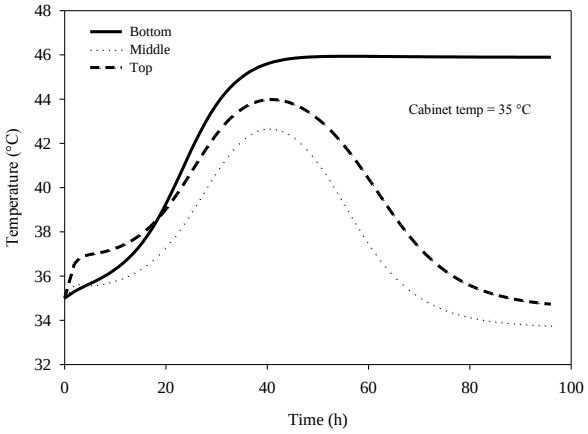
Cabinet temp = 35 °C
Bottom
Middle
Top
Temperature (°C)
Time (h)

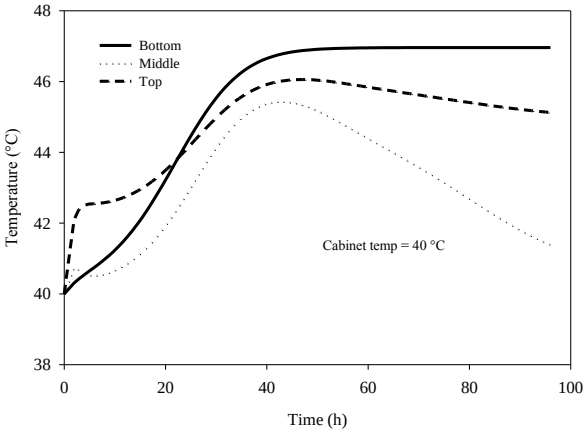
Cabinet temp = 40 °C
Bottom
Middle
Top
Temperature (°C)
Time (h)

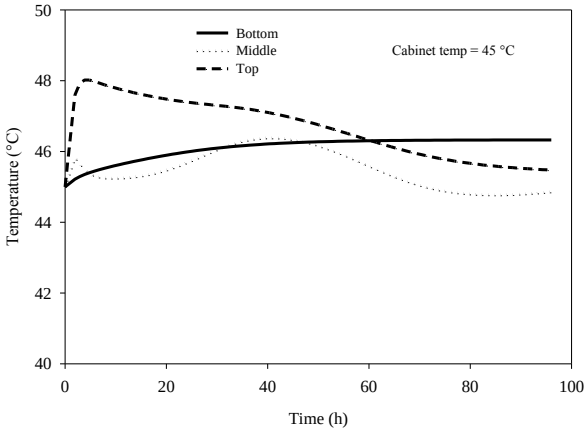
Cabinet temp = 45 °C
Bottom
Middle
Top
Temperature (°C)
Time (h)

b)

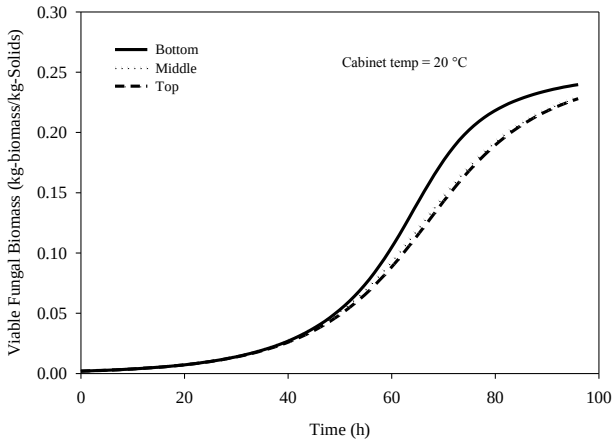
Bottom
Middle
Top
Cabinet temp = 20 °C
Viable Fungal Biomass (kg-biomass/kg-Solids)
Time (h)

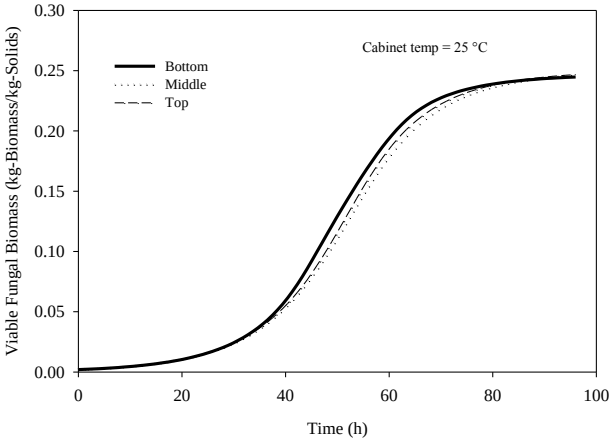
Bottom
Middle
Top
Cabinet temp = 25 °C
Viable Fungal Biomass (kg-Biomass/kg-Solids)
Time (h)

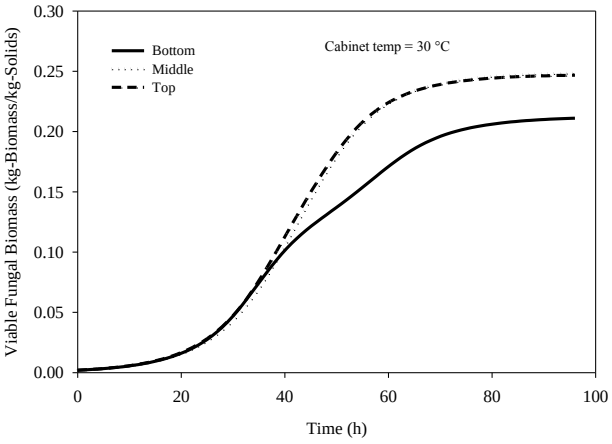
Bottom
Middle
Top
Cabinet temp = 30 °C
Viable Fungal Biomass (kg-Biomass/kg-Solids)
Time (h)

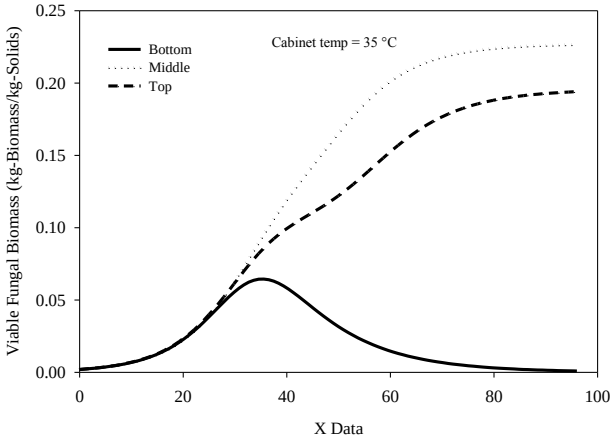
Bottom
Middle
Top
Cabinet temp = 35 °C
Viable Fungal Biomass (kg-Biomass/kg-Solids)
X Data

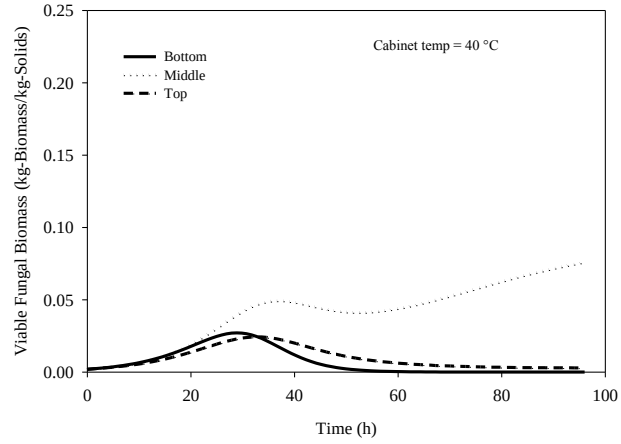
Bottom
Middle
Top
Cabinet temp = 40 °C
Viable Fungal Biomass (kg-Biomass/kg-Solids)
Time (h)

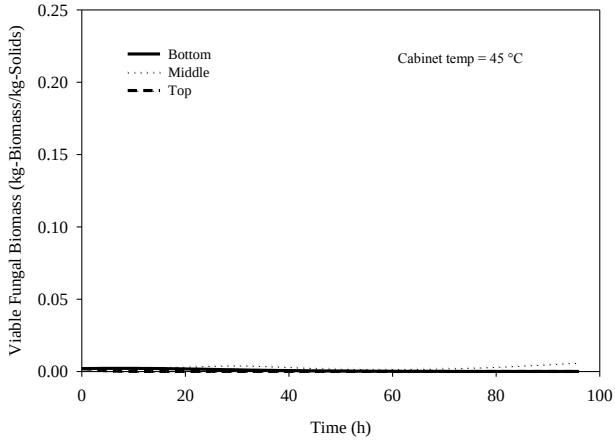
Bottom
Middle
Top
Cabinet temp = 45 °C
Viable Fungal Biomass (kg-Biomass/kg-Solids)
Time (h)

Figure 5.8 Effect of distributor air temperature on bioreactor's performance during full capacity operation. a) Predicted peak bed temperature. b) Predicted peak fungal biomass. Bottom (3 cm from the base); Middle (15 cm from the base); Top (25 cm from the base). Cabinet temperature and distributor flow rate fixed at 30ºC and 3.4 kg h^{-1} during simulations.

a)

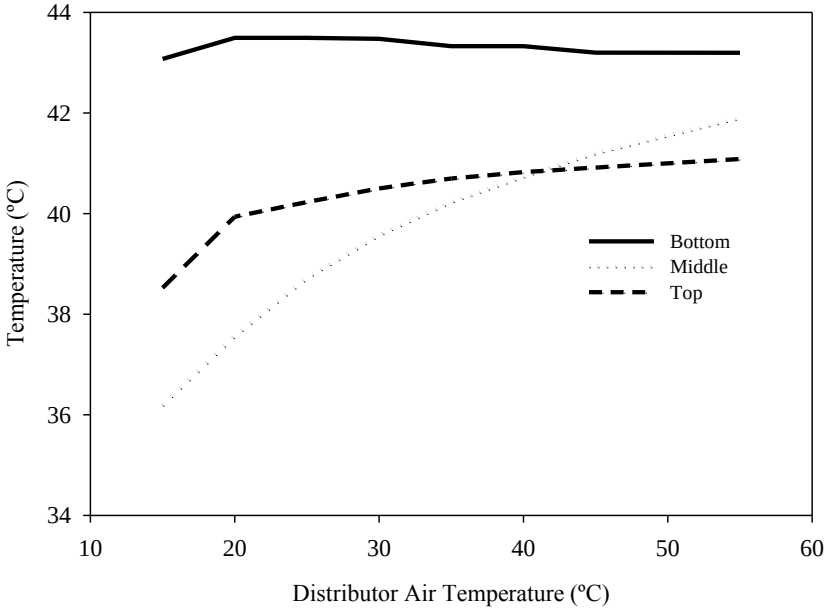

b)

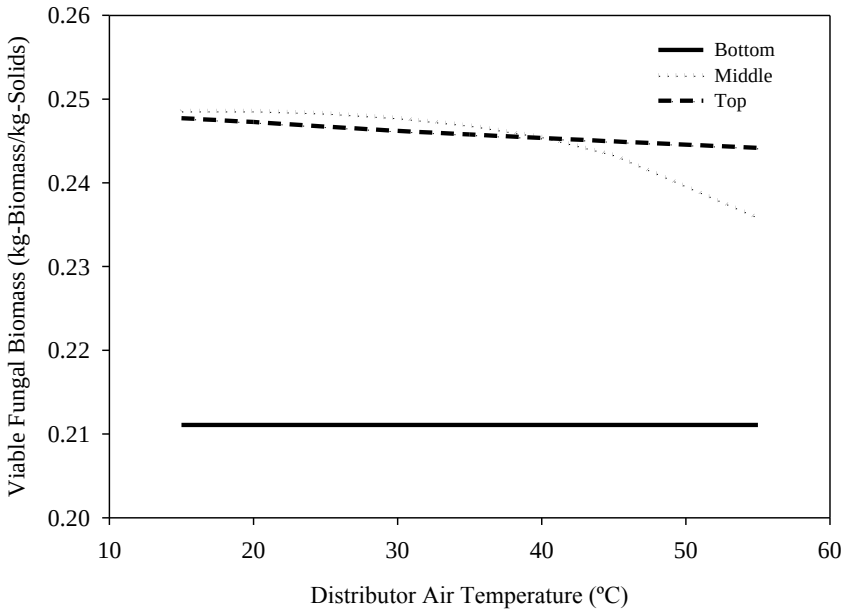
0.26
0.25
0.24
0.23
0.22
0.21
0.20
Viable Fungal Biomass (kg-Biomass/kg-Solids)
10
20
30
40
50
60
Distributor Air Temperature (ºC)
Bottom
Middle
Top

Figure 5.9 Effect of distributor air mass flow rate on bioreactor's performance during full capacity operation. a) Predicted peak bed temperature. b) Predicted peak fungal biomass. Middle (15 cm from the base); Top (25 cm from the base). Cabinet and distributor air temperature fixed at 30 and 25ºC during simulations. Note: data for bottom level not shown due absence of air distributor in bottom tank.

a)

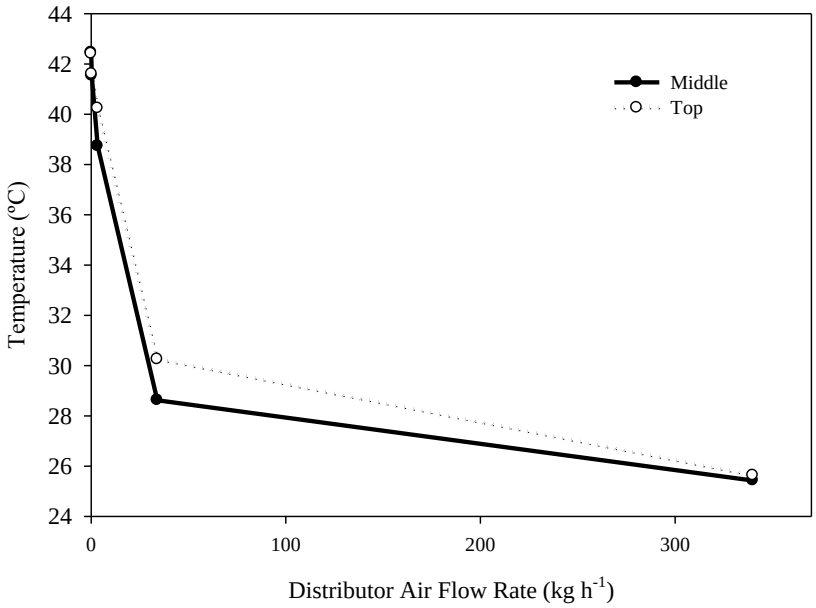

b)

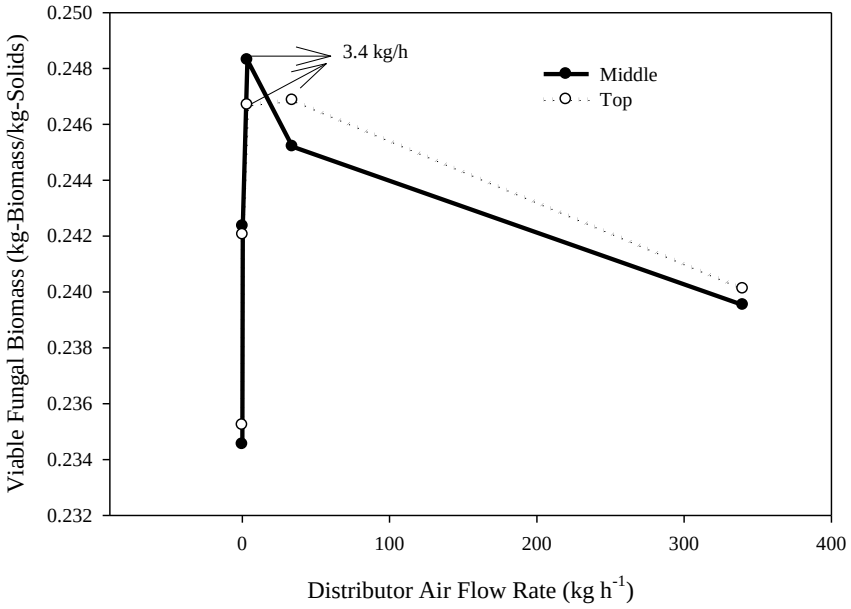
0.250
0.248
0.246
0.244
0.242
0.240
0.238
0.236
0.234
0.232
Viable Fungal Biomass (kg-Biomass/kg-Solids)
3.4 kg/h
Middle
Top
0
100
200
300
400
Distributor Air Flow Rate (kg h-1)

Table 5.1 Supplementary algebraic equations

Symbol	Expression	Eqn.	Reference
k_D	$k_D = A_D exp(\frac{-E_{aD}}{R(Ts+273)})$	8)	[19]
μ_T	$\mu_T = \frac{8.3148 \times 10^{11} \exp(-\frac{70225}{R(T_s+273)})}{1+1.3\times10^{47}\exp(-\frac{283356}{R(T_s+273)})}$	10)	[19]
μ_W	$\mu_W = 1.011325 \exp(618.9218a_W^3 - 1863.527a_W^2 + 1865.097a_W - 620.6684)$	11)	[19]
a_{Wg}	$a_{Wg} = \frac{1}{133.322\exp(18.3036-(\frac{3816.44}{(T_g+273)-46.13}))} \times \frac{P}{(1+(\frac{0.62413}{H}))}$	13)	[30]
W_{sat}	$W_{sat} = (1-X)\times\left(\sqrt[\frac{1}{0.7202}]{(\frac{\ln(1-a_{Wg})}{-4.988})}\right) + X\left(\sqrt[1/0.3596]{(\frac{\ln(1-a_{Wg})}{-2.5503})}\right)$	14)	[29]
h_g	$h_g = 44209.85 \times \sqrt[0.6011]{\frac{(\frac{F}{A})(Tg+273)}{0.0075P}}$	15)	[30]
K_W	$K_W = \left(7.304 - 1.77\times10^{-2}(T_g+273)\right)W - 2.202 - 6.18\times10^{-3}(T_g+273)$	16)	[30]

Table 5.2 Nomenclature and parameter values used during simulation

Symbol	Description	Value (or initial value) and units	Reference
A	Bed area normal to the air flow	0.09 m^2	This study
A_D	Frequency factor for death	8.0164×10^{100} h^{-1}	[30]
a_W	Water activity of the solid phase	Eq. (12), dimensionless	Calculated
a_{Wg}	Water activity of the gas phase	Eq.(13),dimensionless	Calculated
C_{PM}	Heat capacity of dry solids	2500 J kg-water^{-1} $^oC^{-1}$	[30]
C_{PW}	Heat capacity of liquid water	4187 J kg-water^{-1} $^oC^{-1}$	[30]
C_{PV}	Heat capacity of dry air	1000 J kg-water^{-1} $^oC^{-1}$	[30]
E_{aD}	Activation energy for death	621729.234 J mol^{-1}	[30]
F	Distributor air flow rate	3.42 kg h^{-1}	This study
h_g	Convective solid-gas heat transfer coefficient	Eq. (15), J h^{-1} m^{-3} $^oC^{-1}$	Calculated
h_{ov}	Overall heat transfer coefficient system-surroundings	54000 J h^{-1} m^{-2} $^oC^{-1}$	[35]
H	Gas phase humidity	H_o=0.027 kg-vapor kg-dry air^{-1}	This study
k_D	Specific death rate constant	Eq. (8), h^{-1}	Calculated
K_W	Water mass transfer coefficient	Eq. (16), kg-dry solids h^{-1} m^{-3}	Calculated
M	Dry solids	M_o = 3.51 kg (Full capacity) M_o = 2.51 kg (half capacity)	This study
R	Universal gas constant	8.314 J mol^{-1} $^oC^{-1}$	
P	Pressure inside the bioreactor	101325 Pa	
t	Time	t_o = 0 h	
T_g	Distributor gas temperature	T_{go} = 25 ^oC	This study
T_s	Solids temperature	T_{so} = 30 ^oC	This study
T_{surr}	Surrounding temperature	T_{surr} = 30 ^oC	This study
V	Volume of one layer of bed	0.0045 m^3 (layer height = 5 cm)	This study
W	Solid water content (dry basis)	W_o = 1.92 kg-water kg-	This study

		solids^{-1}	
W_{sat}	Saturation water content	Eq. (14), kg-water kg-solids^{-1}	Calculated
X_M	Maximum fungal biomass	0.250 kg-biomass kg-solids^{-1}	
X	Total fungal biomass	X_o=0.002 kg-biomass kg-solids^{-1}	
X_v	Viable fungal biomass	X_v=0.002 kg-biomass kg-solids^{-1}	
Y_{WX}	Yield of water during growth	0.3 kg-water kg-biomass^{-1}	[30]
Y_{QX}	Yield of metabolic heat during growth	8.366×10^6 J kg-water^{-1}	[30]
ε	Bed porosity	0.42, dimensionless	This study
λ	Enthalpy of evaporation of water	2,414,300 J kg-water^{-1}	[30]
μ	Specific growth rate constant	Eq. (9), h^{-1}	Calculated
μ_{opt}	Maximum specific growth rate constant	0.136 h^{-1}	Calculated
μ_T	Fractional temperature based value of μ	Eq. (10), dimensionless	Calculated
μ_W	Fractional water-activity based value of μ	Eq. (11), dimensionless	Calculated
ρ	Air density (dry basis)	1.14 kg-dry air m^{-3}	
o	Used for representing initial conditions		
n	Nth tank		

Table 5.3 Results of statistical analysis featuring significant differences in the peak value of various activities with depth in two modes of operations: Mid H and Full H.

Bed height	Half capacity operation			Full capacity operation			Lab flask data[1]
	Bottom	Middle	Top	Bottom	Middle	Top	
Filter Paper Units (FPU)/g-Solids	$2.95^{A, a}$	$3.22^{A, a}$	$4.94^{A, a}$	$1.60^{B, b}$	$2.71^{B, a}$	$5.39^{A, a}$	5.42
Beta-glucosidase (IU/g-Solids)	$5.34^{B, b}$	$6.61^{B, b}$	$10.47^{A, b}$	$12.97^{B, a}$	$13.36^{B, a}$	$18.76^{A, a}$	15.79
Endoglucanase (IU/g-Solids)	$35.31^{B, b}$	$38.13^{B, b}$	$52.41^{A, a}$	$32.35^{B, b}$	$38.14^{B, b}$	$58.57^{A, a}$	55.51
Xylanase (IU/g-Solids)	$68.10^{B, b}$	$98.35^{AB,a}$	$148.20^{A,b}$	$149.19^{B,a}$	$122.34^{B,a}$	$242.00^{A,a}$	290.22

"A, B, AB indicates significant differences between means for bottom, middle and top levels within the treatments i.e. among Mid H operation and Full H operation." "a, b, indicates significant differences between means across the treatments i.e. for a particular level between Mid H and Full H operations; means followed by different letters differ significantly." Comparison of pair of means were conducted using Tukey Kramer HSD at $P<0.05$.

[1]Represents the data from flask trials of Brijwani and Vadlani [38]

Chapter 6 - Summary

The objectives of the current work are to study micro and macro-scale aspects of fungal solid state fermentation (SSF) of soybean hulls for production of cellulolytic enzymes. At micro-scale the role of physicochemical characteristics of substrate in controlling enzyme production in SSF is discussed. At macro-scale, experimental and theoretical analysis of novel bioreactor design is carried out to demonstrate its scale-up potential.

Optimization of process parameters and cellulolytic enzymes production in static tray bioreactors

In the initial studies feasibility of using mixed culture fermentation of soybean hulls using *T. reesei* and *A. oryzae* in production of complete and balanced enzyme system for lignocellulosic biomass hydrolysis was established. Soybean hulls were supplemented with wheat bran to obtain favorable C/N ratio. Response surface methodology was used to optimize essential process parameters i.e. moisture, pH and temperature. With optimized parameters laboratory scale-up in static tray bioreactor using 100 g substrate was performed to produce enzymes. Optimized production of all cellulolytic activities in static tray was achieved within 96 hours and SDS expression profiles of various enzyme activities further validated the completeness of a cellulolytic enzyme system produced in a static tray bioreactor. Saccharification studies by indigenously produced crude enzyme concentrate demonstrated the potential of a cellulase enzyme complex in hydrolyzing pretreated wheat straw. Almost a 30% conversion of glucan to glucose and 75% conversion of xylan and arabinan, to corresponding xylose and arabinose, were reached during 96 hours of enzymatic hydrolysis. Differences in acid- and alkali-treated wheat straw were attributed to compositional disparities and lignin non-productive binding. The study highlighted the feasibility of solid state fermentation using

soybean hulls as a substrate for producing a system of enzymes with balanced activities that can efficiently saccharify lignocellulosic biomass like wheat straw.

Effect of pretreatments on physicochemical characteristics of substrate and cellulolytic enzymes production in fungal solid state fermentation

By using mild pretreatments physicochemical characteristics of soybean hulls – crystallinity and bed porosity were altered. The altered substrates were used for enzyme production. As crystallinity was an important parameter of the study, sophisticated deconvolution method was used to estimate crystallinity of pretreated and native soybean hulls. It was explicitly shown that steam pretreated soybean hulls with higher crystallinity and bed porosity had significantly higher production of all three important cellulolytic activities-filter paper, beta-glucosidase, and endocellulase activities in *T. reesei* culture. In *A. oryzae* culture, the crystalline and more porous steam pretreated soybean hulls had improved production of endocellulase only, whereas in the mixed culture fermentation, filter paper and endocellulase activities decreased in steam-pretreated soybean hulls.

Effect of bed porosity and crystallinity of substrate on cellulolytic enzymes production in fungal solid state fermentation

Bed porosity of steam pretreated and native soybean hulls was varied by varying the initial moisture content of the substrates. Substrates with higher porosity resulted in higher production of cellulolytic enzymes in both mono and mixed cultures. To understand the role of crystallinity both *T. reesei* and *A. oryzae* were adapted on crystalline substrates like cotton linter and avicel, and amorphous substrate like Walseth. Cotton linter-adapted *T. reesei* had 5.23 FPU/g-ds, 3.8 IU/g-ds beta-glucosidase, and 65.13 IU/g-ds endocellulase activities compared to 3.91 FPU/g-ds, 2.28 IU/g-ds beta-glucosidase, and 55 IU/g-ds endocellulase activities in

Walseth-adapted cultures. Xylanase production in *T. reesei* culture was not significantly different between crystalline and amorphous substrates. Crystalline substrates adapted *A. oryzae* had no significant change in cellulolytic activities with exception of increased endocellulase production compared to amorphous substrate adapted culture. However, the xylanase production in crystalline adapted *A. oryzae* was significantly reduced. Results highlighted the role of substrate properties in controlling enzyme production in SSF.

Experimental and theoretical analysis of novel bioreactor design for cellulolytic enzymes production

A novel deep bed bioreactor with outer wire-mesh frame and internal air distributors was designed. Unique design features (wire-mesh skeleton and internal air distributors) and a near saturation environment within cabinet resulted in improved convective heat transfer with minimum loss of moisture. Enzyme production was faster compared to conventional static tray operation and reached levels during 48 h of incubation period. Those levels were similar to that obtained in laboratory scale trials. A comprehensive two-phase heat and mass transfer model was developed. Model predictions were reasonably good in predicting experimental outcome. Model predictions were extended to simulate the role of critical process parameters on bioreactor performance. It was shown that bioreactor performance was more sensitive to changes in cabinet temperature and mass flow rate of air through distributors. The cabinet temperature of 30ºC and mass flow rate of 3.4 kg h^{-1} was shown to be optimum. These values were concomitant to those used during experimental trials. Lastly, within the range of parameters studied, there was no need to control distributor air temperature, so air could be supplied at ambient.

Chapter 7 - Conclusions and Future Outlook

Solid state fermentation (SSF) is an effective means of producing cellulolytic enzyme system for biomass hydrolysis for biofuels and chemicals. As water is present in bound form attached to solid particles, the particulate nature of the bioprocessing entails such that physico-chemical characteristics can significantly influence the biology of enzyme production in fungal cultures. By virtue of its solid nature the studies on scale-up of the process is important for commercial feasibility. Current work, therefore, explores both micro and macro-scale aspects of SSF of soybean hulls from flask to bioreactor level. In the initial studies process optimization using response surface methodology assisted effective standardization of the process required for further studies on physicochemical aspects and bioreactor scale-up. Compete and balanced enzyme system with 10.7 FPU/g of total cellulase and 10.7 IU/g of beta-glucosidase was produced in optimized process using mixed fungal cultures of *T. reesei* and *A. oryzae*. Crystallinity, bed porosity and volumetric surface area of treated (acid/alkali and steam) and untreated soybean hulls were investigated. It was explicitly demonstrated that steam pretreated soybean hulls with increased crystallinity and porosity had significantly higher enzyme activities, with the exception of xylanase, in *T. reesei*. Total cellulase of 4 FPU/g-ds, and endocellulase of 45 IU/g-ds were obtained in steam pretreated hulls compared to 0.75 FPU/g-ds and 7.29 IU/g-ds (endocellulase) in untreated hulls. In *A. oryzae* significant improvement was noticed only in endocellulase levels as a result of steam pretreatment. However, in the mixed culture fermentation, filter paper and endocellulase activities decreased in steam-pretreated soybean hulls. Additional studies using standard crystalline substrates and substrates with altered bed porosity highlighted that effect of physicochemical characteristics was selective with respect to fungal species and cellulolytic activity. A novel design of bioreactor was developed to

effectively aerate the system to minimize the temperature gradients and to realize the full potential of fungal cultures during scale-up. Unique Bioreactor design consisting of outer wire-mesh and internal air distributors along with a near saturation environment within cabinet resulted in enhanced convective heat transfer without excessive moisture loss. Enzyme production was faster and reached optimum during 48 h period, with activities comparable to those obtained in lab scale trials. Two-phase mathematical model featuring heat and mass transfer phenomena coupled to fungal growth kinetics was developed. Model explicitly predicted the bioreactor performance in various case scenarios, and showed better agreement with observed experimental data.

Scope for future work

The work presented in this dissertation provides necessary knowhow that can immediately contribute towards small scale production of cellulases. The following suggestions are recommended for future work to enhance the level of understanding and to explore new frontiers in the area of cellulolytic enzymes production via fungal SSF.

1. Physicochemical characteristics have been shown to be vital for cellulolytic enzyme production. Future work should elucidate the mechanisms governing the role of physicochemical characteristics at molecular or genomic level.
2. Substrate reactivity apart from bed porosity and crystallinity is also influenced by internal specific area. Effect of internal specific area on enzyme production should be incorporated in future investigations.
3. In the current bioreactor design air circulation through internal distributors is used as heat transfer fluid. Future studies should assess the role of other heat transfer mechanisms like water circulation compared to air distribution in containing the extreme temperature

gradients. It is possible to incorporate water fed cooling surfaces along with internal air distribution in design for effective dissipation of metabolic heat.

4. Current two-phase mathematical model can be improved further by incorporating variation in bed porosity of the substrate bed during the course of fermentation. Further enzyme kinetics can be studied alongside fungal growth kinetics.
5. The validation of present design for variety of other processes and products using array of industrial microorganisms is essential for encouraging commercial usage.